Republic of Iraq
Ministry of Higher Education
and Scientific Research
University of Babylon
College of Engineering
Environmental of Engineering Department

Removal of Methylene blue dye From Colored Wastewater Using Natural Adsorbent

A Thesis

Submitted to the College of Engineering / University of Babylon

In partial Fulfillment of the Requirements for the Degree

of Master in Engineering / Environmental Engineering

By

Maali alamjad Hassan Hussein Jawad Al-himyri

Supervised by

Asst. Prof. Dr. Isra'a Sadi Abdul-Amir Samaka

بسم الله الرحمن الرحيم

((نرفع درجات من نشاء وفوق كل ذي علم عليم))

صدق الله العلي العظيم

((سورة يوسف ألايه ٧٦))

DEDICATION

To

How do I get the description and words that embody your struggle in life…? I dedicate this fruit to efforts that gave me strength and patience… To dear my heart… My Father and Mother … I ask God to protect them for me.

To

Who have the widest hearts which always give…

My Husband mohammed

My Sisters and My brothers.

Maali

2022

Supervisors' Certification

I certify that the preparation of this thesis "**Removal of Methylene blue dye From Colored Wastewater Using Natural Adsorbent**" was prepared "Maali alamjad hassan" under my supervision at Environmental Engineering Department/ College of the Engineering/ University of Babylon, as partial fulfillment of the requirements for the degree of Master in Engineering/ Environmental Engineering.

Signature:

Name**: Asst. Prof. Dr. Isra'a Sadi Abdul-Amir Samaka (Supervisor)**

Date: / 1 / 2022

Examining Committee's Certification

We certify that we have read this thesis entitled "**Removal of Methylene blue dye From Colored Wastewater Using Natural Adsorbent**", and as an examining committee, examined the student "Maali alamjad hassan" in its content and in what is connected with it and that our opinion, it meets the standard of a thesis for the Degree of Master of Science in Environmental Engineering.

Signature:
Name: ***Asst.Prof. Dr. Safaa.K.Hashim*** *(Chairman)*
Date: / 1 / 2022

Signature:
*Name :****Asst. Prof.Dr. suad Mahdi Al fatlawi*** *(Member)*
Date: / 1 / 2022

Signature:
Name: ***Asst. Prof. Dr. Nabaa Shakir Hadi*** *(Member)*
Date: / 1 / 2022

Signature:
Name: ***Asst. Prof. Dr. Isra'a Sadi Abdul-Amir*** *(Supervisor)*
Date: / 1 / 2022

Signature:
Name: ***Asst. Prof. Dr. Hussei A. M. Al-Zubaidi***
Address: Head of the Environmental Engineering Department
Date: / 1 / 2022

Approved by the Deanery of the College of Engineering.

Signature:
Name: ***Prof. Dr. Hatem Hadi Obeid Al-Taei***
Address: Dean of College of Engineering
Date: / 1 /2022

ACKNOWLEDGEMENTS

"In the Name of Allah, the Most Gracious, the Most Merciful"

Praise to Allah his Majesty before anything and after anything and to the prophet “Mohammed and Ahl-Al-Bait” for the strength, courage, and wisdom that Allah gave me to complete this humble work and lengthy journey this degree.

I would like to express my deepest gratitude and respect to my thesis supervisor Asst. Prof. Dr. Isra’a Sadi Abdul-Amir Samaka. I am very grateful for her precious time spent and useful suggestions which provided valuable guidance and important role in the completion of thesis as well as the moral support continued for the duration of the search, calling God richly rewarded him.

I would like to thanks to President of Environmental Engineering Department Asst. Prof. Dr. Hussein Ali Al-Zubaidi. For his help and he never saved an effort to help us and others.

I would also like to thank the staff of Environmental Engineering laboratory at the University of Babylon for their assistance in providing laboratory equipment's through this work.

I wish to express my deepest respect and sincere appreciation to my family especially my father and mother for their support and help during my study.

Also, I would like to thank all those who helped me in one way or another especially my husband mohammed

Maali

2022

Abstract

The capacity of activated carbon derived from naturally occurring plants (Schanginia/sp, SAC) as low cost a biosorbent for methylene blue dye (MBD) removal from wastewater is investigated in this work. In order to assess the potential treatment of industrial aqueous solutions by SAC, a series of laboratory batch and continuous flow experiments were conducted. Before and after MBD removal, a variety of techniques were used to conduct the characterization analysis. Surface area (S_{BET}), FTIR, SEM, and SPM are some of the techniques available. Batch tests were conducted to study different parameters affecting MBD biosorption at room temperature such as pH dye solution, contact time, biosorbent dosage, and initial dye concentration. pH of 9 and dosage of 0.8 g/100 ml dye solution,75 min. contact time for MBD concentration of 50 mg/l, and agitation speed of 250 rpm were found to be optimized conditions for the MBD removal by SAC. The experimental data was analyzed using Langmuir and Freundlich isotherm models. The Langmuir biosorption isotherm was found to be the best model for simulation of MBD bisorption into SAC, with the Langmuir constant linked to the biosorption ability (q_{max}) of 33.34 mg/g and a coefficient of determination (R^2) of 0.9954. The Pseudo-second order model was very well simulated the kinetic experimental data and the biosorption rate parameters values indicating the removal process of MBD onto SAC was chemisorption including the intraparticle diffusion process. A continuous adsorption fixed bed of SAC biosorbent was utilized for the MBD removal from the aqueous solutions at room temperature (25±5°C) to study effects of the flow rate, bed height, and dye concentrations upon removal efficiency. It was noticed that the removal percentage increases with the bed height increasing and decreases as the flow rate increases and increasing of

MBD concentration . The adsorption capacity increases with increasing bed height and concentration and decreases with increasing flow rate. The obtained column data was analyzed and showed that the breakthrough curves were powerfully influenced by those factors. The Bed Depth Service Time (BDST), Thomas, and Yoon–Nelson kinetic models were used to analyze the experimental column data. All applied kinetic models were well described the breakthrough curves with high values of R^2 and the deviation between experimental and estimated value for kinetic parameter was very low. The results indicate that SAC can be used for effectively remove of methylene blue dye from aqueous solutions.

Table of Contents

Content No.	Title	Page No
	Acknowledgement	I
	Abstract	II
	Table of Contents	IV
	List of Tables	VI
	List of Figures	VII
	List of Nomenclature	IX
	List of Abbreviations	XI
Chapter One: Introduction		
1.1	Introduction	1
1.2	Statement of the problem	3
1.3	Research Objectives	4
1.4	Thesis description	5
Chapter Two: Literature Review and Theoretical Concepts		
2.1	Introduction	6
2.2	Environmental and health risks of dyes	6
2.3	Adsorption process	9
2.4	Types of adsorption	11
2.5	Adsorbent materials in treatment wastewater	13
2.6	Activated carbon	15
2.6.1	Agricultural waste based activated carbon	18
2.6.2	Carbonization	20
2.7	Agricultural solid wastes	21
2.8	Mechanism of adsorption	22
2.9	Process factors affecting dye adsorption	24
2.9.1	pH of the solution has an impact	24
2.9.2	The Impact of contact time	25
2.9.3	Adsorbent dosage impact	25
2.9.4	Initial adsorbate concentration impact	26
2.10	Point zero charge of adsorbent determination	27
2.11	Isotherm study	27
2.11.1	Langmuir isotherm	27
2.11.2	Freundlich isotherm	28
2.12	Kinetic study	29
2.12.1	Lagergren pseudo-first-order model	30
2.12.2	Pseudo-second-order model	30
2.12.3	Intra-particle diffusion model	31
2.13	Fixed-bed adsorption column data analysis	31
2.13.1	Process parameter for column study	35
2.13.2	Adsorption models for column study	37
2.13.2.1	The Bed Depth-Service Time model (BDST)	37
2.13.2.2	Thomas model	39
2.13.2.3	Yoon-Nelson model	40
2.14	Previous studies of batch biosorption technique, using agricultural residues as biosorbents to remove dye	41
2.15	Summary	51
Chapter Three: Experimental Work and Procedures		

3.1	Introduction	53
3.2	Materials and methods	55
3.2.1	Adsorbate	55
3.2.2	Biosorbent (SAC) preparation	56
3.3	Characterization techniques of biosorbent	57
3.3.1	Characterization of particular surface region	57
3.3.2	FTIR spectra	57
3.3.3	Scanning electronic microscopy(SEM)	58
3.3.4	Atomic force microscope (AFM)	58
3.4	Experimental methods	58
3.4.1	Batch study	59
3.4.2	Procedure and experimental setup for dynamic biosorption studies	61
Chapter Four: Results and Discussion		
4.1	Introduction	64
4.2	Characterization works	65
4.2.1	Biosorbent physiochemical characterization	65
4.2.2	FTIR spectroscopy of SAC biosorbent	66
4.2.3	Scanning electron microscopy (SEM) of biosorbent	70
4.2.4	Scanning probe microscope (SPM)	73
4.3	The effect of various factors	75
4.3.1	Effect of solution pH	75
4.3.2	Impact of contact time	78
4.3.3	Impact of biosorbent dosage	80
4.3.4	Impact of primary MBD concentration	81
4.4	Isotherm analysis	82
4.5	Adsorption kinetics studies	87
4.6	Study of Mechanism	93
4.7	Experiments of continuous flow (Column test)	96
4.7.1	The impact of flow rate on MBD biosorption	96
4.7.2	Impact of bed height of biosorbent on breakthrough curves	98
4.7.3	Impact of initial MBD concentration on breakthrough curves	99
4.8	Dynamic modeling of a SAC fixed-bed biosorption column	101
4.8.1	The BDST (Bed Depth Service Time) model application	101
4.8.2	Thomas dynamic model of application	105
4.8.3	Application of Yoon-Nelson dynamic model	108
Chapter Five: Conclusions and Recommendations		
5.1	Conclusions	111
5.1.1	Batch experiments mode	111
5.1.2	Continuous flow mode	112
5.1.3	Recommendations for future researchs	113
References		114
Abstract in Arabic		1

List of Tables

Table No.	Description	Page
Table 2-1	The advantages and disadvantages of various decolorization techniques.	8
Table 2-2	Difference between physical and chemical adsorption	13
Table 2-3	Research studies on dye adsorption utilizing adsorbents made from agricultural waste.	22
Table 2-4	Effect of process parameter on breakthrough and exhaustion point	36
Table 3-1	Physical and Chemical Properties of MBD	56
Table 3-2	The main different parameters used in batch experiments	60
Table 3-3	The main parameters used in continuous experiments	62
Table 4-1	Elemental analysis (%W/W) of SAC using EDS spectrum.	65
Table 4-2	Physiochemical properties of SAC.	65
Table 4-3	FTIR analysis for SAC before and after MBD biosorption.	69
Table 4-4	SAC characteristics before and after biosorption of MBD by SPM technique.	75
Table 4-5	Constants of biosorption isotherm for MBD using SAC.	86
Table 4-6	Comparison of maximum adsorption capacity (q_{max}) of SAC with other adsorbents reported for the removal of MBD	86
Table 4-7	Kinetic parameters of various models fitted to MBD biosorption experimental data using SAC.	93
Table 4-8	Multi-linearity parameters of intraparticle model based biosorption mechanism study of MBD onto SAC.	95
Table 4-9	Experimental data analysis for biosorption of MBD onto SAC in a fixed-bed column mode at different operating conditions and breakthrough point of C/C_o was 0.05.	98
Table 4-10	Estimated BDST model parameters at different bed depth height with Q =10 ml/min and C_o =25 mg/l for MBD biosorption onto SAC column.	104
Table 4-11	Comparison between $t_{cal.}$ & $t_{exp.}$ for MBD biosorption onto SAC at different breakthrough point (C/C_o) using estimated BDST model parameters at different bed depth height with Q =10 ml/min and C_o= 25 mg/l for column.	104
Table 4-12	Kinetic models parameters for biosorption of MBD onto SAC fixed bed column at different feed flow rate and bed height.	108

Table of Figures

Figure No.	Description	Page
Fig. 2-1	Basic process of adsorption.	11
Fig. 2-2	Activated carbon comes in different of forms. Illustration of a typical adsorption process. Adapted with permission.	17
Fig. 2-3	Different pore structures of activated carbon.	18
Fig. 2-4	Illustration of a typical adsorption process. Adapted with permission	23
Fig. 2-5	Ideal breakthrough curve.	33
Fig. 2-6	Representation of mass transfer zone movement and formation of breakthrough curve.	35
Fig. 3-1	Flow chart of adsorption process for MBD	54
Fig. 3-2	Structural formulas of Methylene blue (MB)	55
Fig. 3-3	MBD powder used in this study	55
Fig. 3-4	The natural plant and produced activated carbon: Natural plant (b) Prepared SAC.	57
Fig. 3-5	UV Spectrophotometer used in the work	59
Fig. 3-6	Laboratory arrangement of a fixed-bed column structure for MBD biosorption experiments.	62
Fig. 3-7	The schematic of the fixed-bed column structure used in dynamic biosorption experimental investigates.	63
Fig. 4-1	FTIR spectra of SAC (a) before MBD biosorption and (b) after MBD biosorption.	68
Fig. 4-2	The SEM micrograph images of SAC at different magnifications: (a) before MBD biosorption.	71
Fig. 4-2	The SEM micrograph images of SAC at different magnifications: (b) after MBD biosorption.	72
Fig. 4-3	Scanning probe microscope for SAC: (a) before MBD biosorption.	74
Fig. 4-3	Scanning probe microscope for SAC: (b) after MBD biosorption.	74
Fig. 4-4	Impact of initial pH as a function of contact time at different pH on the biosorption of MBD onto SAC.	76
Fig. 4-5	Effect of initial solution pH on the removal efficiency of MBD onto SAC	77
Fig. 4-6	Determination of point zero charge (pH_{pzc}) of SAC.	78
Fig. 4-7	Effect of contact time on the uptake (mg/g) and percentage removal of MBD onto SAC.	79
Fig. 4-8	Percentage removal and uptake of MBD ions in terms of biosorbent dose	81
Fig. 4-9	Percentage removal and uptake of MBD ions as a function of MBD concentration	82
Fig. 4-10	Linearized adsorption isotherm model of MBD onto SAC (a) Langmuir model (b) Freundlich model.	84
Fig. 4-11	Values of Separation Factor, R_L for Biosorption of MBD onto SAC.	85
Fig. 4-12	Comparison of experimental and calculated data	85

	by Langmuir and Freundlich.	
Fig. 4-13	The change of amount biosorbed (mg/g) at various times and initial MBD concentrations.	87
Fig. 4-14	Pseudo -first-order kinetic plots for sorption of MB dye onto SAC at different initial dye concentrations.	89
Fig. 4-15	Pseudo second-order kinetic plots for sorption of MB dye onto SAC at different initial dye concentrations.	91
Fig. 4-16	Linear intraparticle diffusion kinetic model of MBD onto SAC biosorbent at different dye concentrations.	92
Fig. 4-17	Multi- linearity graph of intraparticle diffusion model of MBD onto biosorbent at different dye concentrations.	95
Fig. 4-18	Breakthrough curves for MBD biosorption at different flow rates.	97
Fig. 4-19	Breakthrough curves for MBD biosorption at different column bed heights, where the initial MBD concentration = 25 mg/l, the flow rate = 10 ml/min, the solution pH 9, at ambient temperature.	99
Fig. 4-20	Breakthrough curves for MBD biosorption at different initial MBD concentrations when the bed height = 15 cm, the flow rate = 10 ml/min, the solution pH 9, at ambient temperature.	100
Fig. 4-21	BDST model plot at different values of C/C_o in fixed-bed column for MBD biosorption onto SAC (C_o =25 mg/l, flow rate =10 ml/min).	103
Fig. 4-22	Thomas kinetic plots for adsorption of MBD under various effect flow rate (Co=25 mg/l, H=15 cm, pH 9).	106
Fig. 4-23	Thomas kinetic plots for adsorption of MBD under various effect bed depth (Q =10 ml/min, C_o= 25 mg/l).	107
Fig. 4-24	Yoon-Nelson kinetics plots for the adsorption of MBD on SAC under different flow rate effect (C_o = 25 mg/l, H =15 cm, pH 9).	109
Fig 4-25	Yoon-Nelson kinetics plots for the adsorption of MBD on SAC under different effect of bed depth (C_o = 25 mg/l, Q = 5 ml/min, pH 9).	110

List of Nomenclature

Symbol	Description	Units
A	Cross section area of the column	m^2
C	Intraparticle Diffusion constant	mg/g
C_{ads}	Adsorbed concentration of dye onto biosorbent	mg/g
C_b	Breakthrough point concentration of dye	mg/l
C_e	concentration of dye at equilibrium	mg/l
C_o	Initial concentration of dye	mg/l
K_1	Pseudo-first-order rate constant	min^{-1}
K_2	Pseudo-second-order rate constant	$g.mg^{-1}.min^{-1}$
K_a	Langmuir biosorption equilibrium constant.	1/mg
K_B	Biosorption rate constant	1/mg.min
K_F	Freundlich constant related to relative biosorption capacity of biosorbent	$(mg/g)(1/mg)^{1/n}$
K_{ip}	Intraparticle Diffusion rate constant	$mg.g^{-1}.min^{-1/2}$
K_{TH}	Thomas rate constant	1/min.mg
K_{YN}	Yoon-Nelson rate constant	min^{-1}
m_{total}	Total amount of dye inter the column	mg
N	Freundlich constant related to intensity	---------
q_B	Dynamic breakthrough biosorption capacity per unit volume of biosorbent bed	mg/l
q_e	Amount of dye ions adsorbed per unit mass of biosorbent at equilibrium	mg/g
q_{exp}	Experimental uptake or maximum capacity of the column	mg/g
q_m	maximum biosorption capacity	mg/g
q_t	Amount of dye ions adsorbed per unit mass of biosorbent at time t	mg/g
q_{TH}	maximum biosorption per unit weight of biosorbent	mg/g
q_{total}	Total quantity of dye ions adsorbed in column bed for a given inlet dye ions concentration and flow rate	mg
Q_V	Volumetric feed flow rate	ml/min
R%	The percentage of dye removal	--------
R_L	Separation factor	----------
t_b	Time needed at which the biosorption column reaches the breakthrough point with specific saturation percentage	min
t_e	Time needed to exhaust the bed of column	min
V	Volume of solution	L
U_f	Linear flow velocity	cm/min
V_b	Volume of effluent at breakthrough point	ml
V_{eff}	Volume of effluent at exhaustion	ml
w , m	Mass of biosorbent in batch and column system respectively	g
H	Bed depth of column	cm

Z_c	Critical bed depth	cm
S_c	The column sectional area	cm^2

List of Abbreviations

Abbreviation	Description
SAC	(Schanginia/sp) activated carbon
BET	Brunauer, Emmet and Teller
SEM	Scanning Electron Microscopy
SPM	Scanning Probe Microscope
FTIR	Fourier-Transformed Infrared Radiation
EDS	Energy-Dispersive Spectroscopy
IR	Impregnation Ratio
MBD	Methylene blue dye
MTZ	Mass Transfer Zone
pH_{pzc}	The point of zero charge
R^2	Liner correlation coefficient
Rpm	Revolution per minute
S_{BET}	Specific surface area determined by BET method
S.E	The Standard error of the estimate
ΔH	Heat content
AC	Activated carbon
IUPAC	International Union of Pure and Applied Chemistry
AR	Acid red
MLP	Mango leaves powder
ASS	Annona squmosa seeds
MG	Malachite green
RSM	Reaction surface methodology
CTDLP	chemically treated durian leaf powder
BDST	Bed-depth service time
SPSS	Statistial Package for the Social Sciences
t_{cal}	Calculated time
t_{exp}	Experimental time
R_L	Separation factor
AFM	Atomic Force Microscopy
JLP	jackfruit leaf powder
GNSP	groundnut shell powder
SCW	sugar cane waste
IBSAC	Intsia bijuga sawdust based activated carbon
DP	durian husk
MSH	macadamia seed husks
λ_{max}	The maximum wave length
τ	The time required for 50% adsorbate breakthrough (min)

Chapter One
Introduction

Chapter One

Introduction

1.1 Introduction

In recent decades, urban and industrial activities have greatly contributed to environmental pollution, which has become a serious problem that must be solved or at the very least mitigated. Because of their high polluting ability, the discharge of synthetic dyes in industrial effluents is a major source of concern (Sen et al., 2016). The presence of dyes in the environment causes serious risks, since they hinder the incidence of solar radiation, damaging the development of the existing biota (Naskar and Majumder, 2017). Meanwhile, coloured wastewater is complex in nature, most of which is toxic, mutagenic and carcinogenic to aquatic organisms, causing some health problems based on the problems, several technologies, including flotation (Rubio et al., 2002), aerobic and anaerobic treatment (Seshadri et al., 1994), micro-and ultra-filtration (Choo et al., 2008), ion exchange (Wu et al., 2008), microbial electrochemical technologies (Chen et al., 2019), oxidation (Karthikeyan et al., 2012 ; Chen et al., 2019 a) and adsorption, have been employed for wastewater treatment (Fuat, 2015; Wang et al., 2018; Ait et al., 2018; Enniya et al., 2018; Benkaddour et al., 2018). Among these methods, adsorption has received extensive attention since it is easier, cheaper, more efficient and economical than others. Thus, different adsorbents have been developed and applied to neutralize dyes and other organics in wastewater. The technique is increasingly gaining ground as a competitive, effective and low-cost approach that is more selective than traditional ion-exchange resins and commercial activated carbons (Rafatullah et al., 2010). The economic viability of adsorption depends on the adsorbent option. Because of its wide surface area (up to3000 $m^2.g^{-1}$),

high porosity and high adsorbent potential for a number of contaminants, activated carbon has been more frequently used as a traditional adsorbent (Mahamadi and Mawere, 2019). However, the high cost of activated carbon processing limits its economic viability. In first usage, activated carbon is also depleted and needs to be reactivated, resulting in a (10 - 15 %) loss of the adsorbent. In recent years, the search for reliable and low cost adsorbents have increased significantly. For this purpose, agricultural wastes have a high potential for the removal of various pollutants (Shayesteh et al., 2016; Mohebali et al., 2019). Besides, they are low-cost, available in abundance around the world, renewable resources, environmentally friendly, and easy to regenerate (Zhou et al., 2015). A literature survey has shown that researchers have produced and used a wide range of low-cost adsorbents to extract dyes. Some of the biomass that have been employed for dyes treatments include; fly ash (Mall et al., 2005), coconut shell (Mane et al., 2007), cashew nut shell (Senthil Kumar et al., 2010), rice hulls (El-Maghraby et al., 2011), banana stalk (Bello et al., 2012), orange peels (Mafra et al., 2013), rice husks (Rahman et al., 2012) and maize stem tissue (Vučurović et al,. 2014). Most of these materials have high adsorptive potential for colores due to their composition, which includes cellulose, hemicellulose and lignin, as well as lipids, proteins, enzymes and hydrocarbons (Rangabhashiyam, 2013). Adsorption processes for decontamination of wastewaters can be carried in batch reactors and fixed-bed columns especially in the liquid process (Volesky, 2001; Crini, 2003; Ali, 2014). Batch experiments provide useful information on the best operating conditions for obtaining full dye adsorption, which is critical for fixed-bed works (Ali, 2014). The sorbate is continuously in contact with a given mass sorbent in a continuous method, resulting in the necessary concentration gradients between adsorbent and adsorbate for adsorption. This mode is simple to use and

handle (Aut and Hameed, 2014; Crini et al ., 2018). The breakthrough curves shape and velocity in the bed are established in the design and theory of this mode. The theory of breakthrough curves and bed volumes is used to evaluate this mode (Cheng and Wang, 2000). As a result, the direct application of wastewater treatment on an industrial basis is solely based on fixed-bed studies, which provide readily available support data for application.

1.2 Statement of the problem

The contamination of water resources is one of the extremely contested agenda from a global point, as it causes a severe long-term or even lethal effect on living organisms (Inamuddin, 2018). Water pollution caused by dyes is great apprehension because they elicit changes in the natural appearance of water even at very low concentrations. Untreated effluents from the textile industry are posing a serious threat to the sustainability of aquatic ecosystems as well as to human health (Dod et al ., 2012). The dyes, an important class of pollutants, are the compounds which are organic in nature and present in the industrial effluents. The presence of the dyes in the water ways is easily detectable even when released in small concentrations (Hassan et al., 2013). A variety of techniques have increasingly been used to remove toxic dyes from waste effluents in order to reduce environmental damage and increase water quality (Almeida et al., 2014; Danwittayakul et al., 2015). A mong those techniques, adsorption has been used. However, reported to be ease, rapidity, reliability, low expense, and availability of low-cost adsorbents, adsorption is the most favored approach for wastewater treatment (Prola et al., 2013; Adebayo et al., 2014). Activated carbon have been commonly used for the treatment of industrial wastewater (Calvete et al., 2010; Fernandez et al., 2014; Pezoti et al., 2014). Attention has been

shifted to the usage of eco-friendly and low-cost materials (Pavan et al., 2014). These materials possess high carbon content. They are obtainable from variety of agricultural by-products that are cheap, abundant, and nontoxic (Prola et al., 2013). As a result, since the biomass used in the adsorption phase does not alter the properties or interfere with other chemicals in the wastewater, it is called green technology.

In this study, Schanginia/sp based activated carbon was used as biosorbent for color biosorption.

1.3 The objectives of the study

The goals of the study are as follows:

1- Explore the capacity of prepared activated carbon natural plant biosorbent in batch and fixed-bed biosorption column to remove methylene blue dye from aqueous solutions.

2- Examine the impact of different variables on biosorbent capability, such as dye solution pH, contact time, biosorbent dosage, and initial dye concentration.

3- Assess the biosorption isotherm and kinetics to evaluate the function of biosorption and to demonstrate the form and steps that regulate this operation.

4- Analyze the behavior of fixed bed column by studying the effect of the flow rate, initial dye concentration, and bed height.

5- Simulation of experimental column results utilizing various kinetic models to forecast and analyze breakthrough curve behaviour, and then determining which model best fits the data.

1.4 Thesis description

The structure of the present work is as follows:

Chapter One: Introduces general information of adsorption, MBD.

Chapter Two: Reviews the literature relevant to the present study and related to the scope of the present investigation and illustrates the theoretical aspects of adsorption process, adsorbate, biosorbent and different models.

Chapter Three: shows the experimental work and all the laboratory tests.

Chapter Four: Discusses the results of the experimental work.

Chapter Five: Illustrates the conclusions drawn from the study present and recommendations for future works.

Chapter Two
Literature Review and Theoretical Concepts

Chapter Two

Literature Review and Theoretical Concepts

2.1 Introduction

Removal of dyes from industrial wastewater is a major concern because to the features of these dyes, namely that they are non-degradable and consequently persistent. Furthermore, the majority of contaminants are hazardous to living creatures and have a significant impact on photosynthetic activity in aquatic biota. To comply with environmental regulations, harmful substances should be eliminated from wastewater (Abdelkarim et al., 2017)

A low-cost and environment-friendly substitute approach is taken to determining the adsorption capacity of activated carbon in this thesis (Razi et al., 2017).

2.2 Environmental and health risks of dyes

The most important risks and damages that dyes cause to living organisms are as follows (Nirmal et al., 2019).

1. The absorption and reflection of sunlight into the water is the most significant environmental problem for colors. The photosynthesis activity of algae is reduced by light absorption, which has a significant effect on the food chain.
2. Pigments are carcinogenic, mutagenic, and life-threatening colorants that are primarily transported into the environment through industrial wastewater.
3. Triple primary tumors of the kidney, bladder, and liver have been detected by dye workers.

4. Textile dyes can cause allergies such as contact dermatitis and other diseases, allergic reaction in eyes, skin irritation to mucous membrane and the upper respiratory tract.

5. Reactive dyes form covalent bond with cellulose, woollen and poly amide fibres. Certain reactive dyes have caused respiratory sensitisation of workers occupationally exposed to them.

6. The presence of very small amounts of dyes in the water, which are nevertheless highly visible, seriously affects the quality and transparency of water bodies like lakes, rivers and others, leading to damage to the aquatic environment.

7. The highly toxic and mutagenic dyes decrease light penetration and photosynthesis activity, causing oxygen deficiency and limiting downstream beneficial uses such as recreation, drinking water and irrigation.

Since even a small amount of pigment in water can be toxic and visible, removing color from waste effluents is important for the environment. Since dye removal from wastewater is viewed as an environmental problem, and government regulations require the treatment of colourd wastewater, there is a persistent need for a reliable process that can efficiently remove dyes.

In spite of the availability of many techniques to remove these pollutants from wastewater, such as coagulation, chemical oxidation, membrane separation process, electrochemical and aerobic and anaerobic microbial degradation, these methods are not very successfully due to suffering from many restrictions (Sulyman et al., 2016). Table (2.1) shows the advantages and disadvantages of different dye removal methods.

Table (2.1): The advantages and disadvantages of various decolorization techniques (Robinson et al., 2001).

Technologies	Advantages	Disadvantages
Chemical technologies (Adegoke and Bell, 2015)		
Oxidative process	Simplicity of application	Some means of activating the (H_2O_2) agent is needed
Ozonation	Ozone can be applied in its gaseous state and does not increase the volume of wastewater and sludge	Half-life short (20 min)
Photochemical	No sludge is produced and foul odors are produced	By-products are formed
Sodiumhypochlorite (NaOCl)	Initiates and accelerates the cleavage of azo bonds.	Aromatic amines are released
Electrochemical destruction	There will be no chemical consumption and no sludge build-up	High flow rates result in a direct reduction in dye removal
Fenton's reagent	A appropriate chemical means is Fentons reagent	Generation of sludge
Physical technologies (Adegoke and Bell, 2015)		
Membrane filtration	Removes all kinds of dyes	Production of concentrated sludge
Ion exchange	There is no adsorbent loss during regeneration	Not effective for all dyes
Irradiation	At the laboratory scale, effective oxidation is possible	It necessitates a large amount of dissolved oxygen
Electro-kinetic coagulation	It's economically feasible	Sludge generation is high
Biological technologies (Sivarajasekar and Baskar, 2015)		
Decolorization by white rot fungi	Enzymes are used by white-rot fungi to degrade dyes	The production of enzymes has also shown to be inefficient
Other microbial cultures (mixed bacterial)	Decolorized in 24-30 h	Under aerobic conditions cationic dyes are not readily metabolized
Adsorption by living/dead microbial biomass	Certain dyes have a particular affinity for binding with microbial species	For all dyes, it is ineffective
Anaerobic textile – dye bioremediation systems	Allows the decolorization of azo and other water-soluble dyes	Methane and hydrogen sulfide are generated during anaerobic breakdown

2.3 Adsorption process

The aggregation of atoms, molecules, or ions at the surface of a solid phase is known as adsorption. It is a mass transfer mechanism in which gases or solutes are absorbed by solid or liquid surfaces (Crawford and Quinn, 2017). It's a physical or chemical relation formed by the forming of chemical bonds with effective surface sites in the active material molecules of surface sites through the weak Vander Waals force. The absorption of dissolved solids from a stable surface of a solution or liquid, as well as the retrieval of dissolved solvents from the surface, are common examples of adsorption. This method results in an adsorbate layer on the adsorbent surface. Adsorption on the atom's surface can be limited to the creation of a single molecular coating. As a result, the process is known as unimolecular adsorption. Adsorption necessitates the formation of many molecular layers on the mass's surface. The mechanism is then referred to as multimolecular adsorption (Mhemeed, 2018).

Adsorption techniques have been widely used in the removal of dyes using different adsorbents. These adsorbents include activated charcoal, natural or synthetic zeolites, natural clay crystals, silica gel and activated aluminum, biomass, and silicic acid. However, there are certain restrictions on how these material can be used.

The problems that arise as a result of using these adsorbents are as follows: Any of the adsorbents are too expensive, ineffective, or in short supply. Adsorption methods based on biomass is continuously used as biomass, resulting in low-cost but effective adsorption (Fauzi, 2015).

An economic adsorbent is one that is available in nature or is a by-product of manufacturing and requires little refining. Many analysts have

found low-cost and effective alternatives, such as scrap metals and coconut husks (Tan et al., 2008).

Figure (2.1) illustrates the basic concepts of adsorption theory. The adsorbent is the rigid substance that acts as the adsorption surface; the adsorbate is the species that would be adsorbed (Worch, 2012). It is induced by the species attraction to the solid surface, or by interactions between the solid and gaseous phases of one or more species present in the liquid and solid phases (Sun and Zhang, 2020).

Adsorption has been found to be superior to other strategies for water reuse. Adsorption does not produce any toxic compounds (Nirmal et al., 2019).

Biosorption is a process of attaching pollutants from aqueous solutions to functional groups present on the biomass surface in a rapid and it has been used as a biosorbent for the desired removal of contaminants by a wide range of biomaterials found in nature (Michalak et al., 2013). Biosorption procedures, in general, can reduce capital costs and total treatment costs significantly as compared to conventional schemes (Abdolali et al., 2014).

The relationship between adsorbate and adsorbent, surface region, adsorbent to adsorbate ratio, particle size, pH, and contact time are all factors that influence adsorption performance.

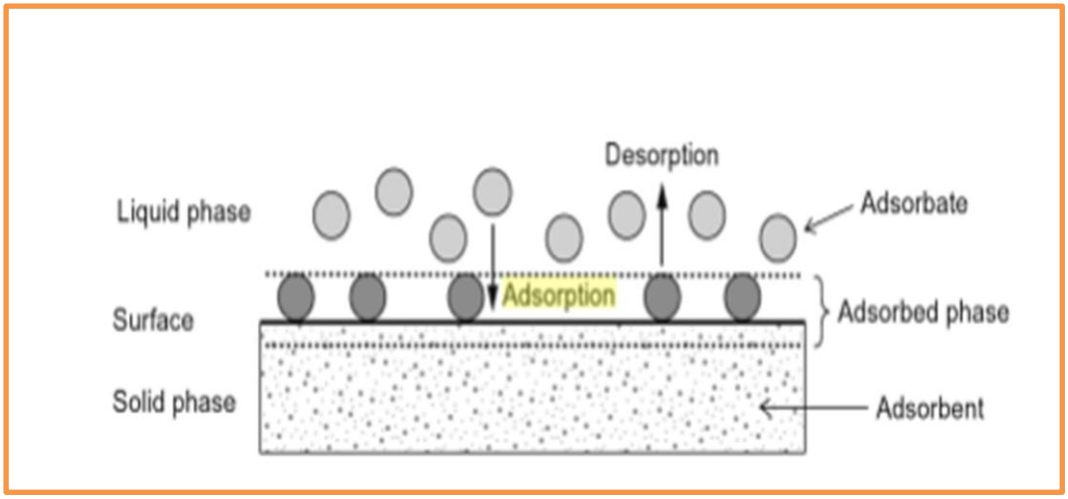

Fig. (2.1): Basic process of adsorption (Worch, 2012).

2.4 Types of adsorption

2.4.1 Physical adsorption

Physical adsorption: When a gas (adsorbate) comes into contact with a rigid surface, physisorption (physical adsorption) occurs (the adsorbent). The adsorbate is the matter in the adsorbed state, as opposed to the adsorptive, which is the gas or vapor that is to be adsorbed. The attraction between adsorbent and adsorbate molecules is caused by van der Waals and electrostatic forces in physical adsorption. Adsorption is an exothermic and reversible process (Bessegato et al., 2015). This mutual forces are caused by nonspecific molecular interactions. Complex interactions occur as polar molecules are adsorbed on ionic or polar surfaces, but the phenomenon is also referred to as physisorption as long as there is no chemical bonding. Physical adsorption mechanisms in porous materials influence the interplay between the strength of fluid-wall and fluid interactions, as well as the effect of restricted pore space on

the environment and thermodynamic equilibrium of fluids confined to narrow pores (Thommes, 2010).

2.4.2 Chemical adsorption

Chemical adsorption, also known as chemisorption, is the second type of adsorption. This sort of hydrogen bond is formed between the surface and the atoms, molecules, or ions that adsorb on it. Chemical adsorption is distinguished by privacy (specific) when it occurs under such circumstances, and adsorption may not occur on another surface under the same conditions or on the surface itself as the ambient conditions change. For a higher heat emission than that produced by physical adsorption, the heat emitted as natural chemical bonds are formed growing be reached. Energizing energy is needed for chemical adsorption (Activation energy). Adsorption occurs quickly and at a low rate, and the reaction is always irreversible and involves close chemical bonds. It also has a specific position (localized) when it is carried out on low-energy adsorption sites. The adsorbent energy requires chemical adsorption to a constant activation energy relative to the homogeneous surface and variable in relation to the heterogeneous surface. Chemical adsorption is described as a single layer of adsorption on the adsorbent's surface (Mhemeed, 2018). Chemical adsorption normally only results in monolayer coverage and is a site-dependent reaction that occurs at specific functional group locations (Najim, 2018). Since the adsorbate forms tight localized bonds at activate centers on the adsorbent, chemisorption has high adsorption energies. Molecules are not considered able to travel on the surface or inside the interface in this situation (Tabrez and Ved, 2010). The following Table (2.2) shows the difference between physical and chemical adsorption.

Table (2.2): Difference between physical and chemical adsorption (Hu and Xu, 2020).

	Physical adsorption	**Chemical adsorption**
Adsorption force	Van der Waals force	Chemical bond force
Selectivity	Nonselective adsorption	Selective adsorption
Adsorption layer	Single or multiple layers	Single layer
Adsorption heat	Low	High
Adsorption rate	Fast	Slow
Stability	Instable	Stable

2.5 Adsorbent materials in wastewater treatment

Via study of adsorption equilibrium and kinetics, adsorbent may be used to describe the changes between molecules in a mixture (Murali et al., 2016). Adsorption was found to be the most efficient way of extracting dyes from aqueous solutions among the techniques. This is done with porous synthetic adsorbents (activated carbons, ion exchange resins, zeolites, silicates, and so on), but natural adsorbents like montmorillonites and smectites can also be used. In the case of adsorption of gases, the most common way of regeneration (desorption) is to increase the temperature while simultaneously lowering the pressure, or to wash the adsorbent bed with solvent in the case of adsorption from liquid solutions.

Desorption usually does not result in a return to the initial sorption potential, and the sorbent is absorbed over time. Due to the high cost of

synthetic adsorbents and the difficulty of regenerating used sorbents, researchers are turning to exotic adsorbents, such as effective and cheap raw, waste materials, biosorbents, and waste materials from industry or agriculture treatment (Orzechowska-Ziba et al., 2019).

Several researchers have sought numerous adsorbents for the elimination of organic compounds from wastewater in recent years, including wheat husk, sugarcane bagasse (Baruah et al., 2016), reverse micelles (Kodal and Aksu, 2017), industrial wastes (Ramrakhiani et al., 2017), apple pomace and wheat straw (Gunturu et al., 2018), industrial agricultural wastes, and various other adsorbents (Mittal et al., 2014). The aim of using waste materials as adsorbents is to have a two-fold benefit in terms of emission reduction.

First, the amount of waste materials could be minimized in portion, and second, if created, a low-cost adsorbent could mitigate wastewater emissions at a fair cost (Bhatnagar and Jain, 2005). The adsorbent must either be discarded or regenerated after it has been filled. The majority of the treatment costs for adsorption water treatment are correlated with regeneration, according to an analysis of the entire life costs (Gupta and Ali, 2012). Despite this, most adsorption research has focused on the production of high-capacity adsorbents, with only a few studies focusing on the development of regenerative adsorbents (Hynes et al., 2020).

The amount of adsorption is determined by the adsorbent nature, including its porosity and surface area. As a result, a variety of adsorbents with better and often selective adsorption have been created. A key feature of better adsorbents is their high porosity, which results in a greater surface area and more specific adsorption sites. The majority of adsorbents used in contamination control have a porous surface. The

porous composition increases not only surface area and, as a result, adsorption, but also the kinetics of adsorption. A larger surface area adsorbent that takes less time to reach adsorption equilibrium is a good adsorbent (Al- Husseiny, 2014).

2.6 Activated carbon

Activated carbon (AC) has been the greatest commonly used, preferred adsorbent for purification effluent due towards its enormous surface area and great rapprochement for color particles (Kaveeshwar et al., 2018). AC is an a porous, amorphous solid with a graphitelattice made up of microcrystallites. There are two stages to the development of activated carbon. Activated carbon is made from a carbon rich precursor by removing much of the volatile non-carbon elements and a small portion of the initial carbon content through thermal or chemical methods (Mopoung et al., 2015 ; Ani et al., 2020).

Carbonisation is the process of converting a carbon-rich piece of substance to pure carbon by heating, which is known as pyrolysis. Since the final result would be extra-porous for activated carbon purposes, very thick carbonaceous content is used at first. The carbonised particles are then activated in the second stage by introducing the AC to an oxidizing agent at a high temperature. During the carbonisation phase, this triggering agent burns away the structures that obstruct the surface pores (Lee et al., 2014).

Activated carbon comes in a variety of ways. Granular activated carbon (GAC), powdered activated carbon (PAC), and woven carbon or activated carbon cloth (ACC). The three types of treatment are used to remove various types of contaminants from water and wastewater. To conform with strict requirements for effluent discharged to receiving

sewage, activated carbon adsorption is often used in industrial wastewater treatment plants. As a separate unit operation, activated carbon adsorption may be used (Bansal and Goyal, 2005). Coagulation/clarification, filtration, and dissolved air flotation are some of the physiochemical treatment measures that it can be installed after. Prior to biological treatment, activated carbon adsorption is another method (Cecen and Aktas, 2011).

Liquid phase applications, gas phase applications, air emissions control manufacturing, electrodes and batteries are activated carbon applications. Activated carbon is used to handle industrial wastewaters in liquid process systems, such as textile processing wastewater. The broad porous surface area and controllable pore structure of activated carbon render it good for wastewater treatment. Because of the reactions that exist between the adsorbate and the adsorbent, activated carbon porosity enables dye uptake in this application, the chemical properties of dye and activated carbon are essential (Inam et al., 2016).

Figure (2.2) depicted the various types of activated carbon. The finely divided powdered shape of activated carbon has large pore diameters and a smaller internal surface region, whereas the granular form has a greater internal surface area and smaller pores. activated carbon fibres have a higher surface area and cover a greater number of larger pores (Bansal and Goyal, 2005).

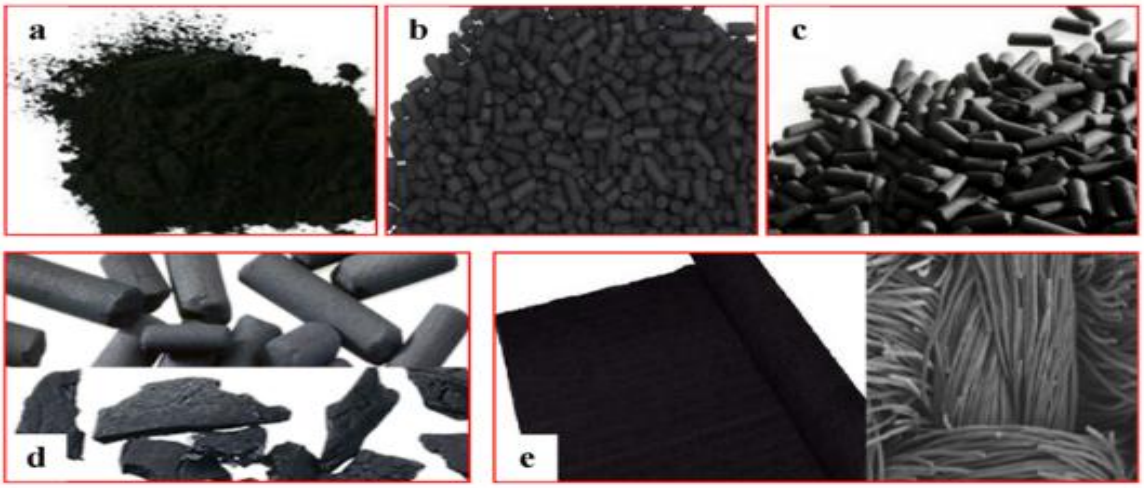

Fig. (2.2): Activated carbon of forms:

(a) powdered activated carbon (b) activated carbon granules (c) activated carbon that has been extruded (d) activated carbon impregnated (e) fabric activated carbon (Mosbah et al., 2020).

as well as surface reactivity, which has been the primary explanation for the widespread usage of activated carbon in recent years. Micropores, mesopores, and macropores are all included in the composition of activated carbon.

These structures play an important role in deciding the properties of activated carbon, such as its performance as an adsorbent. Micropores (less than 2 nm), mesopores (2 nm - 50 nm), and macropores (greater than 50 nm) are the three types of activated carbon pore sizes classified by the International Union of Pure and Applied Chemistry (IUPAC). The internal pore structure of activated carbon is depicted in Figure (2.3).

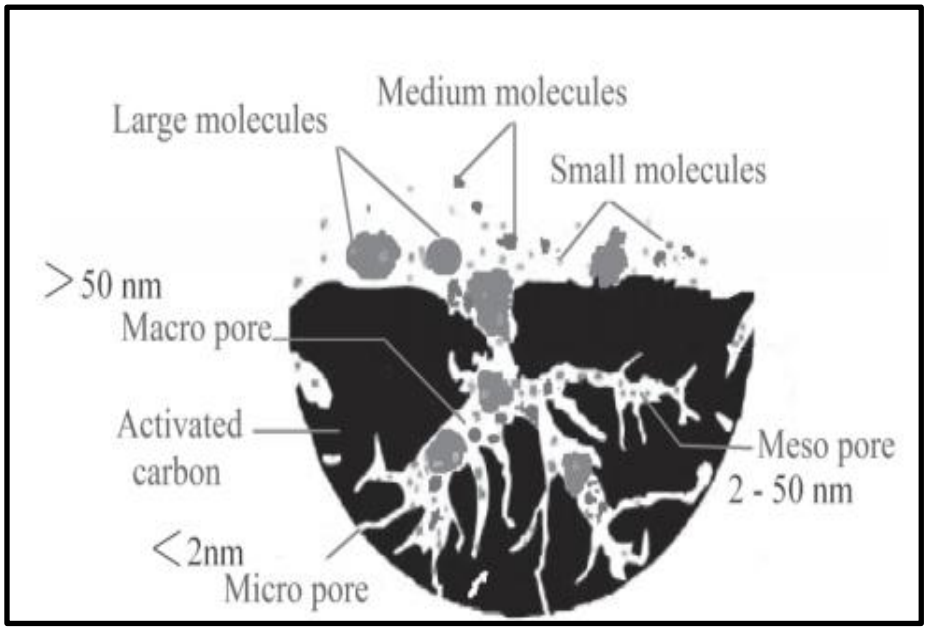

Fig. (2.3): Different pore structures of activated carbon (Sulyman et al., 2016).

Activated carbon (AC) is typically used as an adsorbent for basic dyes (Lakshmipathy et al., 2015). It is widely employed due to its exceptionally high surface area (ranging from 500 to 1500 $m^2.g^{-1}$), well-developed internal microporosity, and wide spectrum of surface functional groups. Hence, we use these wastes as a low-cost precursor for the production of AC.

2.6.1 Agricultural waste based activated carbon

The performance, characteristics, and properties of the activated carbon generated are all determined by the primary material used at the start of the process. Furthermore, the type of activation (physical, chemical, or physicochemical) affects the output of activated carbon (Zhang et al., 2017) and inorganic molecules (Hesas et al., 2013).

Animal, mineral, and plant matter may all be used to make activated carbon. Essentially, price, purity, and future expectancy would be the primary considerations when selecting primary raw materials, whether

they come from animals, minerals, or plants, and they would also be simpler to activate, as well as have low degradation properties when aged (Ahmed, 2016). Agricultural wastes have been used as precursors for the processing of activated carbon by several researchers in recent years for four key reasons: renewable source, little cost, easy obtainability, and environmental friendliness. It may also be a source of income for agro-based industries (Hameed and Daud, 2008).

Activated carbon may be created from carbonaceous materials utilizing the pyrolysis method in a variety of ways, including chemical, physical, and microwave-induced/assisted treatment. Activated carbon was traditionally produced from sulfur, lignite, peat, petroleum waste, and wood, both of which are considered to be costly and finite resources (Ozdemir et al., 2014).

These circumstances prompted a recent innovation in the manufacture of activated carbon, which makes use of agricultural bio-waste (lignocelluloses materials) to lower production costs while still being readily accessible and long-lasting. Palm seeds, fruit shells, groundnut shells, coconut shells, and Ricinus communis seed shells are forms of agricultural waste. Many sections of any plant, including the base, stem, bark, flower, leaf, fruit peel, husk, shell, and stone, may be used to produce activated carbon from agricultural wastes.

Woody and non-woody resources can be used in these wastes. Woody resources are mostly made up of cellulose, hemicellulose, and lignin, while non-woody resources are made up of cellulose, hemicellulose, lignin, lipids, protein, sugar, water, hydrocarbon, starch, and a variety of functional classes that have the ability to remove contaminants (Georgin et al., 2016).

Researchers are often more inclined to use non woody agriculture wastes in studies of activated carbon applications because of their unique formulations, which may contribute to improved pore structure characteristics than woody agriculture wastes. In general, raw material selection is based on seven critical criteria:

1. Carbon content is high.
2. little inorganic matter content results in low ash.
3. Contains a lot of unstable matter and has a high density.
4. Abundant in the sense that the raw material is often available at a reduced rate.
5. The potential for activation
6. When stored, there is a low rate of deterioration.
7. Possibility of obtaining a high percent yield from activated carbon.

2.6.2 Carbonization

The thermal degradation of a raw material and the elimination of non-carbon species is known as carbonization. Carbonization of biomass provides a lot of benefits as compared to traditional biological therapies. It often only takes several hours (instead of months or weeks for biological processes), allowing for a more compact reactor design (Yahya et al., 2015).

Lignocellulosic contents would be decomposed during the process, resulting in the removal of non-carbon elements such as nitrogen, oxygen, and hydrogen. Following that, deposition occurs. In general, low-molecular-weight volatile matter can spread first, accompanied by light aromatics and hydrogen gas. Pore structures begin to form at the same time, and the formed will fill the pore structures.

2.7 Agricultural solid wastes

Agricultural wastes are by-products of a variety of agricultural and foresty operation. Low price, supply, limited recovery time, chemical stability, low treating requirement, keep, and eco-friendly are some of the benefits of utilizing agricultural waste as adsorbents for wastewater treatment (De Gisi et al., 2016; Dai et al., 2018).

Adsorbents made from agricultural wastes and by-products have the high porosity and wide surface area required for wastewater treatment (Abdelhafez and Li, 2016; Anastopoulos et al., 2017; Saxena et al., 2019). The main components of agricultural waste/by-products are cellulose, lignin, and hemicellulose. Polar lignin functional groups such as ether, aldehydes, ketones, alcohols, carboxylic, and phenolic groups have adsorbent properties (Mo et al., 2018; Vardhan et al., 2019) might maybe exist. Agricultural by-products/wastes such as rice husk, onion peel and wheat wastes have been used to remove contaminants from water and wastewater treatment in recent years.

Dye adsorption onto agricultural by-products is emerging as a viable option for inorganic/organic aqueous solution elimination. It is cost-effective, environmentally safe, and effective at removing dyes, and it may substitute the most widely used commercial activated carbon. Adsorbents for dye removal have been made from waste materials and untreated agricultural solid wastes from the timber industry, such as bark and saw dust.

Agricultural by-products, also known as wastes, are widely available in the world. Because of their physiochemical properties, these materials could have potential as sorbents. Many recent studies have shown that different industrial solid wastes can effectively remove organic contaminants, like dyes, when used as adsorbents (Salleh, 2011). Alternative agricultural by-products such as peanut hull, coir pith, and

rice husk are commonly used as pigment adsorbents, as seen in Table (2.3). These wastes are common because they are inexpensive, plentiful, and their organic compositions display a good affinity for certain dyes.

Table (2.3): Research studies on dye adsorption utilizing adsorbents made from agricultural waste .

Materials	Dye	References
Modified saw dust	Methylene Blue	Zou et al., 2013
Mango seed	Methylene blue	Senthil Kumar et al., 2014
Conyzoides leaf	Methylene Blue	Ezechi et al., 2015
Olive pomace	Basic green 4	Koçer and Acemioğlu, 2016
Orange sawdust	Methylene blue	Azzaz et al., 2017
Mango leaf	Methylene blue	Uddin et al., 2017
chickpea shell	Acid Blue25	Krishna et al., 2017

2.8 Mechanism of adsorption

Reichenberg and Boyd's mathematical study of particle, The foundation for sorption of kinetics is laid by mass transfer and mass-action-controlled exchange processes (Fathy and Ahmed, 2012). External transport is usually the rate-limiting stage in systems with: (a) weak mixing, (b) low adsorbate concentration, (c) small particle size, and (d) high adsorbate affinity for adsorbent. In contrast, the intraparticle step limits the overall transfer for those systems that have (1) high adsorbate concentration, (2) good mixing, (3) adsorbent with a big particle size; and (4) low adsorbate affinity for adsorbent (Gulipalli et al., 2011). A standard adsorption mechanism on porous adsorbent is depicted in Figure

(2.4). The solute (adsorbate) is transferred toward the interface layer and added to the adsorbent in the following four stages (Patel, 2019).

1. Advective transport moves solute particles from bulk solutions to the immobile film layer through advective flow, axial dispersion, or diffusion.
2. Solute particle is penetrated and added to an immobile water film sheet during film transition.
3. mass transfer: the binding of a solute particle to the adsorbent's surface, and finally
4. The movement of a solute into the pores of an adsorbent is known as intraparticle diffusion.

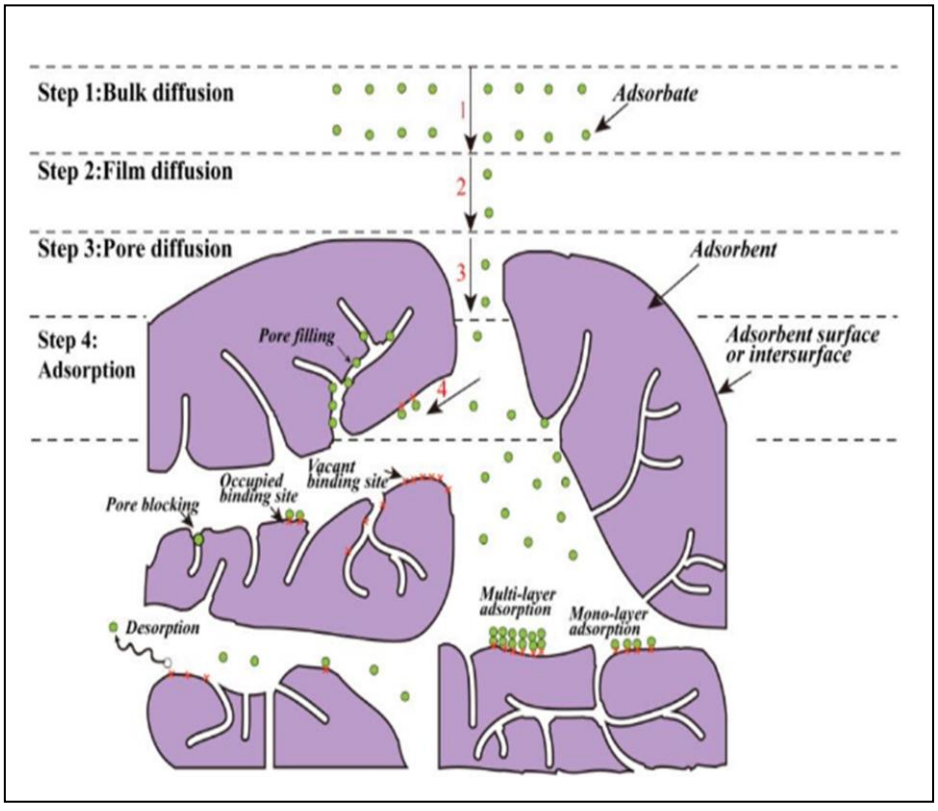

Fig. (2.4): Illustration of a typical adsorption process. Adapted with permission (Wang et al., 2020).

2.9 Process factors affecting dye adsorption

The adsorption mechanism is influenced by a variety of factors. To get rid of the pigment, certain criteria are being investigated.

2.9.1 pH of the solution has an impact

The adsorption mechanism is generally influenced by the pH of the solution, which influences the solution chemistry of dyes as well as the behavior of the adsorbent's functional groups. Different dye groups need different pH ranges when it comes to dyes. Basic dyes, for example, need an alkaline medium , while reactive dyes need a strong acidic environment for optimal dye adsorption (Fahad et al., 2018). The chemical surface of an adsorbent has a significant impact on the adsorption of an adsorbate, which can be influenced by changing the original pH value. According to certain researchers, there is an electrostatic repulsion between the surface of the positively charged adsorbent and the cationic dye molecules at low pH values, which prevents this contaminant from adsorbing (Marrakchi et al., 2017). Since hydrogen ions compete for adsorption sites with the cationic dye molecule if the pH rises, the surface of the biomass acquires a negative charge, allowing for deprotonation of the surface, which encourages cationic dye adsorption and thereby improves the ability of the biomass to adsorb this pollutant (Pang et al., 2017). This is due to the fact that the cationic dye is positively charged in solution, because its adsorption is more successful when the surface charge is negative (Gao et al., 2016). The important element, the point of zero charge (pH_{pzc}), indicates the surface's adsorption potential and the form of surface active centres. The point of zero charge (pzc) is the pH at which the surface charge is zero and is commonly used to measure or describe the electro kinetic

properties of a surface. Only in systems where H+/OH are the possible defining ions is the pH value used to characterize pzc. To better grasp the adsorption process, several researchers looked at the point of zero charge (pH_{pzc}) of different adsorbents made from agricultural solid wastes. At pH > pH_{pzc}, cationic dye adsorption is favored due to the inclusion of functional groups such as the OH^- group, while anionic dye adsorption is favored at pH< pH_{pzc}, where the surface becomes positively charged (Labied et al., 2018).

2.9.2 The impact of contact time

The adsorbate / adsorbent contact time can help in ascertaining the potential prompting of binding and the optimum time for the confiscation of contaminants. Also, the contact time is an essential factor which governs the kinetics of the adsorption process and oversees the inspiring use of an adsorbent for practical application and influences the economic efficiency of the adsorption (Das and Das, 2013). In general, removal efficiency rises quickly at first due to the availability of a large number of vacant surface-active adsorbing sites but, as time passes, the adsorption process slows as the number of surface-active adsorbing sites decreases, forcing the molecule to go further and deeper through the pores, and the adsorption process eventually reaches an equilibrium (Mashkoor and Nasar, 2019).

2.9.3 Adsorbent dosage impact

The quantity of adsorbent used for dye adsorption is an important parameter to control an adsorbent uptake potential under working conditions (Nazarzadeh Zare et al., 2016). When the dosage of adsorbent is increased, the removal efficiency improves while the adsorption

capability decreases. The improved total surface area of the adsorbent and active exchangeable adsorption sites are responsible for the increased removal performance. However, owing to intervening phenomena such as accumulation and/or agglomeration, the effective surface area given by an adsorbent per unit mass decreases significantly at higher concentrations. Since several adsorbent places remained unoccupied, the adsorption ability decreased, and the adsorption did not achieve saturation (Srivastava and Sillanpaa, 2017; Iftekhar et al., 2018). Furthermore, with an increase in adsorbent dosage, the usable adsorbate is insufficient to fully cover the available active adsorbing sites on the adsorbent, resulting in poor adsorbate adsorption per unit mass of adsorbent. In order to diagnose the proficiency of an adsorbent for adsorption from an economic stand point, this parameter provides a indication for the efficiency of dye to be adsorbed for the least amount of adsorbent (Seow and Lim, 2016).

2.9.4 Initial adsorbate concentration impact

The level of dye removal adsorption is heavily influenced by the primary dye concentration. The immediate relationship between the dye concentration and the accessible sites on an adsorbent surface determines the impact of initial dye concentration. In general, as the initial dye concentration rises, the percentage of dye removed declines, perhaps due to adsorption sites on the adsorbent surface being saturated. In the other side, when the initial dye concentration rises, the adsorbent's potential rises, perhaps owing to the strong motivating force for mass transfer at high initial dye concentrations (Bulut and Aydn, 2006; Jawad et al., 2018).

2.10 Point zero charge of adsorbent determination

Investigation on the pH value when the final and initial pH are the same and the biosorbent surface charge is neutral at this value (point zero charge, pH_{pzc}) is a vital property which helps to know which ionic types can be sorbed by biosorbent at desired pH. The amount of SAC (0.5g) was placed in conical flasks which are contained of 50 ml of 0.1M NaCl solution. The primary values of pH (pH_i) (2-10) were organized with 0.1 M solution of NaOH or HCl. After that, suspensions obtained were agitated at 150 rpm for 24 hr. After that, SAC was seperated and the ending pH value of solution was tested. pHpzc is obtained from the point of interception zero with the curve obtained by plotting the ΔpH vs. pH_i (Mohseni et al., 2016).

2.11 Isotherm study

The equilibrium data derived from the initial dye concentration analysis was analyzed using the two most commonly used isotherm equations: the Langmuir and Freundlich equations. The models are simple, well-established and easily interpretable, which are some of the important reasons for their frequent and extensive use. The Langmuir isotherm model considers biosorption in a single layer, while the Freundlich isotherm model considers biosorption on a heterogeneous surface (Kulkarni et al., 2017).

2.11.1 Langmuir isotherm

The Langmuir equation is applicable to homogeneous adsorption where the adsorption of each adsorbate molecule onto the surface has

equal sorption activation energy. The linear form of this isotherm is represented by the expression (Langmuir 1916):

$$\frac{C_e}{q_e} = \frac{1}{q_m K_a} + \frac{1}{q_m} C_e \quad \text{.....(2-1)}$$

where q_e (mg/g) and C_e (mg/l) are the amount of adsorbed adsorbate per unit weight of adsorbent and un adsorbed adsorbate concentration in solution at equilibrium, respectively. The constant K_a (l/mg) is the Langmuir equilibrium constant and q_m is the theoretical monolayer saturation capacity.

The Langmuir isotherm can be expressed in terms of a dimensionless constant known as the separation factor (R_L, also known as the equilibrium parameter), which is specified by the equation below (Nethaji et al., 2012).

$$R_L = \frac{1}{1+K_a\ C_o} \quad \text{.....(2-2)}$$

Where C_o refers to the initial concentration of the adsorbate (mg/l). The value of R_L indicates the adsorption process to be either irreversible (R_L=0), favourable (0<R_L<1), linear (R_L=1) or unfavourable (R_L>1).

2.11.2 Freundlich isotherm

For non-ideal adsorption on a heterogeneous base, the Freundlich isotherm (1906) is used. The existence of different functional classes on the surface, as well as numerous adsorbent–adsorbate interactions, cause heterogeneity (Banerjee and Sharma, 2013; Hameed and El-Khaiary, 2008). The linear form of the Freundlich isotherm is written as:

$$\log q_e = \log k_f + \frac{1}{n} \log C_e \quad \text{.....(2-3)}$$

where q_e is the amount of adsorbate adsorbed at equilibrium (mg/g), C_e is the equilibrium concentration of the adsorbate (mg/l), K_F is the Freundlich adsorption constant related to adsorption capacity of the adsorbent ((mg/g)(l/mg)$^{1/n}$), and 1/n is the adsorption intensity. The values of K_F and 1/n were calculated from the intercept and slope of the plot of log q_e versus log C_e (Akkaya and Güzel, 2013). The numerical value of 1/n less than 1 indicates that adsorption capacity is only slightly suppressed at lower equilibrium concentrations. In comparison to the Langmuir model, the Freundlich isotherm is more widely used, but it offers no details on the monolayer adsorption power. Adsorption on a heterogeneous surface is the basis for this model.

2.12 Kinetic study

Kinetic models are used to specify the controlling mechanisms of the adsorption phase, such as chemical reaction, diffusion control, or mass transfer coefficient. The kinetics of dye adsorption onto adsorbent materials is needed choose the best operating conditions for the fullscale batch operation. The study of adsorption kinetics illustrates how the solute uptake rate and obviously this rate controls the residence time of the adsorbate at the solution interface. This rate is most important when designing the adsorption system and this rate can be calculated from kinetic study. Thus, the kinetics of cationic dye onto adsorbent material was analyzed using different kinetic models which are presented below (Miyah et al., 2016).

2.12.1 Lagergren pseudo-first-order model

Lagergren (1898) proposed the pseudo-first-order kinetic model for the adsorption of solid/liquid structures, which has the formula:

$$\frac{dq_t}{dt} = k_1(q_e - q_t) \quad \text{.....(2-4)}$$

After integration with the initial condition $q_t = 0$ at $t = 0$, Eq (2-5) can be obtained.

$$\ln(q_e - q_t) = \ln q_e - k_1 t \quad \text{.....(2-5)}$$

where, q_t (mg/g) is the amount of pollutant adsorbed at time t (min), q_e is the amount of pollutant adsorbed at equilibrium (mg/g), and k_1 is the Pseudo-first-order rate constant (1/min). Values of q_e and k_1 can be found from the slope and intercept of the plot ln (q_e-q_t) versus t.

2.12.2 Pseudo-second-order model

Ho pseudo second-order kinetics model was used to further interpret the kinetic results. The premise behind this model is that sorption meets second order chemisorption. It can be expressed as (Ho and McKay 1999):

$$\frac{dq_t}{dt} = k_2(q_e - q_t)^2 \quad \text{.....(2-6)}$$

Where k_2 is the constant of Pseudo-second-order rate (g/mg.min). For the similar boundary conditions, the linear arrangement becomes:

$$\frac{t}{q_t} = \frac{1}{k_2 q_e^2} + \frac{t}{q_e} \quad \text{.....(2-7)}$$

Values of q_e and k_2 can be found from the slope and intercept of the graph t/q_t Vs t. The initial biosorption rate h (mg/ g.min) can be found from the Pseudo-second-order model at $t \rightarrow 0$ by the following equation :

$$h = K_2 q_e^2 \quad \text{.....} \quad (2\text{-}8)$$

2.12.3 Intraparticle diffusion model

This model is used to determine the next steps in the adsorption mechanism (Weber and Morris, 1963). The following equation can be used to describe it:

$$q_t = k_{ip} t^{1/2} + C \quad \text{.....} \quad (2\text{-}9)$$

Where k_{ip} is the constant of intra-particle diffusion rate (mg/g.min$^{1/2}$) and C is the constant of intra-particle diffusion provides an idea about the thickness of the boundary layer (mg/g). The plot of adsorption capacity, q_t , versus the square root of time ($t^{1/2}$) explains this model and it should be linear.

2.13 Fixed-bed adsorption column data analysis

Fixed-bed adsorption, as one of the most commonly used separation and purification techniques, has been widely used due to its high performance and ease of operation. How to optimize the design and operation conditions of the fixed-bed adsorption is obviously an important issue to be focused on (Xu et al., 2013). The breakthrough curve may be used to describe the performance of fixed-bed column. The time required for this curve to reach and the shape of its profile are very important characteristics for determining the dynamic and operation

response of adsorption column (Badran et al., 2020). A breakthrough curve is a plot of C/C_o which depict the loading behavior of solute to be sorbed from solution which is refers to the ratio of outlet to inlet solute concentration as a function of time or volume of effluent (V_{eff}) for a given bed depth. When the sorbent bed is saturated with the contaminant, the breakthrough point is reached, and it is described as the time (t_b) when C equals 5% of C_o and the volume of effluent corresponding to this time is V_b. As the sorbate concentration rises quickly after the breakthrough point until it approaches the exhaustion point, the column becomes totally saturated and the sorbed bed is exhausted. The volume of effluent (V_{eff}) at exhaustion time is determined as below:

$$V_{eff} = Q_V t_e \quad \text{.....(2-10)}$$

The volumetric feed flow rate (ml/min) is Q_v, and the exhaustion time is t_e (min). The value of V_b can be calculated as:

$$V_b = Q_V t_b \quad \text{.....(2-11)}$$

For a given inlet solute concentration and feed flow rate, the total amount of solute adsorbed q_{total} (mg) in the column is equal to the area under the curve of adsorbed solute concentration against time as shown in Figure (2.5), which can be determined using the equation below (Kapur and Mondal, 2015):

$$q_{total} = \frac{Q_v}{1000} = \int_0^{t_{total}} C_{ad}\,dt = \frac{Q_v A}{1000} \quad \text{.....(2-12)}$$

Where C_{ad} =(C_o-C) denotes the adsorbed solute concentration (mg/l) at time t, The volumetric feed flow rate is Q_v (ml/min), and the outlet and inlet solute concentrations are C and C_o.

In the column, the experimental uptake or maximum capacity q_{exp} (mg/g) is calculated as follows:

$$q_{exp}\ (mg/g) = q_{total}\ /m \qquad \ldots\ldots\ldots\ldots\ldots\ldots\ldots\ldots\ldots\ldots (2\text{-}13)$$

The total amount of adsorbent is represented by m(g). The total mass of solute that enters the column (mg) is calculated as follows:

$$m_{total}\ (mg) = C_o\ V_{eff}\ /1000 \qquad \ldots\ldots\ldots\ldots\ldots\ldots\ldots\ldots\ldots\ldots (2\text{-}14)$$

The percentage removal of solute is calculated as below:

$$\text{Total removal } (R\%) = q_{total}/m_{total} * 100 \qquad \ldots\ldots\ldots\ldots\ldots\ldots\ldots\ldots\ldots\ldots (2\text{-}15)$$

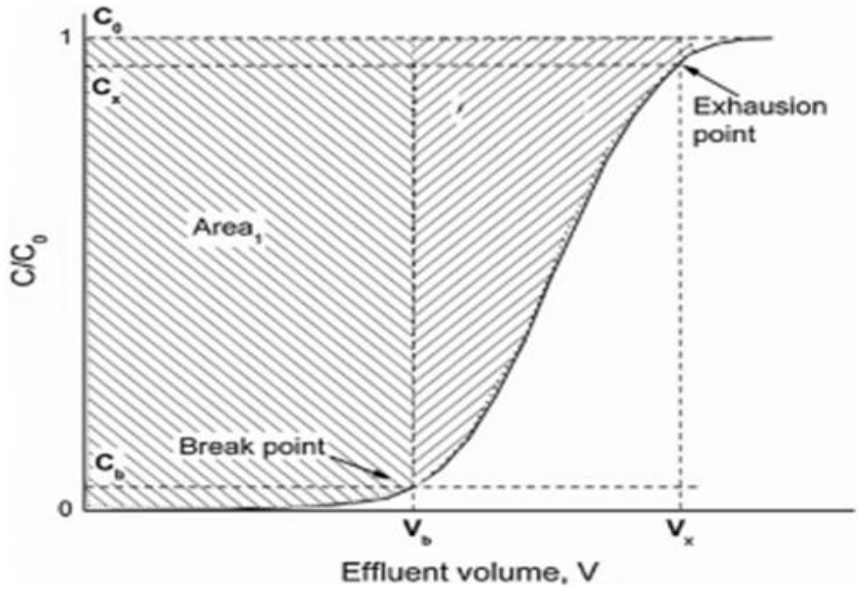

Fig. (2.5) Ideal breakthrough curve (Chowdhury et al., 2015)

Continuous mass transfer happens between two phases during the adsorption process in continuous flow mode utilizing a fixed-bed column (the mobile phase which represents the contaminated solution and the solid phase of the column bed). The concentration of solute in both phases is a function of contact time and adsorption zone height (MTZ). A

mathematical model dependent on mass balance may be used to describe this adsorption phenomenon and its characteristic parameters.

To illustrate the relationship between the breakthrough curve and fixed-bed adsorbent, consider the following: as feed wastewater enters the column inlet, the contaminant is adsorbed more quickly and effectively by the upper few layers of the unused sorbent during the initial period of operations. The feed wastewater is continuously in contact with the upper layers at its initial concentration, C_o. The lower strata of the bed trap the tiny amounts of adsorbate that did not adsorbed in the first few layers. No solute escapes the adsorbent at first (effluent concentration, C=0). Near the influent end of the column, the mass transfer zone (MTZ) is focused (Figure 2.6). As contaminated solution continues to flow through the column, the top layers of the bed become saturated with the pollutant and be less effective for further adsorption process. As a result, the MTZ begins to move downwards fresher adsorbent layers. This region moves as a wave, followed by the movement of the initial concentration front, although at a much slower rate than the feed wastewater linear velocity. As MTZ decreases, more pollutants seem to escape through the effluent, as shown in Figure (2.6). For a constant flow rate, plots of C/C_o against time or effluent volume display a rise in the C/Co ratio as the region moves along the column. The majority of column sorption breakthrough curves have a S shape, but with varying degrees of steepness (Chowdhury et al., 2015).

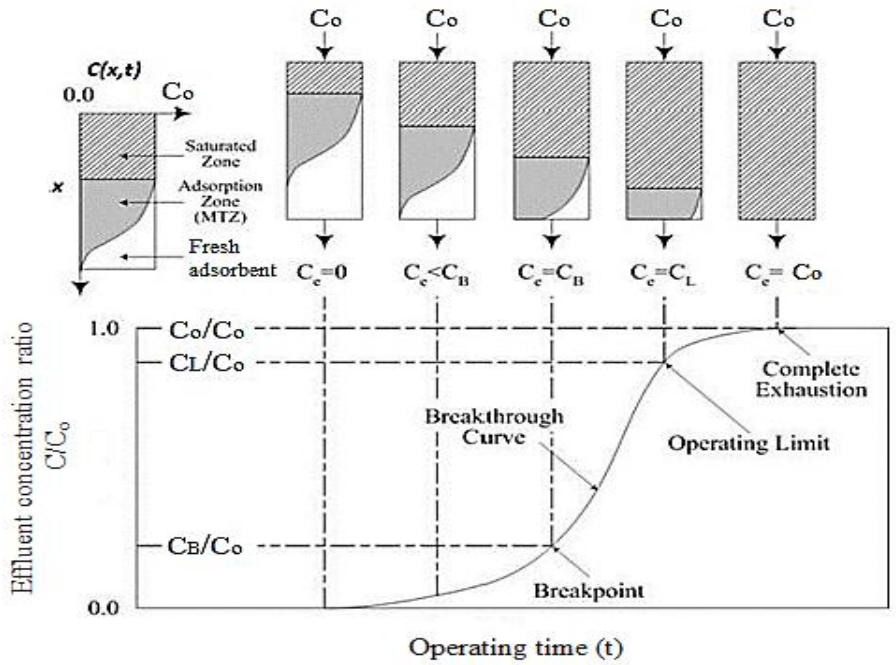

Fig. (2.6): Representation of mass transfer zone movement and formation of breakthrough curve (Chowdhury et al., 2015).

2.13.1 Process parameter for column study

The majority of adsorption experiments utilized synthetic wastewater as an adsorbate, in which a dye solution was equipped and processed with an adsorbent. The effect of different process parameters such as the initial adsorbate concentration, adsorbate flow rate in column, column bed height, and breakthrough and exhaust points was calculated. All of these factors are critical in determining the efficiency of an adsorbent in a continuous effluent treatment operation on a pilot or industrial scale . The impact of process parameters on breakthrough and exhaust point is shown in Table (2.4), along with its features and description. Initial adsorbate concentration, bed height, and flow rate are the most feasible parameters, since most researchers are actually focusing on these parameters and utilizing natural and synthetic adsorbents to eliminate different forms of contaminants such as dyes, metals, radioactive waste, and so on.

Table (2.4): Effect of process parameter on breakthrough and exhaustion point (Patel, 2019).

Process parameter	Features	Explanation
Initial adsorbate concentration	With increasing influent concentrations, breakthrough and exhaustion points happen earlier. Following that, as the inlet concentration increased, the breakpoint time decreased.	Because of the large number of available vacant sites, adsorption was initially fast. Following that, increasing the initial adsorbate concentration causes a greater driving force to overcome mass-transfer resistance in the liquid process, and the sites are quickly exhausted, resulting in a decrease in the amount of effluent treated (Moyo et al. 2017; Saravanan et al. 2018)
Flow rate of adsorbate	With a higher flow rate, breakthrough points are more likely to occur. With a reduction in flow rate, the saturation of breakthrough time increases significantly.	The rate of mass transfer increases, i.e., the amount of adsorbate adsorbed onto unit bed height (mass-transfer zone) increases as the fow rate increases, leading to faster saturation. (Lopez-Cervantes et al. 2017). With a lower flow rate, the adsorbate has more time to contact the adsorbent, resulting in higher adsorbate removal in the column (Ahmad and Hameed 2009; Sheng et al. 2018)
Bed height of column	With rising bed depth, breakthrough and exhaustion times take longer. It was also found that as the bed depth was raised, the volume of effluent handled increased.	The increase in surface area and the number of binding sites available for adsorption is attributable. When the amount of adsorbent was raised, the time it took for the adsorbate and adsorbent to interact increased as well (Fathi et al. 2014; Teutscherova et al. 2018)

2.13.2 Adsorption models for column study

The concentration profiles in the liquid and adsorbent phases differ in place and time in continuous biosorption systems. For the design and optimization of fixed bed columns, mathematical and quantitative modeling approaches are used. As a consequence, the dynamic behavior of a fixed bed column can be defined in terms of the effluent concentration time profile, i.e. the breakthrough curves, from the perspective of process modeling (Abdolali et al., 2017). Multiple models are used to forecast breakthrough results, measure column kinetic constants, and determine the adsorption ability of fixed bed columns. During the operation of a column utilizing adsorption dynamics acquaintance and simulation, numerous functional features such as sorbent capability, operational life span, regeneration period, and time prediction play an important role. These models often include detailed conclusions regarding the process mechanism. Axial dispersion, external film tolerance, and intraparticle diffusion resistance are both tested on the adsorption column. As a consequence, axial dispersion, outward mass movement, and intraparticle diffusion are presumed in the calculated associations for adsorption in fixed-bed columns (Cruz Olivares et al., 2013). For evaluating the efficiency and applicability of column models for large-scale operations, a number of mathematical models have been created. To study the column actions of an adsorbent–adsorbate system, the Thomas, bed depth service time, and Yoon–Nelson models are most widely used.

2.13.2.1 The Bed Depth-Service Time model (BDST)

The aim of fixed bed adsorbed operation is to reduce the concentration in the effluent to a degree that does not surpass a predetermined breakthrough value (C_b). The real effluent concentration is smaller than

C_b at first since the activated carbon is unsaturated, so when the effluent is drained into the bed, the carbon becomes saturated and the effluent concentration reaches C_b, i.e. the breakthrough point is achieved. Bohart and Adams (1920) suggested a link between bed depth (Z) and the period it takes for breakthrough to occur. The process requirements and operational parameters were connected to the service time (t):

$$\ln\left(\frac{c_0}{c_b}-1\right)=\ln\left[\exp\left(\left(\frac{K_B q_B}{u}\right)z\right)-1\right]-K_B C_o\, t_b \quad \text{..... (2-16)}$$

Hutchins (1973) suggested that the bed depth and service period had a linear relationship:

$$t_b=\frac{q_B}{C_o U_f}\,z-\frac{1}{K_B\,C_o}\ln\left(\frac{C_o}{C_b}-1\right) \quad \text{.....(2-17)}$$

The service time is represented by t_b, which is the time it takes for the adsorption column to reach the saturation breakthrough point with a given percentage of saturation (Kratochvil and Volesky, 2000), q_B is the dynamic breakthrough adsorption capacity per unit volume of adsorbent bed (mg/l), K_B is the adsorption rate constant ($l.mg^{-1}.min^{-1}$), z is the column bed depth (cm), U_f is the linear flow velocity (cm/min) described as the ratio of the volumetric flow rate Q_v (cm^3/min^{-1}) to the column cross-sectional area S_c (cm^2). The inlet and breakthrough point concentrations of adsorbate (mg/l) are C_o and C_b, respectively. The values of the model constants (q_B and K_B) are determined using linear regression methods and SPSS system V.20, using the slope and intercept of a linear plot between the t_b and z at various percentage breakthroughs.

Various applications with varying feed flow rates and bed heights (Unuabonah et al., 2015). In this case, the model parameters q_B (mg/l) and K_B (l/mg.min) were determined by plotting the intercept and slope of

ln [(C_o/C_b) – 1] against t.

When the service time is zero, the critical bed depth (Zc) is measured, which is the theoretical depth of the adsorbent sufficient to prevent the adsorbate concentration from reaching breakthrough concentration:

$$Z_C = \frac{U_f}{K_{BD} q_{BD}} \ln\left(\frac{C_0}{C_b} - 1\right) \quad \text{.....(2-18)}$$

2.13.2.2 Thomas model

One of the most popular hypotheses for fixed-bed column efficiency is the Thomas model**.** The Thomas model is based on the hypotheses that (1) the adsorption is not limited by chemical interactions but by mass transfer at the interface and (2) experimental evidence is compatible with Langmuir isotherms and second-order kinetics. It is used to measure the adsorption rate constants and the maximum solid phase adsorbate concentration on adsorbents (Thomas, 1944 ; Foo et al., 2013). Using the kinetic model developed by Thomas, the data obtained in column in continuous mode studies was used to measure the maximum solid phase concentration of dye on biosorbent and the adsorption rate constant (Thomas, 1944). The Thomas model equation is as follows:

$$\left(\frac{C}{C_o}\right) = \frac{1}{1+\exp\left[\frac{K_{TH}}{Q_v}(q_{TH}\, m - C_o V_{eff})\right]} \quad \text{.....(2-19)}$$

After logarithmic transformation, the linear form is:

$$\ln\left(\frac{C_o}{C} - 1\right) = \frac{K_{TH}\, q_{TH}\, m}{Q_v} - K_{TH} C_o t \quad \text{.....(2-20)}$$

Where K_{Th} (l/min.mg) is the Thomas rate constant; q_{TH} (mg/g) is the equilibrium dye uptake per g of the adsorbent; C_o (mg/l) is the inlet dye concentration; C (mg/l) is the outlet concentration at time; m (g) the

mass of adsorbent, Q (ml/min) the flow rate and t (min) stands for flow time. The intercept and slope of a linear plot of ln [(C_o/C -1] vs. time t, respectively, provided the Thomas parameters (q_{TH} and K_{TH}).

2.13.2.3 Yoon-Nelson model

The Yoon and Nelson model is regarded as the less complicated column model since it does not necessitate specific information on adsorbate features, adsorbent kind, and adsorption bed physical properties (Afroze et al., 2015). The concept behind this model is that the rate of decrease in adsorption likelihood for each adsorbate molecule is proportional to the probability of adsorbate adsorption and adsorbate breakthrough on the adsorbent (Yoon and Nelson, 1984).

The Yoon-Nelson equation relating to a single component system is written as below:

$$\frac{C}{C_0} = \frac{1}{1+\exp[K_{YN}(Z-t)]} \quad \text{.....(2-21)}$$

The linearized form of Yoon–Nelson model for a single component system is expressed as:

$$\ln\left(\frac{Ce}{C_0-Ce}\right) = k_{YN}t - \tau k_{YN} \quad \text{.....(2-22)}$$

where k_{YN} is the rate constant (min^{-1}), τ the time required for 50% adsorbate breakthrough (min), the concentrations of effluent and influent adsorbate, respectively, are C and C_o. and t is the breakthrough time (min).

A plot of ln (C/C_o– C) vs t. gives a straight line with K_{YN} as the slope and - τk_{YN} as the intercept, which are referred to as the model constants. Using the following equation, the amount of adsorbate in a packed-bed,

q_{YN}, which is semi of the total adsorbate entering the adsorption bed for 2 τ periods (Patel and Vashi, 2012), can be determined:

$$q_{YN} = \frac{q_{total}}{m} = \frac{C_0\, Q_v \tau}{1000\, m} \quad \text{.....(2-23)}$$

The adsorption capacity (q_{YN}) is calculated using Yoon-Nelson equation, which takes into account the concentration of inlet adsorbate (C_o), volumetric feed flow (Q_v), adsorbent mass (m), and the 50 percent breakthrough time (τ).

2.14 Previous studies of biosorption technique, using agricultural residues as biosorbent to remove dyes

Numerous experiments have shown the effectiveness of dye adsorption using raw adsorbents made from agricultural wastes and used plant pieces (Rangabhashiyam et al., 2013).

Aydin and Baysal (2005) found that the adsorption efficiency to remove dye from wastewater made it an ideal alternative to other expensive treatment options. Touch duration, pH, adsorbent dose, and initial dye concentration were used to investigate the removal of acid red 183 (AR) and acid green 25 (AG) into bittim (Pistacia khinjuk Stocks) (BTS) shells from aqueous solutions. Dye adsorption isotherms on BTS were measured and compared to traditional isotherm equations including the Langmuir and Freundlich models. Within 30 minutes, adsorption equilibrium was achieved. The Langmuir isotherm tends to match the isotherm data more than the Freundlich isotherm, according to the results. Adsorption data are used to establish the parameters of the Langmuir and Freundlich isotherms. AR and AG had gross adsorption capacities of (33 and 28) mg/g on BTS. The pseudo-secondorder reaction model could be used to explain the adsorption kinetics of AR and AG.

Ponnusami et al (2009) studied Gulmohar (Delonix regia) as adsorbent for the removal of Methylene blue from aqueous solution. The material was studied without chemical treatment. The adsorption was observed to be more beneficial at higher pH. The Langmuir isotherm matched the equilibrium data well, and an appreciable Langmuir ability of 0.3 mg/g was discovered.

Sentruk et al., (2010) used a batch biosorption technique for the elimination of Rhodamine 6G, a new biosorbent almond shell (Prunus dulcis) was tested. For all of the Rhodamine 6G initial concentrations tested, the biosorption kinetics fits a pseudo second order paradigm. Both the Langmuir and Freundlich isotherm models work well with equilibrium results. The best match of the Langmuir isotherm model revealed that almond shell has a monolayer biosorption capacity of 32.6 mg/g.

Senthil Kumar et al. (2010) studied the use of a low-cost absorbent, which is the cashew nut shell prepared from agricultural waste, to remove the Congo red (CR) dye from the aqueous solution. Adsorbent dose, pH, initial dye concentration, and time had an impact on adsorption. The findings suggest that, when compared to other commercial adsorbents, CNS can be used to remove dyes from wastewater at a lower cost. Langmuir and Freundlich analyzed the experimental data, resulting a Langmuir isotherm with a maximum biosorption capacity of 5.184 mg/g.

Santhi et al. (2011) investigated the possibility of removing green malachite (MG) and methylene blue (MB) dyes from aqueous solutions using a low-cost substance made from annona squmosa seeds (ASS). The results show that malachite green and methylene blue have removal efficiencies of 75.66 percent and 24.33 percent, respectively, and that the

adsorption process is pH-dependent. The optimum pH for dye removal was found to be 6.0. With increasing initial dye concentration, the amount of dye adsorbed from aqueous solution increase. The equilibrium data (R^2 > 0.97) fit the Langmuir model well, and the adsorption kinetics (R^2 > 0.99) followed the pseudo-second-order equation. On ASS, MG and MB have maximum adsorption capacities of 25.91 mg/g and 8.52 mg/g, respectively. These findings suggest that annona squmosa seed could be a low-cost adsorbent for removing dyes from industrial wastewater. ASS has a higher adsorption capacity for MG than MB.

Hussin et al. (2015) studied durian leaf powder processing with NaOH to introduce more carboxyl groups in order to improve their performance as an adsorbent. A Fourier Transform Infrared (FTIR) spectrometer was used to analyze the relationship of chemically treated durian leaf powder (CTDLP) with methylene blue (MB). A scanning electron microscope (SEM) was used to analyze the surface alteration of CTDLP. The results of touch duration, initial dye concentration, adsorbent dose, and dye solution pH on MB adsorption studied use a batch adsorption sample. The Langmuir model (R^2 > 0.989) better match the experimental results, with a maximum monolayer adsorption ability of 125 mg/g. The kinetic experiments demonstrated strong alignment with the pseudo-second-order model, meaning that the MB adsorption method required chemisorption. CDTLP was discovered to be a possible adsorbent for the removal of MB from wastewater in this analysis.

Etim et al. (2016) studied coconut coir dust at low cost from agricultural residues in the batch process of removing methylene blue pigment. Adsorption was investigated over time as a feature of absorbent quantity, pH, and concentration. The adsorption ratio is observed to differ linearly with the quantity of adsorbent and concentration over time,

although non-linearly with pH. Two isotherm models, Langmuir and Freundlich, were studied, and adsorption was found to fit well into both with $R^2 \geq 0.90$. The pseudo-second order kinetic model accurately represented the kinetic data. They discovered a potential for absorption (q_m =29.50mg/g). The dye was adsorbent by a chemical reaction of the othe adsorbent.

Abbas et al. (2018) dried fungi waste from white mold fungi to use it to remove methylene blue pigment from aqueous solution in batch mode. The equilibrium isotherm as well as the kinetics have been studied. To determine the adsorption capacity and analyze the suitability of the biosorption process, several parameters were evaluated, including pH, contact time, dye concentration, and biosorbent dosage. The Langmuir and Freundlich isotherms were used to model the process equilibrium, also pseudo-first-order and pseudo-second-order kinetic models were used to fit the kinetic data indicated a better fit of process to a pseudo second order model. The equilibrium isotherm data fit well to the Langmuir isotherm with a maximum biosorption capacity of 23.69 mg/g and a determination coefficient R^2 of 0.9909

Gebrezgiher and Kiflie (2020) studied removing reactive red dye from aqueous solutions by cactus peel. The initial dye concentration, pH, biosorbent dosage, contact time, and pH were investigated. Response surface methodology was used to examine the interaction effects of process variables. As the initial dye concentration and solution pH decreased, as well as the biosorbent dosage and contact time increased, removal efficiency increased. At solution pH, initial dye concentration, biosorbent dose, and contact time of 3.0, 40 mg/l, 6 g, and 120 min, the highest removal efficiency (99.43%) was achieved. According to regression analysis, the Langmuir isotherm (R^2=0.9935) was better

represented the biosorption process than the Freundlich isotherm (R^2=0.9722). The absorption capacity (q_m) with the highest percentage is 0.2796 mg/g.

Felista et al. (2020) studied the possibility of using macadamia seed husks (MSH) as a low cost absorbent material to eliminate Basic Blue3 Dye (BB3). Batch adsorption experiments were carried out to assess MSH ability to remove BB3 under a variety of experimental conditions. Increases in interaction time, MSH dosage, initial BB3 dye concentration, and pH increased the percentage BB3 dye uptake. At optimum pH 12, the adsorption equilibrium was reached in 40 minutes, with an adsorption efficacy up to 99.8%. The experimental data fit a pseudo second order kinetic model with (R^2> 0.9970), indicating chemisorption dominance. Freundlich adsorption isotherms fit the experimental data well, with high value R^2=0.9991, implying multiple layer adsorption and a maximum BB3 adsorbed q_m mg/g =1.4. The findings show that MSH is a viable and effective alternative for removing synthetic dyes from industrial effluents.

Using a fixed-bed adsorption, Ahmad and Hameed (2009) examined the adsorption ability of granular activated carbon dependent on bamboo waste (BGAC) to extract. Reactive Black (RB5) from aqueous solution. On the breakthrough characteristics of the adsorption method, the effects of inlet RB5 concentration (50-200) mg/l, feed flow rate (10-30) ml/min, and activated carbon bed height (40-80) mm were investigated. With a 100 mg/l inlet dye concentration, an 80 mm bed height, and a 10 ml/min flow rate, the highest capacity of 39.02 mg/g was achieved. The adsorption data is mounted to Adam –Bohart, Thomas, and Yoon–Nelson models, which are all well-known fixed-bed adsorption models. The findings were well-fitting to the Thomas and Yoon–Nelson models, with

R^2 of 0.93 at various conditions. Using a fixed-bed adsorption column, the BGAC was shown to be a good adsorbent for RB5 adsorption.

Han et al. (2011) examined the impact of different method parameters on the effectiveness of jackfruit leaf powder (JLP) for extracting methylene blue (MB) from aqueous solution, including bed depth (5-10) cm, flow rate (30-50) ml/min, and initial MB concentrations (100-300) mg/l. The cumulative adsorbed concentrations and equilibrium absorption decreased with increasing flow rate and raised with the initial MB concentration, according to the findings. At pH 10, the longest breakthrough period and highest MB adsorption were achieved. The column worked well at low flow rates, according to the data. With increasing bed height, breakthrough time and exhaustion time have increased. To forecast the breakthrough curves and evaluate the characteristic parameters of the column that are useful for process design, the bed-depth service time (BDST) model and the Thomas model were applied to the adsorption of MB at various bed depths, flow rates, influent concentrations, and pH. At all of the process parameters tested, the two models predictions were very similar to the experimental findings, suggesting that they were very suitable for JLP column design.

Kumar et al. (2012) studied low groundnut shell powder (GNSP) to remove methylene blue using a fixed bed. The adsorption kinetics and breakthrough curves for the GNSP were studied using the bed service depth model and the Thomas model. Both models had very large R^2 values and matched the experimental results very well. The percentage of color removed improved as bed height increased. It was found that adsorption capacity of GNSP was in the range of 0.238 to 0.272kg/kg of adsorbent. These findings suggest that the GNSP may be used as a low-cost alternative adsorbent for pollutant removal in aqueous solution.

Yagub et al. (2014) used the fixed bed column to investigate the efficacy of pine cone biomass for removal of methylene blue (MB) dye from aqueous solution. The adsorption column breakthrough curves (BTCS) revealed that feed flow rate, initial MB dye concentration, and column bed height had influences on dye adsorptive behavior. The total amount of adsorbed dye, equilibrium dye absorption, mass transfer region, and total percentage of dye removal increased as MB dye concentration and bed height increased, but decreased as the initial flow rate increased. Thomas, Yoon–Nelson, and Bed Depth Service Time (BDST) models were used to match the experimental BTCS collected from dynamic experiments to assess the fixed-bed column adsorption kinetic parameters. All of these parameters are important for the design of an adsorption column, and all three kinetic models were found to be applicable. The overall solid-phase concentration (q_o) decreased as the flow rate and bed height increased, but increased as the original MB dye concentration increased, according to the Thomas model. The value of the Thomas kinetic rate constant (K_{Th}) increased as the flow rate increased, but decreased as the original MB dye concentration and bed height increased. In the entire column adsorption method, the Yoon–Nelson model showed that the time needed to achieve 50% adsorbate breakthrough matched well with the experimental results (50 percent exp). The rate constant K_{YN} increased as the flow rate and initial MB dye concentration increased, but decreased as the bed height increased. The rate constant (K_o) decreased as bed heights and initial MB dye concentrations increased, but increased as flow rate increased, according to the BDST model. With growing flow rate, initial MB dye concentration, and bed height, the volumetric sorption capability of the bed (N_o) raised. the experimental data was well-fitted by all three models.

Sajab et al. (2014) applied cationic and anionic modified oil palm fruit fibers to remove methylene blue (MB) and phenol red (PR) using single- and multiple-melting systems in a fixed bed system for an adsorption assay. To test various experimental situations, the experimental data is fitted with Thomas and Clark column adsorption models (adsorbate dose, bed height, column temperature, and flow rate). The findings point to a monolayer and heterogeneous adsorption process. Using a bed depth service time model and the adsorption rate, the service time of each bed were calculated. The adsorbent was regenerated for up to five adsorption/desorption cycles, indicating that the adsorbent column is extremely reusable. Both fibers packed in separate arrangements were used to remove mixed MB and PR at the same time.

afroze et al. (2015) verified the efficacy of eucalyptus bark biomass absorption in removing methylene blue (MB) pigment from solution in a sustainable and cost-effective manner. To evaluate breakthrough curves with a fixed bed flow column, a series of column tests were performed using crude eucalyptus bark with varying MB dye flow rate (10-15) $ml.min^{-1}$, initial MB dye concentration (50-100) $mg.l^{-1}$, and adsorbent bed height (10-15) cm. The best conditions for optimum dye adsorption were found to be a high bed height, low flow rate, and a high initial dye concentration.The Thomas model, Yoon–Nelson model, and bed depth service time model were added to experimental breakthrough data to simulate breakthrough curves and evaluate the characteristic parameters of the column dynamics for industrial applications and process design. In terms of MB flow rate, initial dye concentration, and adsorbent bed height, all models were considered to be ideal for representing the dynamic behaviour of the column. The researchers discovered that eucalyptus bark biomass has a strong adsorption capacity for extracting

MB dye from aqueous solutions in a column method and could be used to handle dye-containing effluents.

Yu et al. (2015) determined the possibility of eliminating the cationic dyes methylene blue and rhodamine B from aqueous solution using continuous mode utilizing modified sugar cane waste (SCW). In a fixed bed column, the effects of flow rate on dye adsorption were investigated. In a binary method, the competitive adsorption kinetics of the two dyes were explored in detail. The changed sorbent's adsorption capacities for methylene blue and rhodamine B in a one-component system were 1.7 and 0.4 mmol $.g^{-1}$, respectively, according to the results. Free adsorption, replacement adsorption, and adsorption equilibrium are the three stages of the competitive adsorption mechanism in the binary scheme. In the second step, the 0.19 mmol of rhodamine B that had been absorbed was substituted by 0.35 mmol of methylene blue. For the first time, a simple updated Yoon -Nelson model was used to predict adsorption kinetics. The adsorption rate constants for the two dyes in the three phases were found to be in the following order: phase I > phase III > phase II, demonstrating that the substitution adsorption phase is the rate deciding stage. Desorption experiment showed that the loaded two dyes could be separated and recycled by using the mixture solution of HCl (0.1 $mol.l^{-1}$) and ethanol as eluent. The prepared fixed bed column had great potential in industrial wastewater treatment.

El Messaoudi et al. (2016) studied the possibility of removing Congo red (CR) from aqueous solution in a fixed bed column system using an environmentally friendly bio absorbent jujube shell (JS). Bed depths (2, 4 and 6) cm, flow rate (2.8, 4.5 and 6.4) min/l, and influent CR concentrations (100, 200, and 300) mg/l were all variables in the experiment. With a flow rate of 2.8 ml/min and a bed depth of 4 cm, the

maximum biosorption potential (80.49mg/g) on a 100 mg/l of CR solution was achieved. This research found that CR can be effectively adsorbed on JS. With increased flow rate, decreased bed depth, and increased influent CR concentration, the breakthrough and exhaustion times decreased. The models of Thomas and Bohart-Adams were successful in predicting breakthrough curves for CR removal with various parameters. The biosorption of CR onto JS was discovered to be very similar to the Thomas model. The desorption of JS was investigated using a NaOH solution (0.1N) as the desorbing agent, and the reuse of JS over four cycles was investigated.

Kopsidas et al. (2016) investigated the usage of traditional urban solid waste like coffee grounds to clean commercial wastewater polluted with simple dyes like methylene blue. Two popular models, namely Bohart and Adams and Clark, were used to evaluate data from the continuous fixed-bed column method. For a bed depth of 15 cm, an initial dye concentration of 800 $mg.l^{-1}$, and a flow rate of 20 $ml.min^{-1}$, the Bohart and Adams capacity was up to N = 46,166 $mg.l^{-1}$ or q_o = 104.5 mg/g. Methylene Blue is well-adsorbed on coffee residues, according to the findings. As a result, this method may be used to remove simple dyes from aquatic environments at a low cost.

Thuong et al. (2018) verified the removal of methylene blue (MB) and crystal violet (CV) from wastewater using a fixed-bed column of pretreated durian husk (DP). Bed depths (2-6) cm, flow rate (5–20) ml/min, and influent dye concentrations (200-600) mg/l are all investigated variables in the system. On a 600 mg/l of methylene blue and crystal violet reached within a 4 cm bed height and a flow rate of 10 ml/min, the highest adsorption level of pretreated DP was 235.80 mg/g and 527.64 mg/g, respectively. As a result, the breakthrough curves were

developed and modeled using the related theoretical models when considering the results of various experimental conditions. In an initial concentration of 200-600 mg/l, pre-treated durian peel was found to have a strong adsorption potential for cationic dye, with full elimination.

2.15 Summary

The disposal of colored dye wastewater in the environment has depleted freshwater resources and compelled scientists to rethink the availability of clean and safe water. It has been reported that the presence of toxic and colored compounds in dye-containing wastewater results in carcinogenic, mutagenic, allergic, and dermatitis effects on living organisms. Adsorption is recognized as an effective and low cost technique for the removal of organic pollutants from water and wastewater, and produce high-quality treated effluent. This chapter highlighted the studies of removal of organic pollutants using adsorption technique with different kinds of natural and synthetic activated carbon. Also, it provides extensive literature information about synthetic dyes, their classification and toxicity effects.

Many researches have given considerable attention aimed at establishing to the removal efficiency of organic pollutants by adsorption technique. To decrease treatment costs, attempts have been made to find inexpensive alternative activated carbon (AC), from waste materials of industrial, domestic and agricultural activities.

Commercial activated carbon is used widely as an adsorbent in the removal of dyes with great success due to its excellent adsorption capacity, large surface area and mesoporous structure . However, due to the high cost and difficulties associated with its regeneration, various researchers have explored alternative nonconventional and cost-effective adsorbents in the removal of dyes. Agricultural solid waste based activated carbon are considered interesting alternative to available commercial activated carbon. These natural waste materials are available locally in a large quantity and have little or no commercial value. This literature review provides an overview and up to date of current uses of biomass based carbon in the removal of organic dyes from wastewater. Also, the mechanism of adsorption and identification of various process parameters such as solution pH, initial adsorbate concentration, adsorbent dose, contact time have been critically analysed here. Further, this review describes the different continuous column adsorption studies based on using various natural biosorbents and the application of various column dynamic models.

From the established studies, it can be concluded that there has been a vast focus on natural adsorbents. This was reasoned by multiple studies to be based on their inexpensive economic potential. However, to decisively make this conclusion, this work aims to explore a biosorbent derived from Iraqi natural plant as a natural, cheap and environmentally friendly adsorbent.

Chapter Three
Experimental Works and Procedures

Chapter Three

Experimental Works and Procedures

3.1 Introduction

Preparation and characterization of the biosorbent (SAC) in this chapter are explained. The effectiveness of SAC in removing of methylene blue dye (MBD) from colored industrial effluent was investigated in a series of laboratory batch and continuous flow experiments. The batch tests at room temperature (25 ± 5°C) are based on the effects of the pH of dye solution, contact time , biosorbent dosage and initial concentration of MBD. While continuous flow studies have been carried out to investigate the effect of MBD solution flow rate, bed depth of biosorbent and initial MBD concentration on the MBD removal efficiency. Figure (3.1) indicates the flow chart of this work.

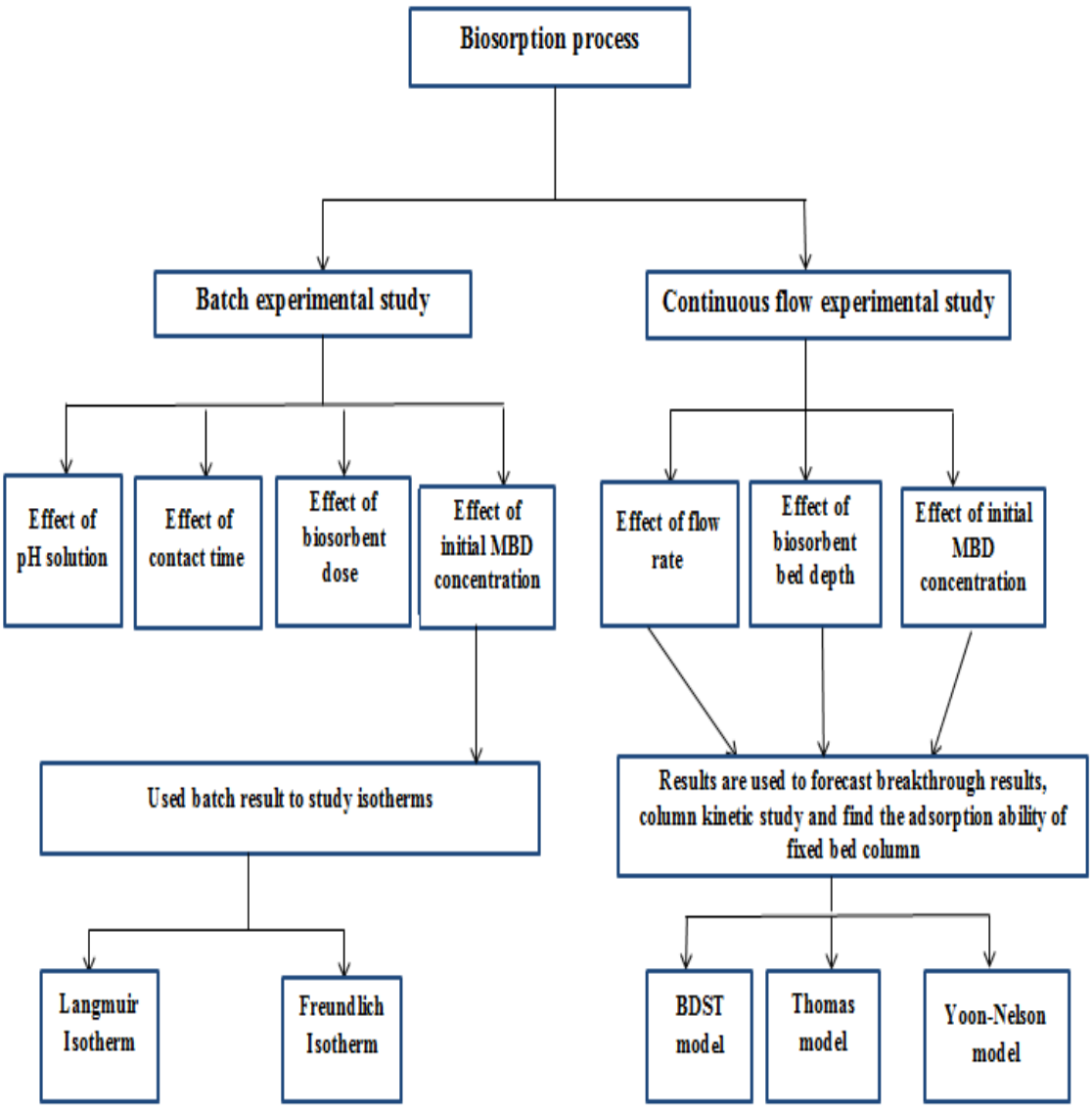

Fig. (3.1): Flow chart of adsorption process for MBD.

3.2 Materials and methods

3.2.1 Adsorbate

Methylene blue dye (MBD) has broader uses, including coloring paper, temporary hair coloring, fabric dyeing, wool, etc. With the molecular formula $C_{16}H_{18}N_3ClS$ (molecular weight 319.85 g/mol). The chemical composition of the dye is shown in Figure (3.2). The Iraqi commercial markets supplied the methylene blue used in this work and some of its physical and chemical properties are shown in Table (3.1) and Figure (3.3) shows the MBD powder that was employed in this study. The desirable concentrations of MBD solution were prepared by diluting the stock solution using distilled water. The pH of dye solution was adjusted using HCL and NaoH with molarity of 0.1.

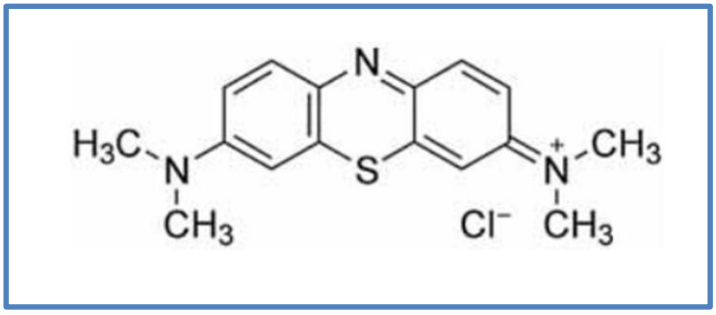

Fig. (3.2): Structural formula of (MBD) (Zazouli et al., 2016).

Fig. (3.3): MBD powder used in this study.

Table (3.1): Physical and chemical properties of MBD (Acemiolu et al., 2010; Azha et al., 2016).

Property	Value
Chemical formula	$C_{16}H_{18}N_3CIS$
IUPAC name	3,7-bis (Dimethylamino)-phenothiazin-5-ium chloride.
Molecular weight (g/mol)	319.85
Type	Cationic dye
Color	Blue
Physical state and form	Solid
Odor	Odorless
Absorption maximum (nm)	664
Solubility	1 g/25 ml
Other name	Swiss blue

3. 2.2 Biosorbent (SAC) preparation

Activated carbon derived from natural and local Iraqi plant (Schanginia/sp) was the biosorbent used in the present research. The activated carbon production consisted of activation by carbonization of the respective plant material. The raw material was split into small parts, and was washed several times using tap water followed by using distilled water to remove water soluble substances, soil, dust, etc, and followed carbonization was carried out for one hour in a muffle furnace at 250 C° (Ukanwa et al., 2019). Based on previous trials with various heating durations, this heating degree and time is based. The plant was totally carbonized to ash when the degree of heating and period were increased. After carbonization, the carbon collected was washed with distilled water several times, then dried in an electric oven at 100 C° (Yuan et al., 2019)

to eliminate any unwanted moisture inside the particles and stored in desiccators. The biosorbent was finally ground and sieved through a 100 mesh sieve. In the Ministry of Oil/ Petroleum Production and Research Center, the physiochemical properties of activated carbon prepared from natural Iraqi plants were carried out.

The natural plant and produced activated carbon are shown in Figure (3.4 a,b), respectively.

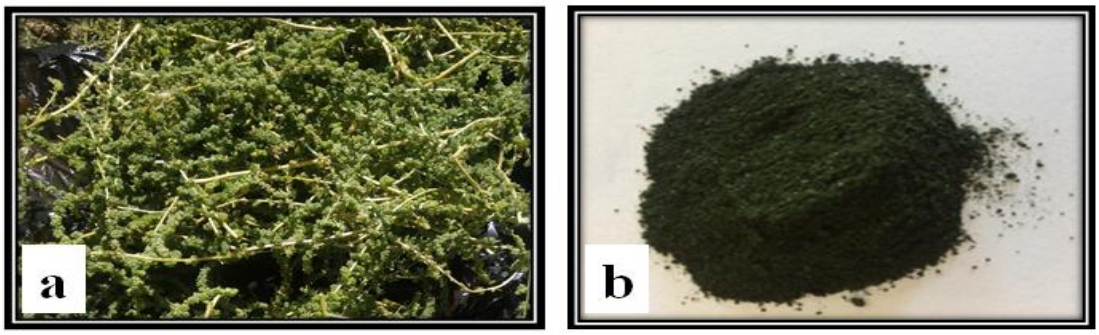

Fig. (3.4): (a) Natural plant (b) Prepared SAC.

3.3 Characterization techniques of biosorbent

3.3.1 Characterization of particular surface region

The nitrogen adsorption-desorption isothermal analysis measurements were defined by the precise surface area (S_{BET}) of the prepared SAC. The evaluation will be carried out at the Ministry of Oil/ Petroleum Development and Research Centre. Nitrogen adsorption-desorption isotherms obtained in a relative pressure < 0.35 p/p^o by using an analyzer, Model No. Qsurf 9600, Themo Finnegan Co., USA.

3.3.2 FTIR spectra

In the College of Pharmacy, University of Kufa, Fourier transform infrared spectroscopy (FTIR; SHIMADZU, IRPrestige-21, Japan) is

conducted to feel the surface functional groups of studied biosorbent at wavelengths of 400-4000 cm^{-1}. This test is the most appropriate measuring tool based on the adsorption of FTIR in the chemical bonds associated with the mineral composition.The pattern of biosorption on biomass materials is closely related to the presence of SAC's active functional groups and surface bonds. FTIR spectroscopy, thus, is an effective means of defining the signature functional groups that can adsorb dye ions. Before and after MBD biosorption, FTIR spectroscopy was conducted on SAC for elucidation of the positions of these active sites along with the change of their locations after MBD biosorption.

3.3.3 Scanning electron microscopy (SEM)

A high-resolution scanning electron microscopy (SEM; TESCAN, Mira3, France) was used to scan the surface texture morphological composition of the surface and examine the outline of the biosorbent used before and after the biosorption of MBD with various magnifications. This test was carried out the University of Tehran, along with energy dispersive spectroscopy (EDS).

3.3.4 Atomic force microscope (AFM)

To describe and examine the topography of SAC before and after MBD biosorption, the CSPM with AFM test (SPM AA300 Angstrom Advanced Inc., USA with AFM contact mode) was performed. This test is carried out at the Department of Chemistry, University of Baghdad, College of of Science.

3.4 Experimental methods

Two types of studies were used in the experimental process of this study; batch and continuous trials. The biosorption method was divided

into two sets: isothermal and kinetic equilibrium, while using fixed-bed columns, the continuous system was performed.

3.4.1 Batch study

To obtain the best operating condition for SAC in the removal of MBD 100 ml of solution of known dye concentration was added to conical flasks of 250 ml volume. The mass of the SAC was applied to each flask, then the flasks were constantly stirring by an orbital shaker at everage speed and allow sufficient time for the equilibrium of SAC at room temperature (25 ± 5°C). The samples were eventually removed and filtered. In College of Engineering Environmental department Engineering. The concentration of MBD are measured using double beam UV-VIS spectrophotometer (UV/VIS-6800JENWAY) with maximum wavelength. The maximum wavelength, λ_{max} for MBD was measured at 664 nm. Concentrations during experimental work were determined from a standard calibration curve. A photo of the UV Spectrophotometer used in the study is shown in Figure (3.5).

Fig. (3.5): UV Spectrophotometer used in this work ((UV/VIS-6800JENWAY).

The key distinct factors used in batch studies are shown in Tables (3.2)

Table (3.2): The main different parameters used in batch experiments.

Factor	Rang	Purpose
pH of MBD solution	2 - 10	To identify the best pH
Contact time, min	5 - 120	Determining the optimal contcat time for the removal of MBD
Dose, g/ 100 ml dye solution	0.1 - 1.5	To determine the optimum bisorbent quantity
Initial dye concentration, mg/l	10 – 100 25, 50, 100, 200	For isotherm analysis and study of kinetics.

The removal efficiency and uptake was estimated using the following equations.

$$R\% = \frac{C_O - Ce}{C_O} * 100 \qquad \text{.....(3-1)}$$

$$q_e = \frac{Co - Ce}{m} \times v \qquad \text{.....(3-2)}$$

Where:

R % = Percentage removal

C_o = Initial concentration of dye (mg/l)

C_e = Concentration of dye at equilibrium time (mg/l)

v = Volume (l)

q_e = Biosorption capacity at equilibrium time (mg/g)

m = Biosorbent mass (g).

3.4.2 Procedure and experimental setup for dynamic biosorption studies

Contintious flow biosorption tests were conducted in a fixed bed column made using apyrex glass column with an inner diameter of 2 cm and a length of 75 cm. To avoid channeling and for even distribution of the solution, glass wool and glass beads layer of particle size 5 mm were inserted near the column inlet. To prevent biosorbent loss, the bottom of the bed was covered with a layer of glass wool. SAC was sieved to get the 600 µm particle size. The photo and schematic illustration for this system is seen in Figures (3.6 and 3.7), respectively . In the fixed bed column, a known quantity of biosorbent was applied to achieve the required bed height of 15, 20, and 30 cm. The MBD solution was pumped downward through the column using a peristaltic pump (ISMATEC model, IDEX Corporation, Germany). Biosorption investigation must begin with the biosorbent bed being wetted with purified water in a downward flow to remove any occupied air from the particles. The column tests were carried out at room temperature. Determining the dynamic and operative response of a biosorption column needs defining the time for breakthrough appearance and shape of the breakthrough curves which are very vital features. So, breakthrough curves were plotted by C/C_o vs. time. The breakthrough curves were studied in relation to different operating factors. Samples were collected at regular intervals (15min) form the exit of the column for all the experiments effluent until equilibrium and saturated capactity for dye biosorption of the column bed was reach. The distinet factors used in continuous flow biosorption study is show in Table (3.3).

Table (3.3): The main factors used in continuous experiments.

Factor	Rang	Purpose
Dye solution flow rate, ml/min	10, 15, 20	To evaluate the effects of different flow rates of dye solution on breakthrough curves
Biosorbent bed height, cm	15, 20, 30	To study the influence of different bed heights of biosorbent on breakthrough curves
Initial dye concentration, mg/l	25, 50,75	To study the effects of different initial concentrations of dye on breakthrough curves

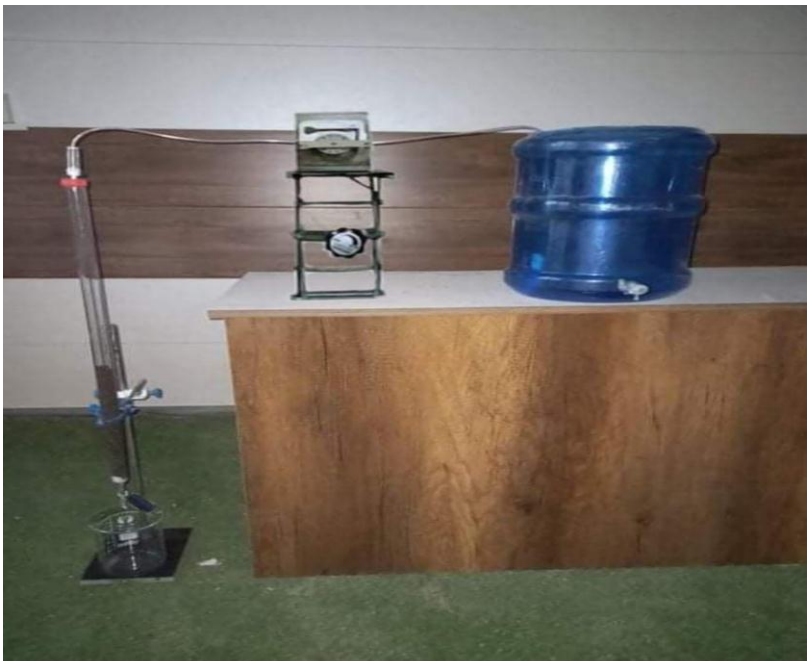

Fig. (3.6): Laboratory arrangement of a fixed-bed column structure for MBD biosorption experiments.

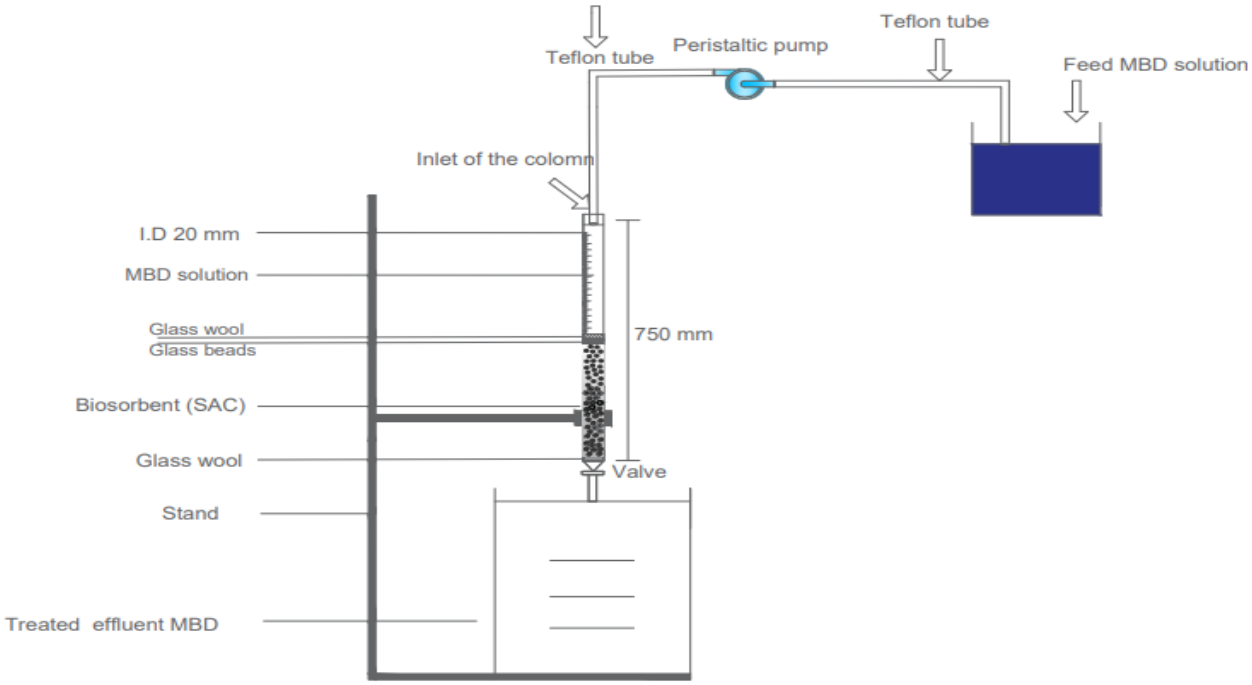

Fig. (3.7): The schematic of the fixed-bed column structure used in dynamic biosorption experimental investigates.

Chapter Four
Results and Discussion

Chapter Four

Results and Discussion

4.1 Introduction

This chapter investigates the potential effectiveness of SAC as an biosorbent in the removal of MBD from its aqueous solution by biosorption process. SAC is deemed environmentally sustainable since it does not involve the usage of chemicals such as acids and bases in its processing. The purpose of the characterization analysis is to show how important features of the biosorbent, such as surface area, surface topography, and active sites, change before and after MBD removal. The biosorption activity of SAC to ward MBD removal is studied using batch and dynamic systems. The effect dye solution pH, contact time, biosorbent dose and initial dye concentration, on biosorption capability is investigated in batch mode at room temperature (25 ± 5^0C) . The equilibrium data were fitted into Langmuir and Freundlich isotherm models to better grasp the adsorption isotherm and MBD - SAC interaction. Additionally, batch experimental data was analyzed using pseudo-first-order, pseudo-second-order, and intra-particle diffusion models to establish adsorption kinetics and mechanism. In continuous flow system , the obtained data is evaluated in order to determine the impact of operational variables on the breakthrough curves. The kinetic analysis uses various kinetic models to forecast the breakthrough curve under various conditions.

4.2 Characterization works

4.2.1 Biosorbent physiochemical characterization

The elemental analysis was obtained by EDS analysis which is occupied with SEM technique. EDS analysis of produced activated carbon is summarized in Table (4.1).

Table (4.1): Elemental analysis (%W/W) of SAC using EDS spectrum**.**

Biosorbent	**C**	**O**	**N**	**H**	**S**	**Other contents plus L.O.I.**
SAC	69.52	12.36	1.93	6.24	1.3	8.65

In comparison to other elements, the SAC sample has a very high carbon content. As a consequence, it can be inferred that carbon is the most abundant component in the sample, meaning that it is carbonaceous and ideal for adsorption. Since the quantity of S was so tiny, it meant there were just a few impurities present. Table (4.2) mentions the other physiochemical properties of SAC .

Table (4.2): Physiochemical properties of SAC.

Property	**SAC**
Specific surface area, S_{BET} ($m^2 g^{-1}$)	27.92
Moisture content %	0.3
Bulk density (g/ml)	0.356
Point zero charge (pH_{pzc})	4.4

4.2.2 FTIR spectroscopy of SAC biosorbent

The FTIR is a technique of vibrational spectroscopic usually used to characterize functional groups present in SAC based biosorbent surface that could be possibly involved during the interactions / biosorption of MBD (Saroyan et al., 2017; Giannakoudakis et al., 2018).

The FTIR spectra of SAC before and after MBD biosorption in the range of 400 – 4000 cm^{-1} are shown in Figure (4.1 a, b) for explanation the locations of active sites of these functional groups besides of the shifting of their locations after MBD removal.

Figure (4.1 a) presents the complex nature of SAC as evidenced by the presence of a large number of IR bands which are appeared that important various functional groups, accordance with their respective wavelengths (cm^{-1}). The intense and broad absorption peaks in the range of 3414 – 3236.55 cm^{-1}represent the –OH stretching vibrations of hydrogen bonded hydroxyl group of polymeric compounds such as phenols, alcohols and carboxylic acids as in pectin, cellulose group founded on the surface of biosorbent.

The oxygen functional groups on the SAC surface greatly enhance its hydrophilic properties and also act as binding sites for the organic pollutant molecules (Chen et al., 2015; Reddy et al., 2014; Lakshmipathy, 2015). The –NH asymmetric stretching of amino groups also appeared in this region (Üner et al., 2015; Latif et al., 2019).

The peaks at 2924.09 and 2852.72 cm^{-1} are attributed the symmetric and asymmetric C-H stretching vibrations of aliphatic acids (Somaia and Sahar, 2017). The peaks at 1637.56 and 1618.28 cm^{-1} indicate to the C=O stretching in organic groups of carboxyl and bending vibration of the functional group of

–OH (Zhang et al., 2017; Francisco et al., 2019). The peaks at 1517.98, 1460.11, and 1440.83 cm^{-1} are attributed to aromatic C=C groups stretching vibrations in aromatic rings (Hesas et al., 2013; Amin et al., 2017; Jamiu et al., 2020). The peaks at 1375.25 and 1323.17 cm^{-1} represent the $–COO^-$ symmetric stretching vibrations as well as the C-N stretching vibrations (Hassan et al., 2017; Das et al., 2020) and N-O stretching vibrations of aliphatic amines (Ansari et al., 2016).

The IR bands around 1000-1300 cm^{-1} indicate to C-O and C-O-C stretching vibrations of carboxylic acids, alcohols, phenols or esters groups (Reddy et al., 2012; Jawad et al., 2018). The peaks at 785.03 and 719.45 cm^{-1} represent C-N stretching vibrations (Schiewer and Patil, 2008; Zhang et al., 2013). Finally, the peaks below 700 cm^{-1} indicate to presence of alkyl halides compounds with C-Br (stretching vibration) bond (Kanthasamy et al., 2020).

The details of FTIR analysis for SAC before and after MBD biosorption are listed in Table (4.3). As shown in Figure (4.1a), the SAC surface prior to MBD biosorption is rich in hydroxyl, carbonyl, and carboxylic groups, which serve as proton donors to bind the cation MBD, as well as other medium and poor functional groups that contribute to dye removal.

Absorption peaks change, new peals emerge, and others vanish after SAC is filled with MBD (Figure 4.1b). These differences suggested that these functional groups can play an important role in MBD biosorption through electrostatic attraction with positively charged MBD molecules. H-bonding interactions between H atoms on the SAC surface and N atoms in the MBD structure are also part of the biosorption process. Other study on MBD biosorption utilizing coal activated carbon (Jawad et al., 2019) came up with similar theories.

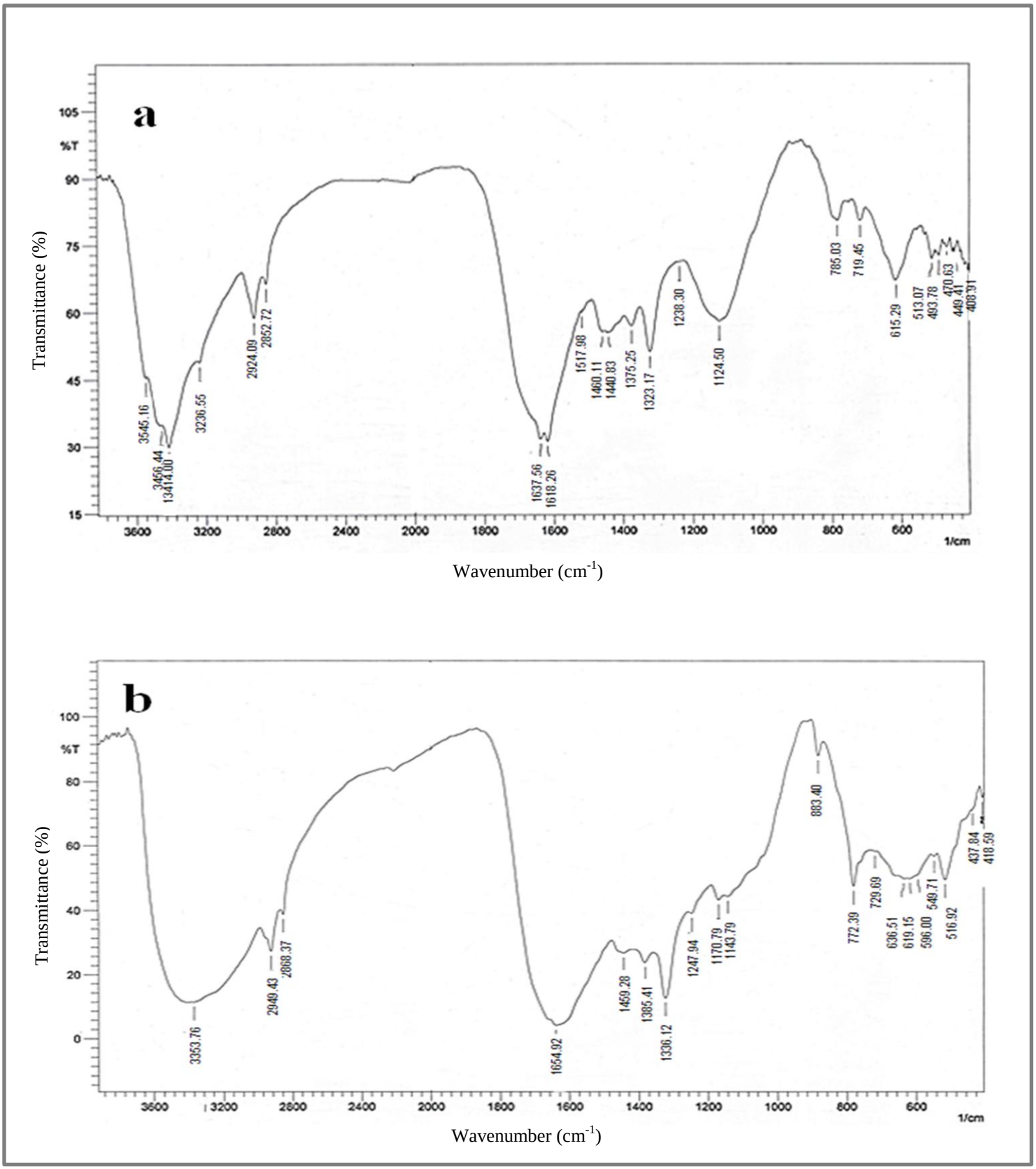

Fig. (4.1 a,b): FTIR spectra of SAC (a) before MBD biosorption and (b) after MBD biosorption.

Table (4.3): FTIR analysis for SAC before and after MBD biosorption.

Functional group	Wavenumber (cm^{-1})		Differences
	SAC	MBD-loaded SAC	
–OH stretching vibrations of hydrogen bonded hydroxyl group of polymeric compounds such as phenols, alcohols and carboxylic acids as in pectin, cellulose group, also the –NH asymmetric stretching of amino groups	3545.16	--------	--------
	3456.44	--------	--------
	3414.00	3353.76	-60.24
	3236.55	--------	--------
Symmetric and asymmetric C-H stretching vibrations of aliphatic acids	2924.09	2949.43	25.34
	2852.72	2868.37	15.65
C=O stretching in organic groups of carboxyl and bending vibration of the functional group of –OH	1637.56	1654.92	17.36
	1618.28	--------	--------
aromatic C=C groups stretching vibrations in aromatic rings	1517.98	--------	--------
	1460.11	--------	--------
	1440.83	1459.28	18.45
$–COO^-$ symmetric stretching vibrations as well as the C-N stretching vibrations and N-O stretching vibrations of aliphatic amines	1375.25	1385.40	10.15
	1323.17	1336.12	12.95
C-O and C-O-C stretching vibrations of carboxylic acids, alcohols, phenols or esters groups	1238.30	1247.94	9.64
	--------	1170.79	--------
	1124.50	1143.79	19.29
C-N stretching vibrations	--------	883.40	--------
	785.03	772.39	-12.64
	719.45	729.69	10.24
Alkyl halides compounds with C-Br (stretching vibration) bond	615.29	636.51	21.22
	--------	619.15	--------
	--------	596.00	--------
	513.07	549.71	36.64
	493.78	516.92	23.14
	470.63	--------	--------
	449.41	437.84	-11.57
	408.91	418.59	9.68

4.2.3 Scanning electron microscopy (SEM) of biosorbent

The SEM technique was used to acquire photographs of the surface morphology and shape of the SAC surface before and after MBD biosorption at varying magnifications. Before MBD biosorption, the SEM images (Figure 4.2a) showed an irregular structure with crevices and many non-homogeneous ravines developed on the SAC surface, which provide a wide surface area for dye removal. There are some visible differences after MBD biosorption (Figure 4. 2b), such as a smooth surface with shiny and white spots. In addition, the surface of SAC tended to be coated in sediments, suggesting that biosorbed MBD had fully filled the pores (Boulaiche et al 2019; Jabar et al 2020) all agreed with this conclusion.

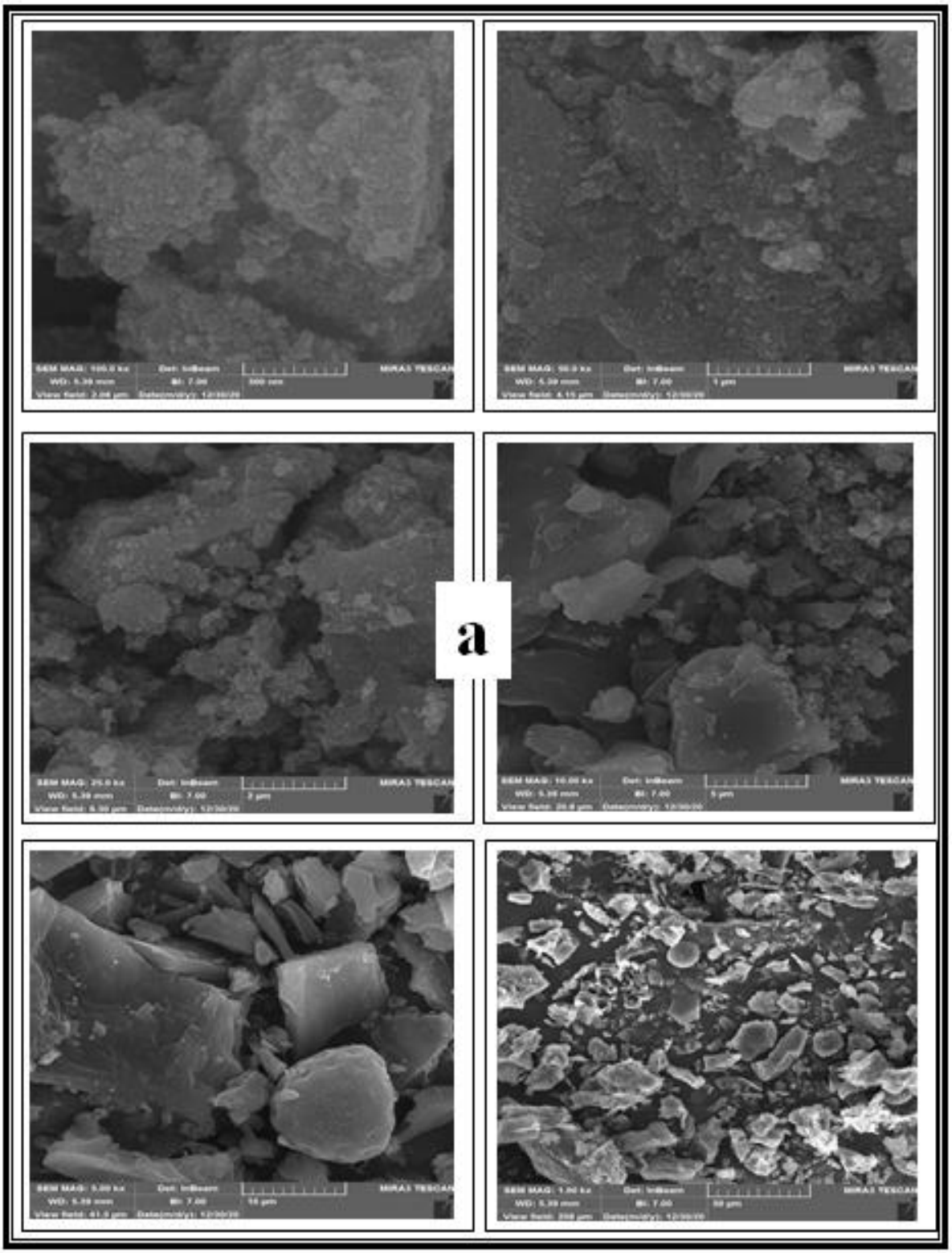

Fig. (4.2 a): The SEM micrograph images of SAC at different magnifications before MBD biosorption

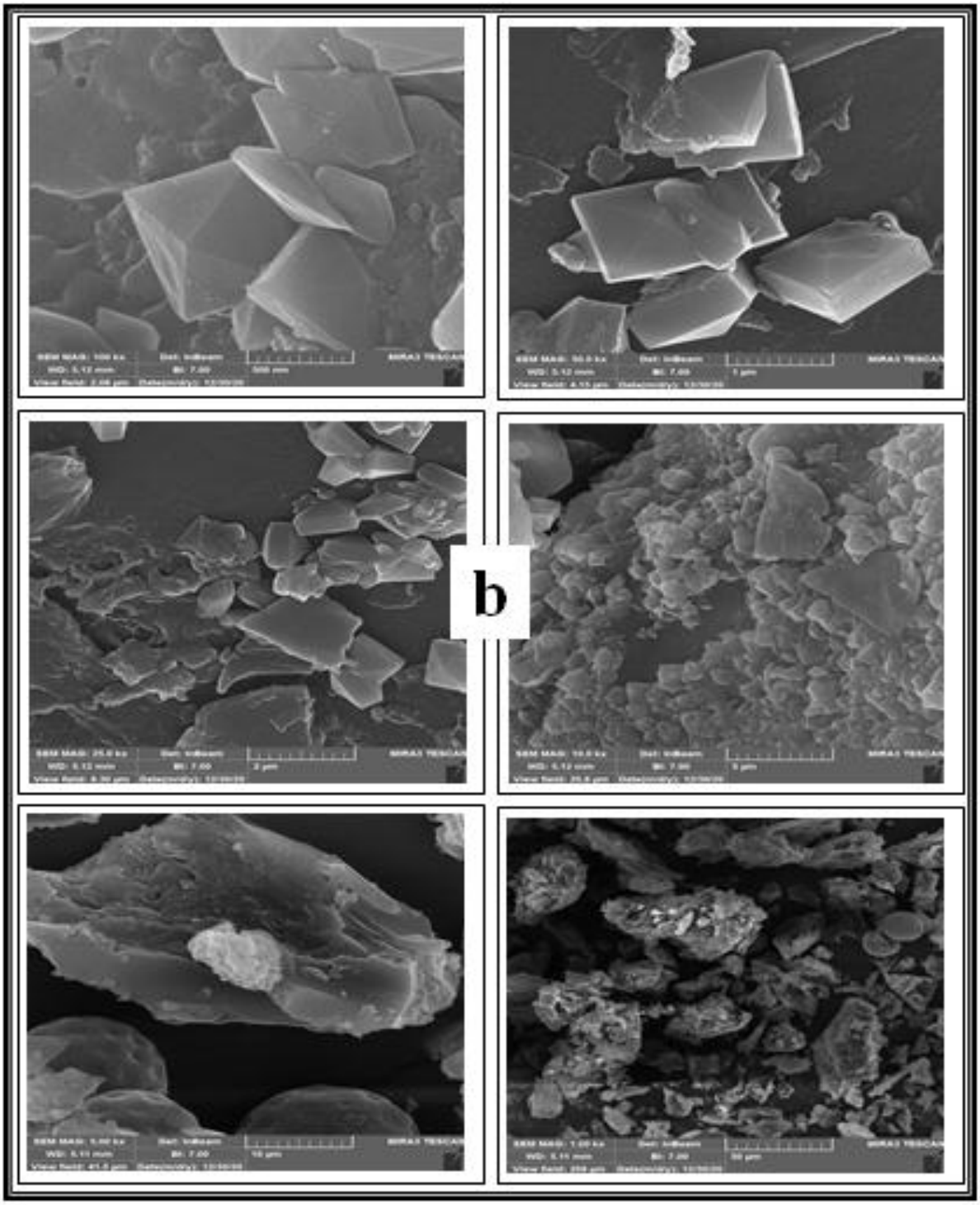

Fig. (4.2 b): The SEM micrograph images of SAC at different magnifications after MBD biosorption.

4.2.4 Scanning probe microscope (SPM)

The SPM test was used to identify and examine the topography of the SAC before and after MBD biosorption, as seen in the Figure (4.3a,b). According to Figure (4.3a), the SAC before MB adsorption has an irregular and distorted surface with large layers of coarse heterogeneous pores, suggesting a high likelihood of dye molecules being adsorbed. The (CSPM) image of SAC after MB adsorption in Figure (4.3b) reveals clearer surface properties with decreased pore structures, meaning that MBD molecules are absorbed and trapped by the accessible pore vicinities of the SAC surface (Jawad et al., 2018 a). The tables (4.4) below display the main findings from this test.

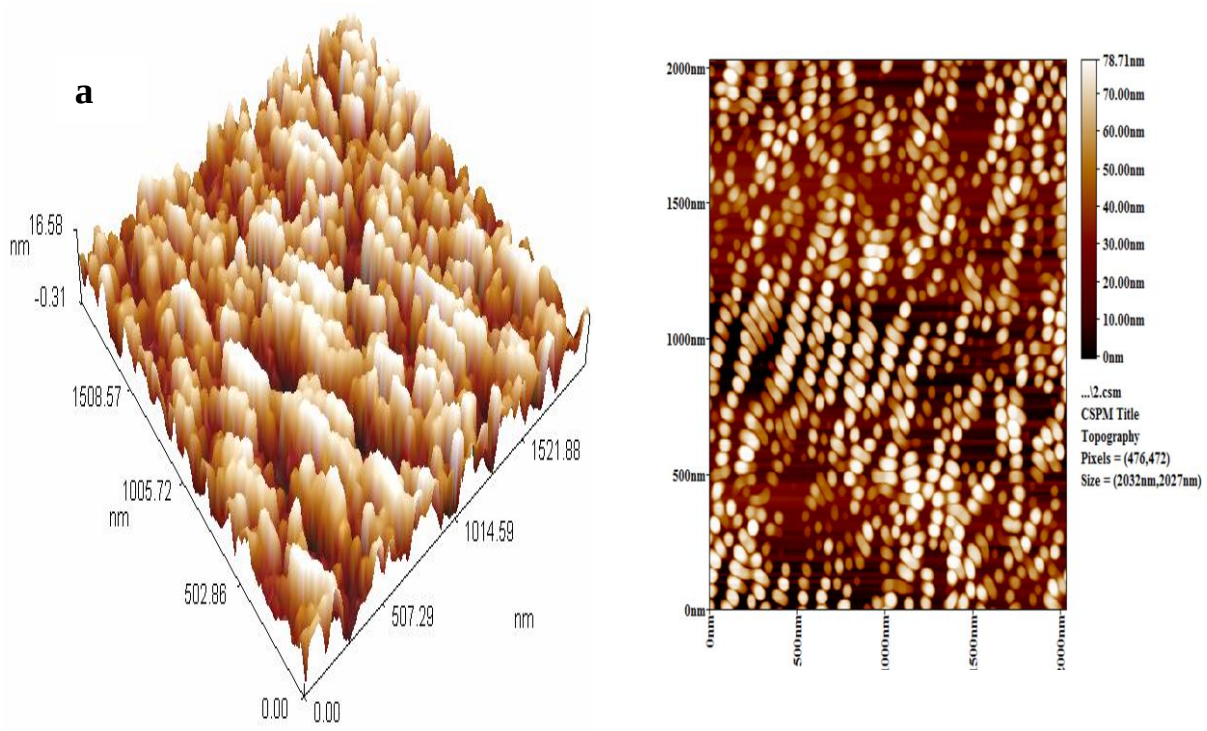

Fig. (4.3 a): Scanning probe microscope for SAC before MBD biosorption.

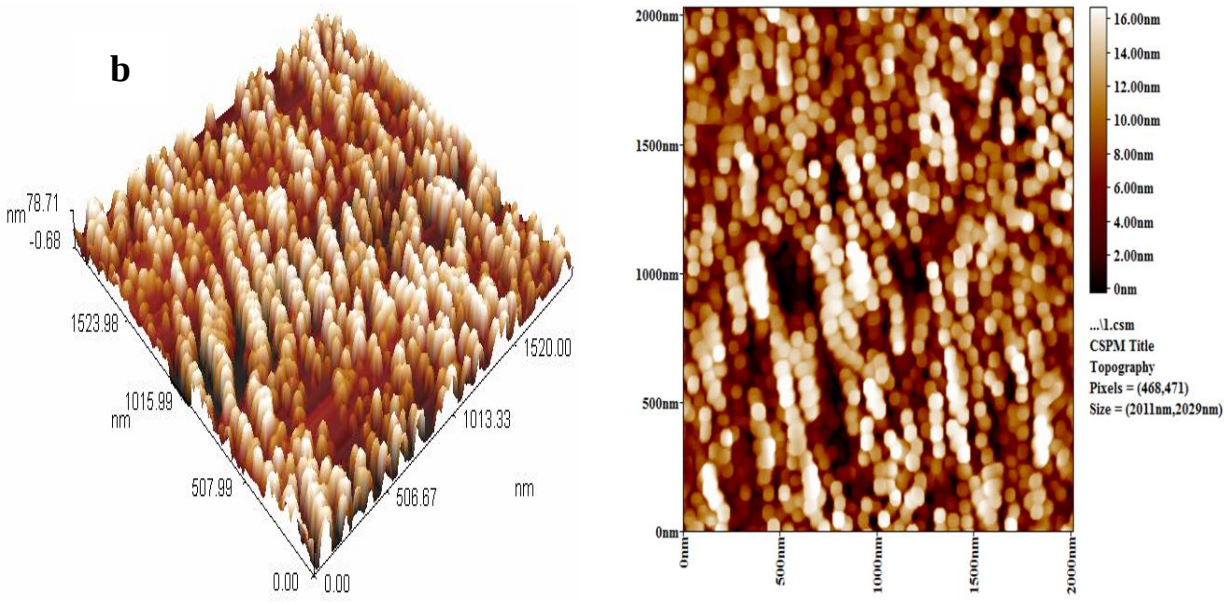

Fig. (4.3 b): Scanning probe microscope for SAC after MBD biosorption.

Table (4.4): SAC characteristics before and after biosorption of MBD by SPM technique**.**

Character	Before	After
Sa (roughness average) (nm)	19.9	3.8
Ssk (surface skewness)	0.00378	0.222
Sz Ten point height (nm)	79.2	16.9
Sdr (surface area ratio)	147	4.06
Sk (core roughness depth) (nm)	69	13.4

4.3 The effect of various factors

4.3.1 Effect of solution pH

The solution pH value plays an important role in the adsorption process, and can affect the adsorbent surface charge, the degree of ionization, and even the adsorbate molecular structure in the solution (Kuang et al., 2020). As shown in Figure (4.4 a,b), the results of initial solution pH of MBD biosorption onto SAC were examined in the pH range of 2 to 10 at room temperature. Figure (4.4 a) shows with a rise in pH values in the range of 2 - 10, the capacity of SAC indicate a substantial increasing pattern from 3.88 to 6.14 mg/g, and the MBD removal efficiency increased from 62.08 to 98.24 % as seen by Figure (4.4b). Therefore, the MBD removal percentage and capacity were increased with the increase of pH value. The pH value of dye solution governs the extent of ionization of the acidic and basic compounds and affect the surface charge of SAC (Fu et al., 2015 ; Asghar et al., 2015). The optimum removal of MBD was noted at pH 9 and was recorded as 98.24 percent, which is also verified by Figure (4.4b). However, no significant changes in adsorbent removal efficiency were found after pH 9, so pH 9 is considered the optimum pH for SAC as a consequence, further studies were carried out at pH 9.

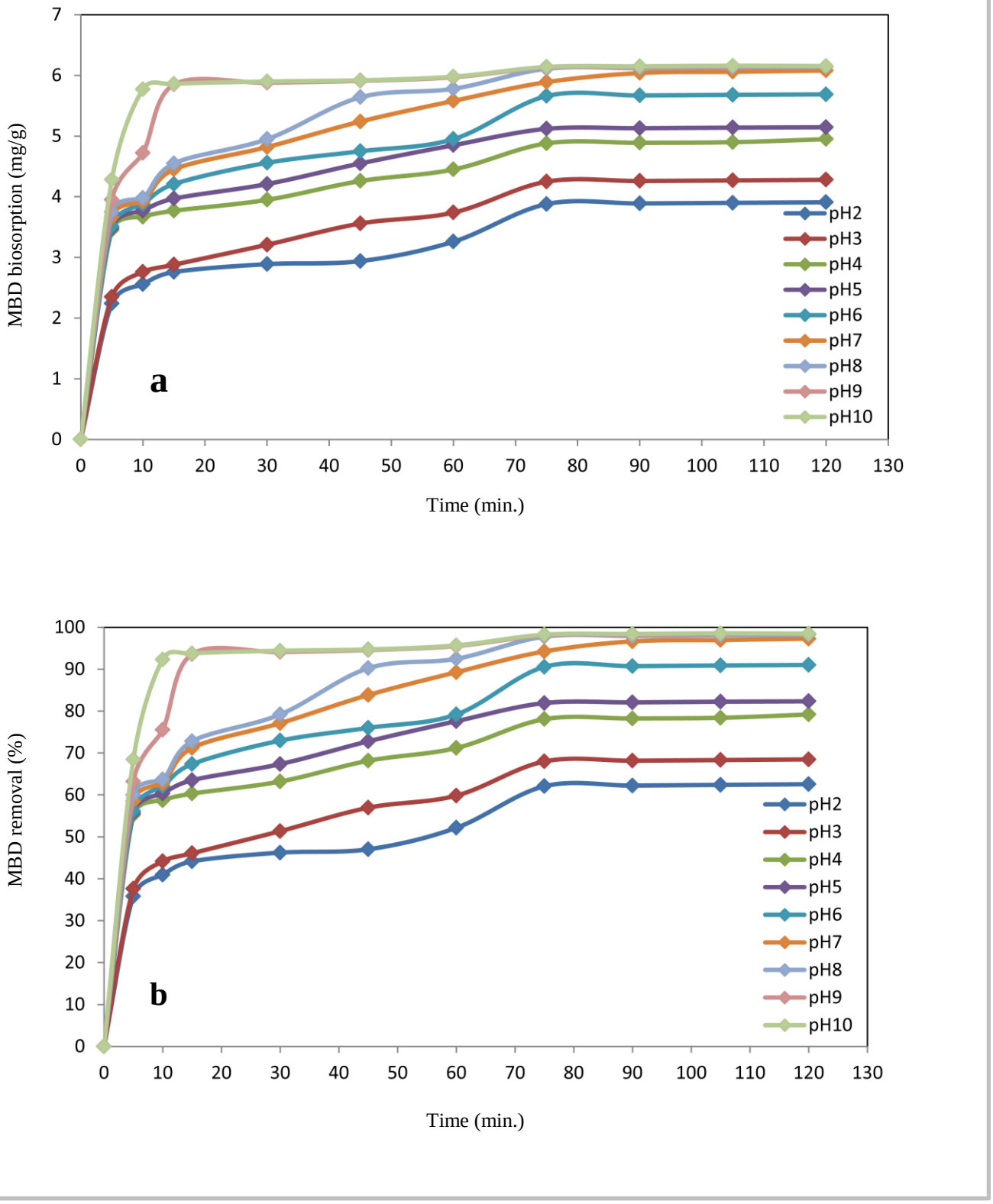

Fig. (4.4 a,b): Impact of initial pH as a function of contact time at different pH on the biosorption of MBD onto SAC.

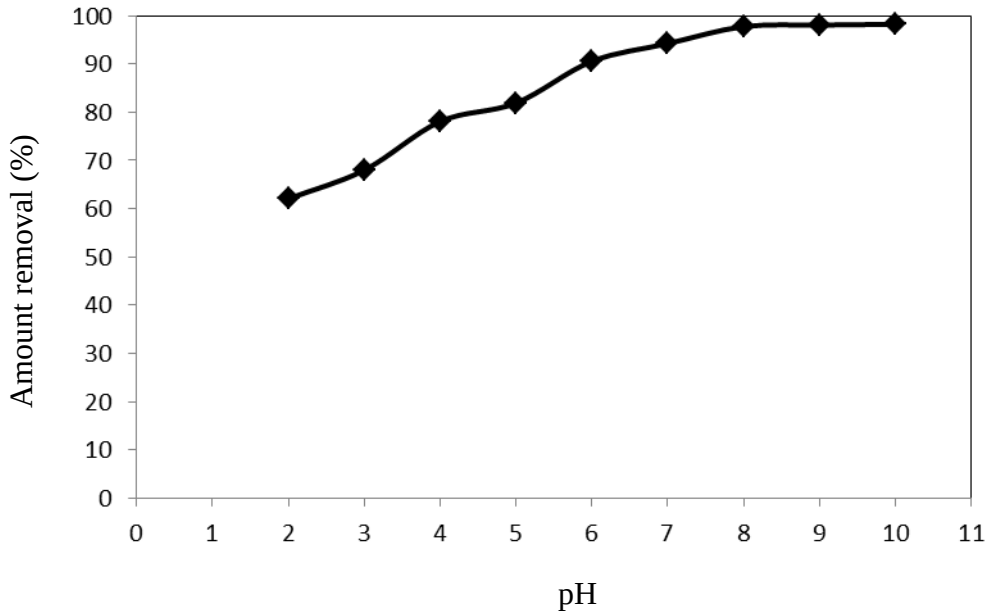

Fig. (4.5): Effect of initial solution pH on the removal efficiency of MBD onto SAC.

At pH 9, the biosorption of MBD onto SAC was the largest, whereas at pH 2, it was the lowest. This indicates that the maximum percentage removal of MBD will be accomplished while the solution is at the greatest fundamental level as can be seen in Figure (4.5). This is attributable to the dominance of negative charges on the biosorbent of surface, which results in increased electrostatic attractions and adherence to MBD due to its cationic composition. A number of other researchers reported the similar conclusions (Auta and Hameed, 2013; Hassan et al., 2014; Rizzi et al., 2017).

Lower percentage removals at acidic conditions (pH 2) can be clarified by the fact that the sorbent of surface seemed positively charged for the cationic adsorbate, resulting in electrostatic repulsion and fewer biosorption (Al-Ghouti and Al-Absi, 2020; Mahmoudi et al., 2015).

The point zero charged (pH_{PZC}) of SAC is 4.4 as shown in Figure (4.6). Since the surface of SAC is positively charged at $pH<PH_{PZC}$ ($pH < 4.4$), there is a heavy repulsion between excess H+ on the biosorbent surface and positively cations of MBD, resulting in poor dye adsorption. When the pH

of the solution > pH_{PZC} (pH > 4.4), the negatively charged surface of SAC acts as a cation attractor, causing intense attraction between the biosorbent surface and the cation MBD, resulting in fast dye biosorption (Belhouchat et al., 2017)

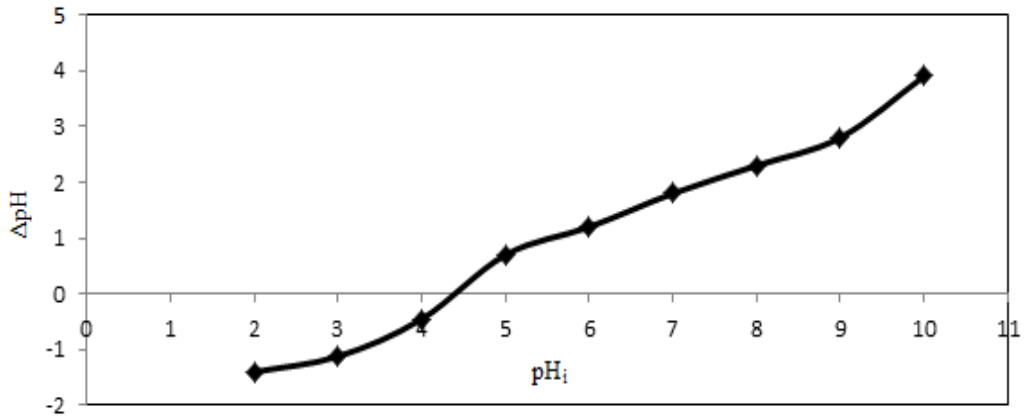

Fig. (4.6): Determination of point zero charge (pH_{pzc}) of SAC.

4.3.2 Impact of contact time

The impact of contact time on biosorption has been investigated in batch biosorption experiments. Contact period between biosorbent and adsorbate has a significant impact on the biosorption mechanism (Saleem et al., 2016). Figure (4.7 a,b) depicts the influence of contact time as a significant experimental factor on the biosorption mechanism in time intervals varying from 5 to 120 min on the biosorption of MBD by SAC. Figure (4.7 a,b) shows that as contact time grew, the removal efficiency and potential of MBD by SAC increased , eventually reaching a maximum value. SAC had a maximum biosorption ability of 6.152 mg/g. Figure (4.7 b) shows the impact of contact time on MBD removal for SAC, and 75.52 percent dye removal occurs in the first 10 minutes. The sharp increase in the slope of the curve (in the first 10 minutes) indicated that the dye was bound to the SAC surface quickly (rapid biosorption region). The higher initial biosorption rate was attributed to the larger number of active sites on SAC and the strong

attractive forces between the dye molecule and the biosorbent. The number of active sites decreased over time, which resulted in a slower rate of dye binding (Pathania et al., 2017). The slope became less steep after that (transition region), because there are few active sites on the surface of biosorbent, suggesting a slow biosorption of up to 75 minutes. The equilibrium period for MBD biosorption at the surface of SAC was observed to be 75 minutes, after which the biosorption capacities of SAC biosorbent did not change significantly (ElSayed, 2018; Hassan et al., 2013).

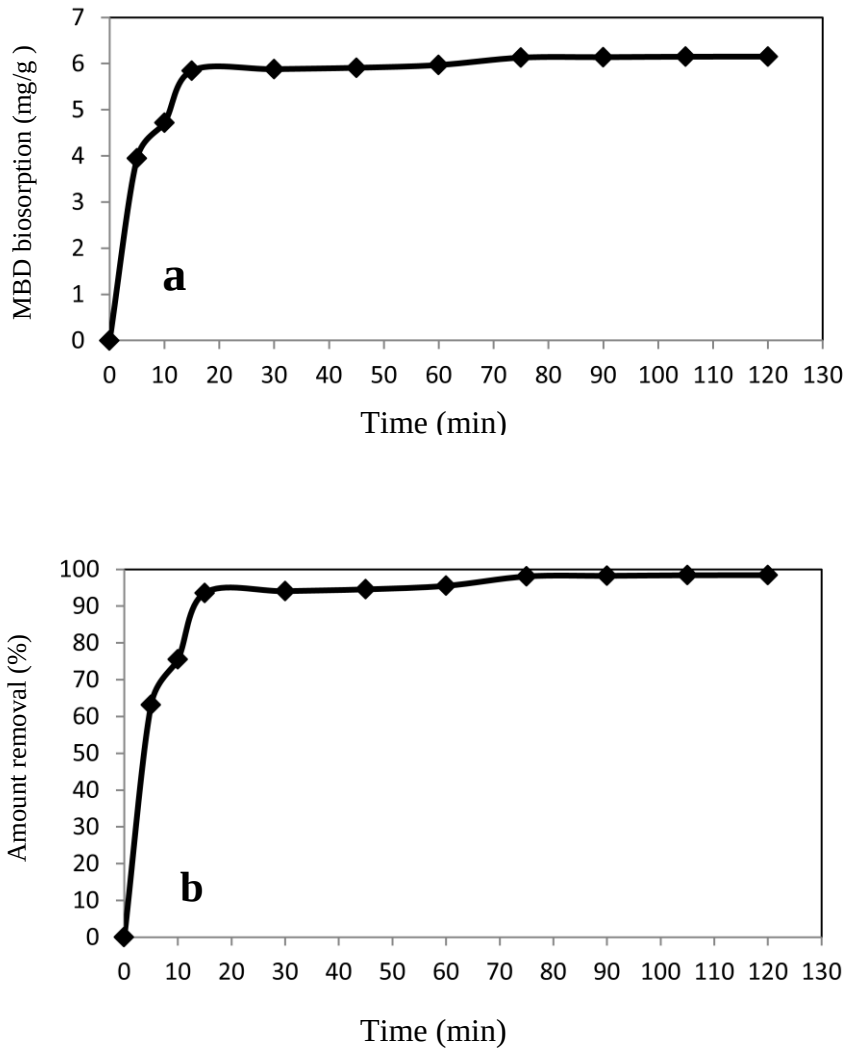

Fig. (4.7 a, b): Effect of contact time on the uptake (mg/g) and percentage removal of MBD onto SAC.

4.3.3 Impact of biosorbent dosage

To investigate the role of the biosorbent dose in the capacity of biosorption and MBD removal performance from aqueous media. The biosorbent dosage of SAC ranged from 0.1 to 1.5 g/100 ml at an initial MBD concentration of 50 mg/l. Figure (4.8) shows the percentage removal and uptake of MBD ions in terms of biosorbent dose. It was observed from the figure that the removal efficiency of MBD improved dramatically from 85.92 to 98.68 % as the dosage of biosorbent increased from 0.1 to 0.8 g. A substantial improvement in MBD biosorption is not detected with the further rise of the biosorbent dose greater than 0.8 g, and thus the optimal SAC dosage was considered to be 0.8 g/100 ml. The improvement in the accessibility of more active adsorbent sites for MBD biosorption with an increase in the adsorbent dose can be accompanied by this periodic increase in removal efficiency. It is noteworthy, however, to note here that the ability of biosorption has followed the surprising drop pattern in the biosorption capacity from 42.96 to 3.31 mg g^{-1} for SAC was observed with a rise in the biosorbent dosage from 0.1 to 1.5 g/100 ml (Uddin and Rahman, 2017). This can be due to the fact that the increased adsorbent concentration most likely increases the interactions of the biosorbent, such as agglomeration and accumulation, contributing to a significant decrease in the biosorbent total surface area and consequently to a decrease in its biosorption ability (Mashkoor and Nasar, 2020).

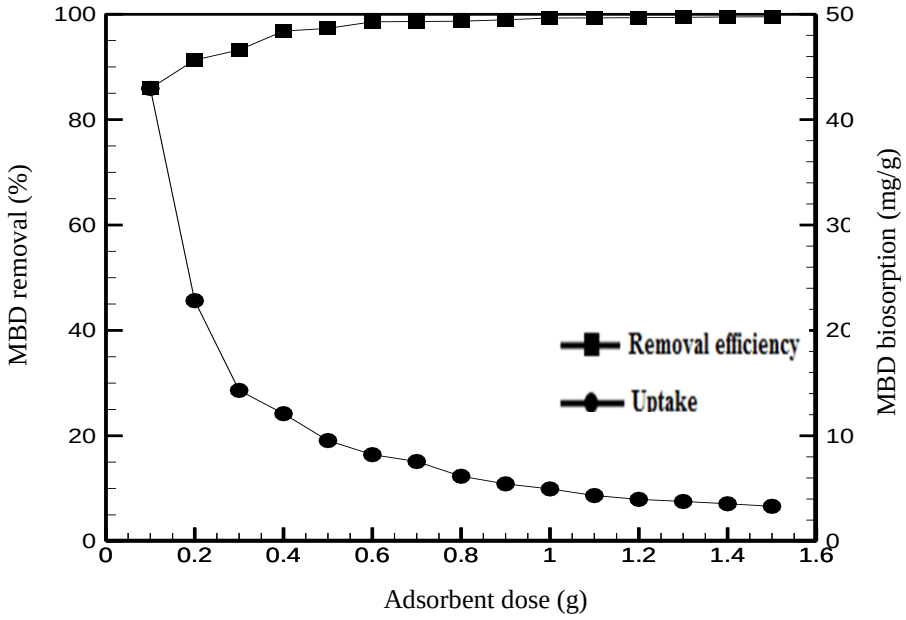

Fig. (4.8): Percentage removal and uptake of MBD ions in terms of biosorbent dose.

4.2.4 Impact of primary MBD concentration

In biosorption experiments, the initial dye concentration is a critical element. The effect of the primary concentration of MBD solution (10 - 100 mg/l) on removal efficiency and biosorption capacity in this sample is shown in Figure (4.9). The efficiency of dye removal decreased as MBD concentration rose from 10 to 100 mg/l, with a drop in the range of 100 - 96.8%. The biomass removal capacity, on the other side, increased in direct relation to the initial MBD solution concentration. The biosorption increased from 1.25 - 12.1 mg/g while the primary MBD concentration was increased from 10 - 100 mg/l. The removal efficiency was also stated to decrease as the dye concentration was increased in various studies. If the dye content rises, the number of possible active adsorption sites on the biomass surface decreases, and there are no more places to adsorb dye onto SAC (Geetha et al., 2015). In other studies, biomass adsorption was found to increase with

the initial dye concentrations. This may be as a result of the increasing driving force (Oguntimein, 2015; Dahiru et al., 2018).

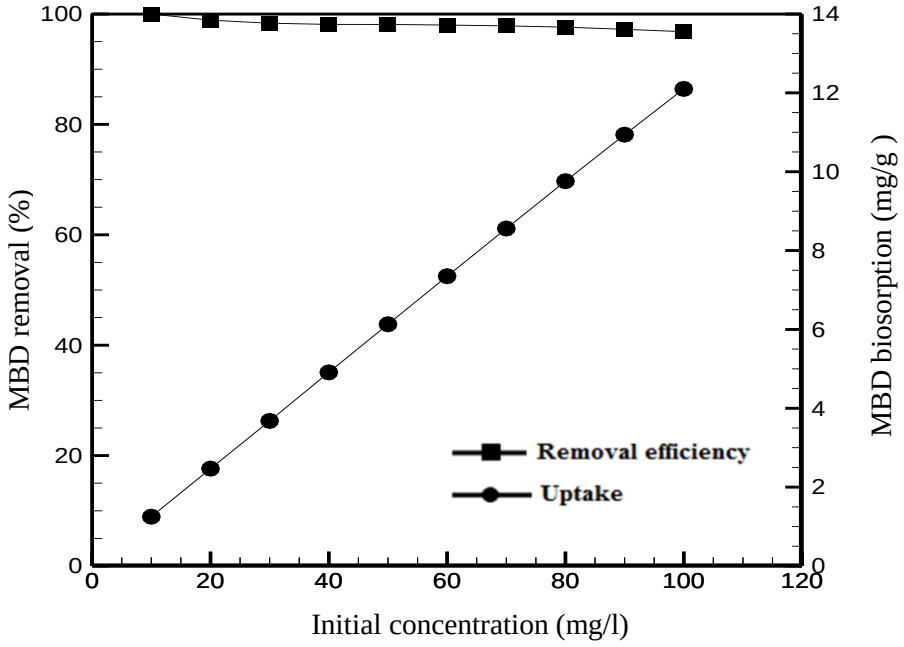

Fig. (4.9): Percentage removal and uptake of MBD ions as a function of MBD concentration.

4.4 Isotherm analysis

At constant temperature and pH, adsorption isotherms define the relationship between the quantity of adsorbed content on the adsorbent (q_e) and the equilibrium concentration in the bulk fluid (C_e). The applicability of the SAC in remediating MBD from wastewater was evaluated using two isotherm models such as Langmuir and Freundlich (Figure 4.10 a,b). The R^2 values of the two isotherm models were both very high, with the Langmuir model R^2 value being the largest at 0.9954. Despite the strong R^2 (0.9785) of the Freundlich model, the simulation plots in Figure (4.10 b) reveal that it is clearly not the right match for the biosorption of MBD onto SAC. This is also supported by the model higher standard error of the estimate (S.E.) value (Table 4.5). While both the R^2 and (S.E.) value of the Langmuir

isotherm model yield identical simulation curve, the Langmuir model is better adapted to characterize the adsorption mechanism of MBD onto SAC. This experimental result of creating a monolayer on the surface of SAC is supported by the volume of the MBD molecule. According to the Langmuir model, SAC has a maximum potential of 33.34 $mg.g^{-1}$ for the removal of MBD, which is far higher than many other recorded biosorbents (Table 4.6). SAC, on the other hand, may be called a very good low-cost biosorbent for the removal of MBD since it is a natural biosorbent that has not been processed or chemically changed. The excellent fit for the Langmuir model indicates that with monolayer coverage, MBD biosorption is limited and the surface is generally homogeneous in terms of functional groups, and there is no the MBD molecules interact greatly.

A dimensionless constant called the equilibrium parameter, R_L defined by the dimensionless constant, will represent the significant characteristic of the Langmuir isotherm in Eq (2.5). R_L was between (0 – 1), indicating a desirable isotherm. The R_L values were in the range of 0.0467 - 0.3333, suggesting a desirable dye adsorption mechanism on activated carbon (Nibret et al., 2019) as can see the separation factor in Figure (4.11).

An isotherm of Freundlich implemented as an analytical model. adsorption intensity or surface heterogeneity was described by the slope (1/n) values. When the value of (1/n) is between 0.1 and 1.0, it is commonly considered to be a symbol of a successful adsorption operation. The index value in this study was within the range (0.39), meaning that the adsorption method is suitable. Thus, the magnitude of the Freundlich constant indicates the easy sorption capacity of MBD from an aqueous media (Mahmoud, 2015; Quansah et al., 2020).

The comparisons of the MBD uptake potential between the experimental results and that derived by the use of Langmuir and Freundlich models are seen in Figure (4.12).

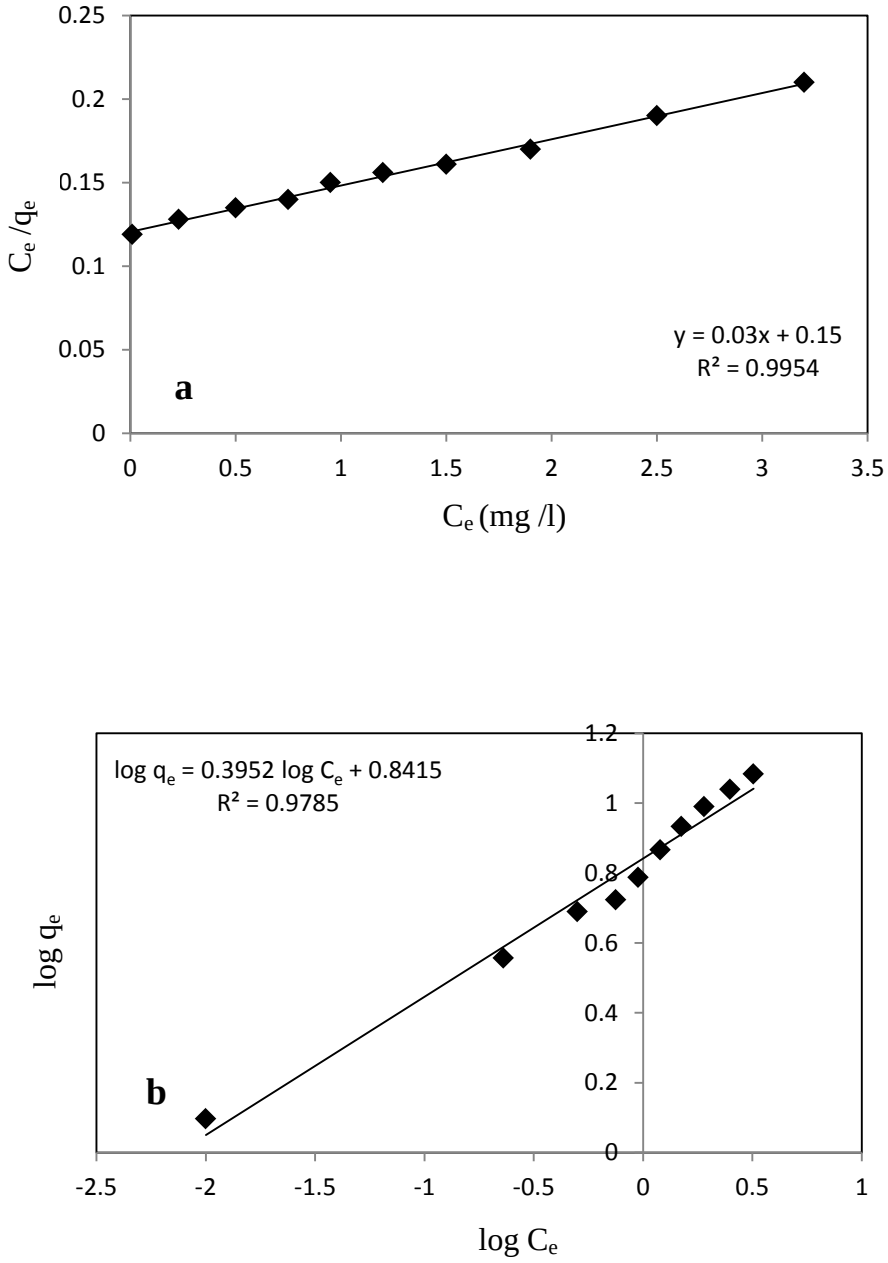

Fig. (4.10): Linearized biosorption isotherm model of MBD onto SAC (a) Langmuir model (b) Freundlich model.

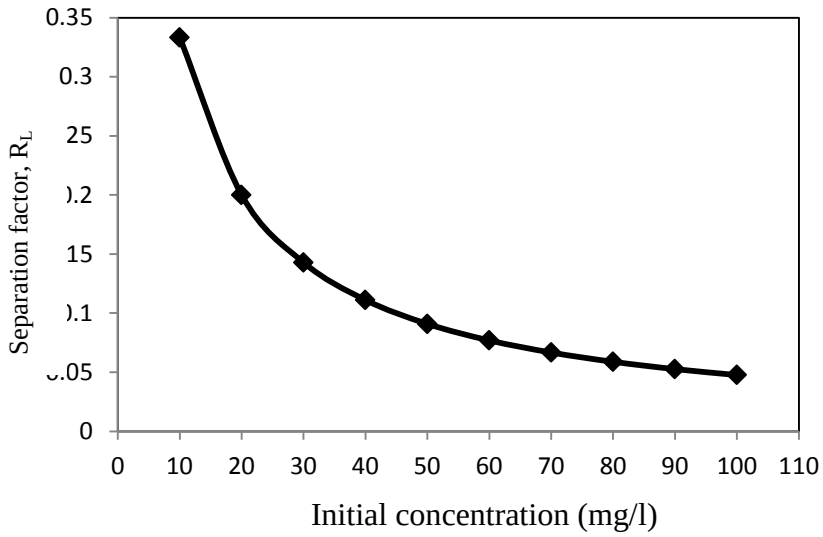

Fig. (4.11): Values of separation factor, R_L for biosorption of MBD onto SAC.

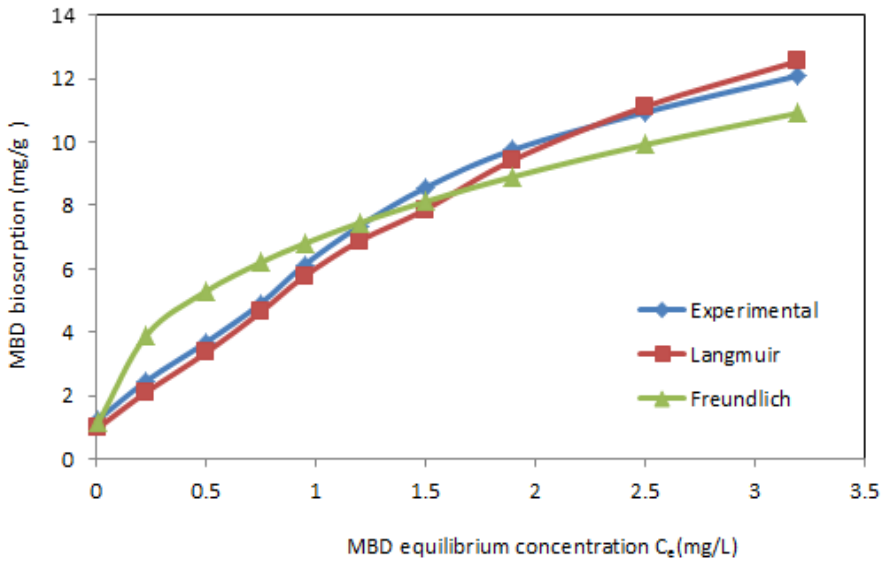

Fig. (4.12): Comparison of experimental and calculated data by Langmuir and Freundlich.

Table (4.5): Constants of biosorption isotherm for MBD using SAC.

Langmuir (95% Confidence level)		Freundlich (95% Confidence level)	
q_m (mg/g)	33.34	K_F (mg/g)(l/mg)$^{1/n}$	6.94
K_a (l/mg)	0.2	1/n	0.39
R^2	0.9954	R^2	0.9785
S.E.	0.00204	S.E.	0.04522
R_L	(0.0476 - 0.3333)		
Equation	$q_e = 6.67C_e / 1+0.2C_e$	Equation	$q_e = 6.94\ C_e^{0.39}$

Table (4.6): Comparison of maximum biosorption capacity (q_{max}) of SAC with other biosorbents reported for removal of MBD.

Adsorbent	**q_{max} (mg.g^{-1})**	**Reference**
Neem (Azadirachta indica) leaf powder seeds	19.6	Bhattacharyya and Sharma, 2005
NaOH-modified rejected tea	2.44	Nasuha and Hameed, 2011
Alginate grafted polyacrylonitrile beads	3.51	Salisua et al., 2015
Artocarpusheterophyllus (Jackfruit) seed	26.4	Kooh et al., 2016
Wild carrot	21	Swamy et al., 2017
Bush Cane Bark Powder	23.49	Enenebeaku et al., 2017
Defattedalgal biomass	7.8	Guarín et al., 2018
Water hyacinth root	2.8969	Nibret et al., 2019
Rice husk	25.46	Quansah et al., 2020
Natural plant (Schanginia/sp.)	**33.34**	**The present study**

4.5 Adsorption kinetics studies

The biosorption was measured using a concentrations of (25, 50, 100, 200) mg/l and a mass of 0.8 g, with a contact time between the biosorbent and MBD ranging from 5 to 120 minutes at pH 9 at room temperature (25 ± 5^0C). According to Figure (4.13) the biosorbent experienced a fast rise in capacity of biosorption in the first 10 minutes. Later this period, it became slower and remained practically constant at 75 min (equilibrium time). The findings are attributed to the fact that the dye to be biosorbed was almost entirely present in the solution during the initial step of the biosorption, with a high chance of reaching the biosorbent surface, and the active sites were unoccupied at the start of the method. Through the passage of time, the concentration of MBD decreased due to movement of dye to unoccupied sites, which hampered the biosorption process by the competition for the remaining available sites through residual dye particles. The literature (Wong et al., 2016; Kumar and Jena, 2016; Pang et al., 2017; Heidarinejad et al., 2018) has already published on the results of this behavior. These studies are conducted to find the rate and mechanism of adsorption

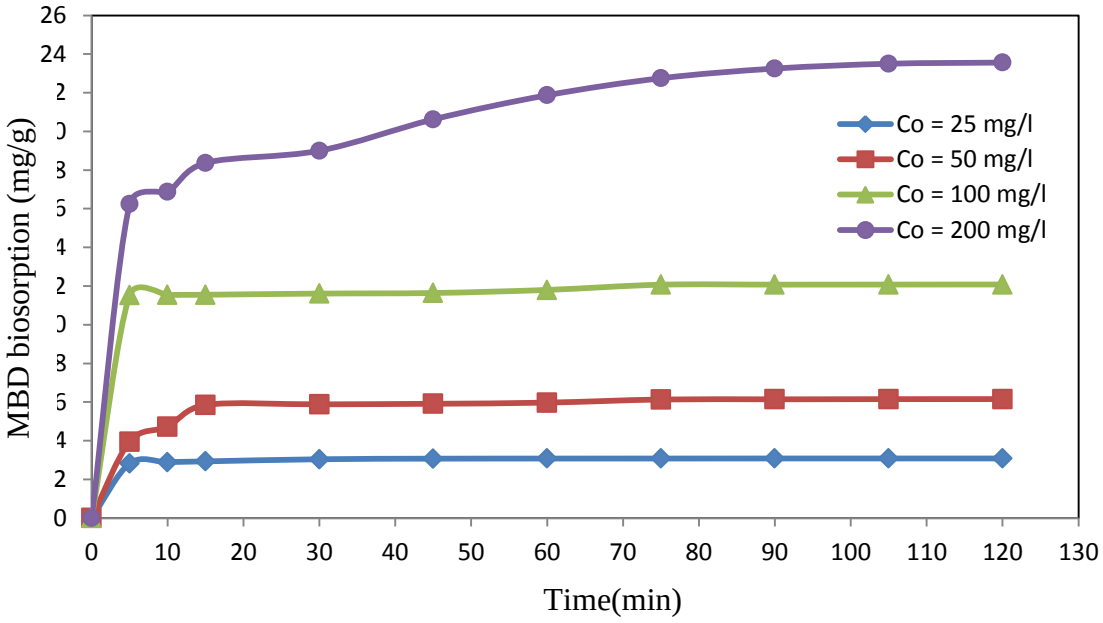

Fig. (4.13): The change of amount biosorbed (mg/g) at various times and various initial MBD concentrations.

The experimental data are fitted using the three kinetic models which cited in section (2.11)

4.5.1 Model of pseudo first order lagergren

Figure (4.14) displays the linearized version of the pseudo first order kinetic model plotted at various dye concentrations. Table (4.7) shows the measured rate constants, experimental and expected q_e, and the related correlation coefficient values. The estimated q_e values from the first-order kinetic model are not rational compared to experimental q_e values. The rate constant k_1 is a function of the process conditions. It is reported to decrease with increasing initial dye concentration (Naushad et al., 2015; Chinoune et al., 2016), reduction in k_1 and hence in rate could be a result of the increased diffusional resistance across the boundary layer (Bayomie et al., 2020) which may be understood as follows: $1/k_1$ is the time scale for the process to reach equilibrium; a longer time is needed (smaller k_1) if the initial concentration (C_o) is larger. If the biosorption kinetics obey the pseudo-first-order model, an improvement in the dye solution concentration would result in a linear increase in the rate constant changeover (Kahori et al., 2017). According to the pseudo-first-order kinetic model, the rate of biosorption site occupancy is proportional to the number of unoccupied sites (Salam, 2013; Farooq et al., 2010). In certain instances, Lagergren first-order equation does not match the full spectrum of interaction time and is only appropriate for the initial stages of adsorption processes (Dileepa et al., 2013). As comparing the value of R^2 obtained for pseudo-first order model with the second model showed that MBD biosorption onto SAC did not follow this model. These observations lead us to say that the biosorption of MBD does not express a controlled diffusion process since it does not follow the pseudo-first order equation given by Lagergren (El-Maghraby and Nahla, 2014)

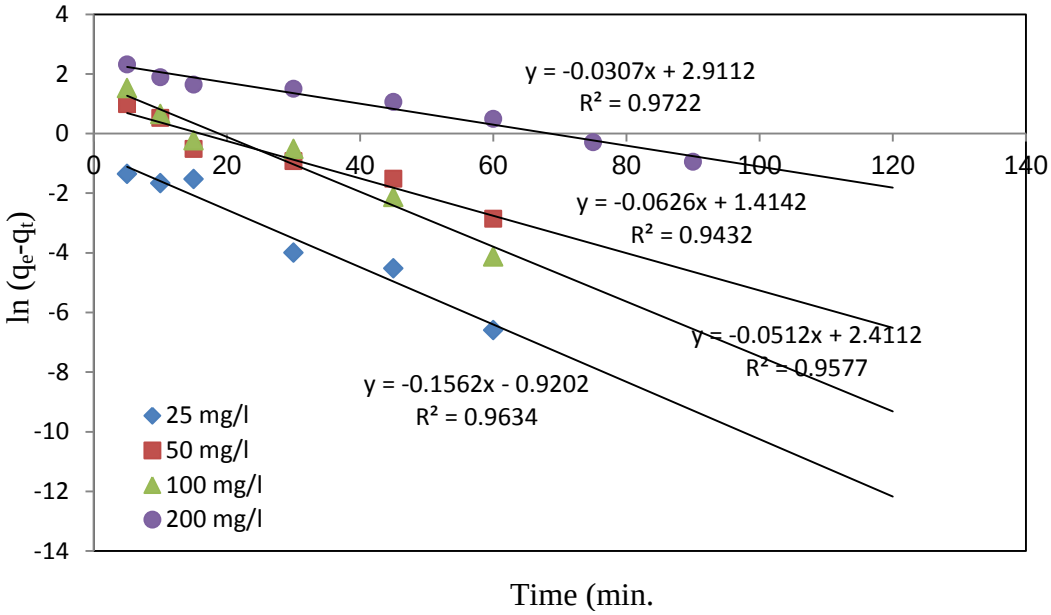

Fig. (4.14): Pseudo -first-order kinetic plots for biosorption of MBD onto SAC at different initial dye concentrations.

4.5.2 Model of pseudo second order

Figure (4.15) depicts plot of the linearized version of the pseudo second order kinetic model at different dye concentrations. Straight lines emerge from plot of t/q_t vs. t, showing that the mechanism approaches pseudo second order kinetics. In comparison to many other kinetics methods, this model biggest benefit is the potential to predict over a wide variety of studies. If this model is right, the electrostatic interaction and chemisorption process is the rate-controlling phase that includes electron sharing and exchange between the adsorbate and biosorbent (Dileepa Chathuranga et al. 2013; Li et al. 2014). According to Table (4.7), adsorption ability increases with increasing initial dye concentration and k_2 (0.4476 to 0.0282 $g.mg^{-1}.min^{-1}$) for SAC decreases with initial dye concentration increased. This behavior can be explained by the fact that at lower concentrations, there is less competition for sorption sites. The competition for the surface active sites would be fierce at higher concentrations, resulting in lower sorption rates (Ansari et al., 2016). And the failure of the first-order to provide a

clearer explanation of the adsorption mechanism may be due to boundary layer constraints controlling the adsorption method (Obayomia et al., 2019). The rise in the driving force for mass transfer, which allows more dye molecules to enter the surface of the biosorbents in a shorter period of time, may be due to the increase in the initial adsorption rates, h (Table 4.7) with an increase in the initial dye concentration (Han et al., 2011; Dawood and Sen, 2012; Nanganoa et al., 2014), if the dye adsorption is chemically rate controlled, the pseudo-second-rate constant will be independent of particle diameter and flow rate will depend on concentration of the ions in solution (Fideles et al., 2018) as seen in Table (4.7). For all initial dye concentrations, the correlation coefficients R^2 of determination obtained from the plots were found to be quite near to unity. As R^2 values of pseudo first order model for all dye concentrations are less than the values of R^2 for the pseudo second order model and the values of q_e, cal from the first model are diverged to the experimental values of q_e (q_e, exp), but those values are closed by using the second model. In comparison to the pseudo first order kinetic model, straight lines obtained from pseudo second-order kinetic plots mean that the pseudo second order kinetic model will match the experimental data across all stages of the biosorption period. As a result, it is concluded that pseudo second-order model is the best match for the biosorption operation, and that the rate-controlling phase could be electrostatic interaction and chemisorption mechanism. These findings show that the pseudo second-order sorption mechanism is the most common (Malik, 2004; Kannan and Sundaram, 2001; Nemeş et al., 2016) and its rate is proportional to the square of the biosorbent's available adsorption sites (Ho and McKay 1999). These findings are consistent with MBD adsorption on pomegranate jackfruit peels (Hameed, 2009) and (Punica granatum) peels (Jawad et al., 2018).

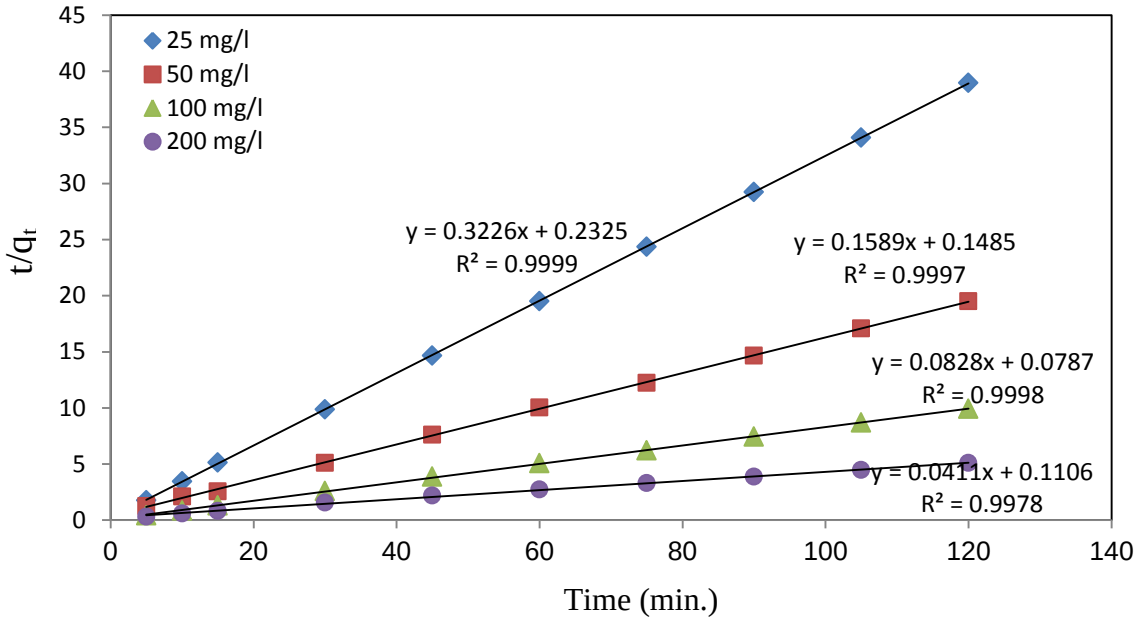

Fig. (4.15): Pseudo second-order kinetic plots for sorption of MB dye onto SAC at different initial dye concentrations.

4.5.3 The intraparticle diffusion model

The diffusion mechanism was identified using an intraparticle diffusion model. The q_t versus $t^{1/2}$ plot for various concentration were explained by Figure (4.16). The intraparticle diffusion model was used to further investigate the kinetic processes, because of the intense electrostatic attraction between the dye and the exterior surface of the adsorbent. Table (4.7) lists the intraparticle diffusion model parameters, k_{ip} and C . The higher k_{ip} values indicate a higher intraparticle diffusion rate. Furthermore, The thickness of the boundary layer can be measured using C values of an intraparticle diffusion model , which is positive and increases with time for biosorbent, indicating that the thickness of the boundary layer is increasing and controlling the MBD biosorption rate into this biosorbent (Boudechiche et al., 2016; Zarrabi, 2016). For the biosorption of MBD onto SAC, the k_{ip} values for MBD improved as concentration increased at all levels. With increasing initial dye concentration, the value of intercept, C increased from the first to the third step, which may be attributable to the boundary layer

influence. If the thickness of the boundary layer rises, outward mass transfer reduces, increasing the probability of internal mass transfer (Samiey and Ashoori, 2012 ; El-Haddad et al., 2014; Cai et al., 2019; Pholosi et al., 2020). Low-cost biomass content lotus leaf (Han et al., 2011), sugar beet pulp (Vučurović et al., 2012), biosorption of MBD onto activated carbons prepared from NaOH-pretreated rice (Chen et al., 2013) and Luffa cylindrica fiber-activated carbons (Cherifi et al., 2013) have yielded similar results.

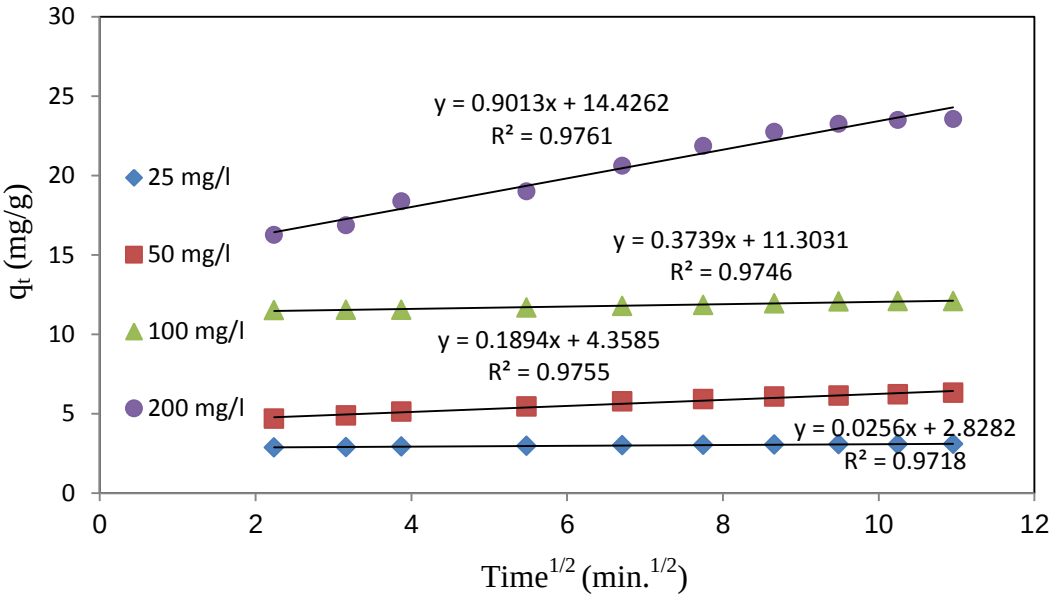

Fig. (4.16): Linear intraparticle diffusion kinetic model of MBD onto SAC biosorbent at different dye concentrations.

Table(4.7): Kinetic parameters of various models fitted to MBD biosorption experimental data using SAC.

Kinetic models	**MBD concentration(mg/l)**			
	25	**50**	**100**	**200**
Pseudo- first- order				
q_e, exp (mg/g)	3.10	6.13	12.16	24.50
q_e, calc.(mg/g)	2.51	4.11	11.14	18.37
K_1 (min^{-1})	-0.1562	-0.0626	-0.0512	-0.0307
R^2	0.9634	0.9432	0.9577	0.9722
Pseudo –second- order				
q_e, calc. (mg/g)	3.01	6.29	12.07	24.33
K_2 (g mg^{-1} min^{-1})	0.4476	0.1702	0.0871	0.0282
h (mg $g^{-1}min^{-1}$)	4.27	7.09	12.68	16.71
R^2	0.9999	0.9997	0.9998	0.9978
Intraparticle diffusion				
K_{ip}(mg g^{-1} $min^{-0.5}$)	0.0256	0.1894	0.3739	0.9013
C (mg/g)	2.8282	4.3585	11.303	14.4262
R^2	0.9718	0.9755	0.9746	0.9761

4.6 Study of Mechanism

In systems with high adsorption rates, high adsorption mass concentrations, and large adsorbent particle sizes, the intraparticle diffusion mechanism helps to regulate the rate of adsorption. The adsorption dynamics in the MBD attachment phase normally consist of three steps:

The first part of the Figure (4.17) is due to the transport of solute from bulk solution to the biosorbent exterior surface via a liquid film. Following that, the intraparticle diffusion is attributed as a slower process in the second half. In reality, the rate of adsorption is determined by the slope of the linear portion: a lower slope means a slower adsorption process (Oguntimein., 2015). Since the slope of the first linear segment was higher than the slope of the second linear portion, the rate of diffusion of MBD molecules across boundary layer film in the early stages of the adsorption phase was faster than the rate of intraparticle diffusion. The MBD molecules are easily adsorbed onto the surface of the activated carbon at first, and the MBD molecules diffuse into the interior of biosorbent particles until saturation is

achieved. Finally, the final equilibrium stage is related to the intraparticle diffusion slowing down due to the low concentration dye in the aqueous solution (Hong and Wang, 2017; El maguana et al., 2020). Figure (4.17) shows the plot of the intraparticle diffusion model, which is linear to show that the biosorption process involves the intraparticle diffusion and does not proceed through the origin, suggesting that intraparticle diffusion was not the only rate limiting stage of the biosorption process of MBD onto SAC, and that other pathways may be working at the same time. The description of parameter with respect to part are described in Table (4.8) for various concentration utilizing SAC biosorbent. Film diffusion was found to be more dominant than pore diffusion based on correlation coefficient (R^2) values. The results for the removal of MBD using various low-cost adsorbents were considered to be in close alignment with literature (Kushwaha et al., 2014; Banerjee et al., 2016; Singh et al., 2017). Surface adsorption and intraparticle diffusion defined the entire adsorption mechanism, which was complicated. As a result of the deprotonated acidic groups, the surfaces of the SAC sample are negatively charged at a functioning pH 9. Because of intense electrostatic forces, oxygen atoms have a high affinity for positively charged molecules and cations. Since MBD is a cationic dye, it is obvious that electrostatic interactions play a role in its biosorption onto SAC. The chemical structure of MBD, on the other hand, contains many aromatic rings and cationic atoms, making it ideal for biosorption on the surface of SAC via ionic interaction (Liu et al., 2019). In certain instances, cations can improve anionic species biosorption by improving the binding of negatively charged anions. Because of pH buffering effects, cation loading of biomass can enhance biosorption of another cation in some cases (Cheriti et al., 2011).

So, the MBD biosorption onto SAC may be involved (i) chemical interaction between MBD molecules and surface functional groups (ii) electrostatic interaction between the electron-rich sites on the biosorbent

surface and MBD molecules, and (iii) weak physical forces, hydrogen bonding and van der Waals interactions between the biosorbent and MBD molecules. Therefore, the MBD biosorption onto SAC surface occured by both physical and chemical adsorption.

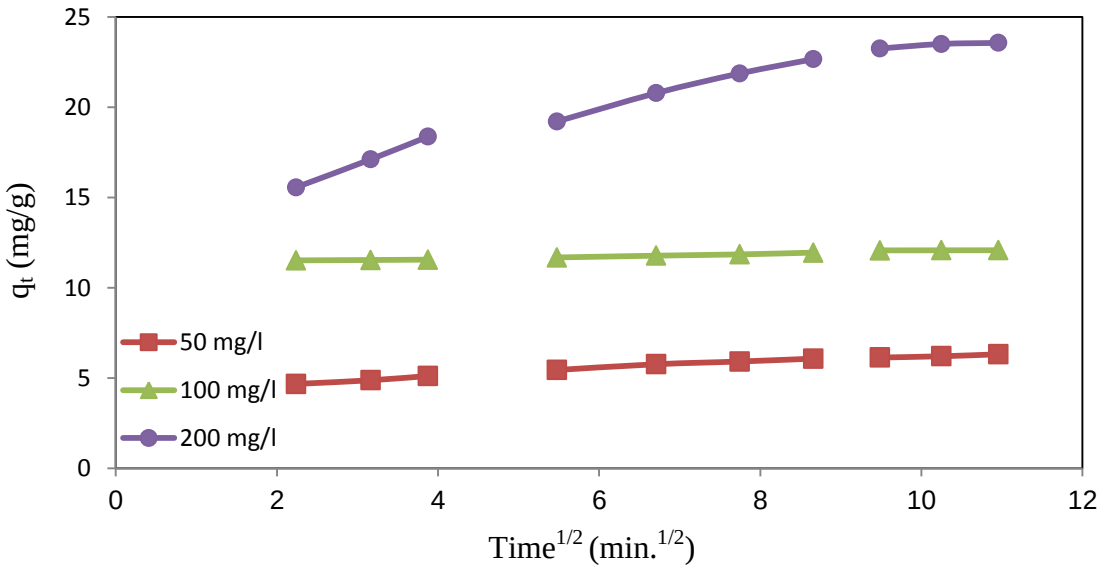

Fig. (4.17): Multi- linearity graph of intraparticle diffusion model of MBD onto biosorbent at different dye concentrations.

Table (4.8): Multi-linearity parameters of intraparticle model based biosorption mechanism study of MBD onto SAC.

MBD (mg/l)	K_{ip1} (mg g^{-1} $min^{-0.5}$)	C_1 (mg/g)	R_1^2	K_{ip2} (mg g^{-1} $min^{-0.5}$)	C_2 (mg/g)	R_2^2
25	0.0306	2.81	0.9985	0.0255	2.84	0.9979
50	0.2662	4.07	0.9836	0.1942	4.41	0.9823
100	0.9593	7.88	0.9927	0.1184	10.96	0.9738
200	1.7145	11.71	0.9997	1.0868	13.36	0.9928

4.7 Experiments of continuous flow (Column test)

This experiment help in understanding and forecasting process behavior. Understanding the adsorption dynamic and modeling is critical for calculating sorbent potential and the time it takes to reach the breakthrough curve. It is important to conduct an adsorption experiment utilizing a fixed bed column. The nature of the breakthrough curves and the breakthrough time at which MBD concentration reaches the threshold values were calculated and studied for various operating parameters such as MBD solution bed inlet flow rate , bed height , and initial dye concentration. The residual MBD was quantified using a spectrophotometrically evaluated at a wave length of 664 nm. When C/C_o = 0.05, a biosorbent bed quality warning, 5% breakpoint time is applied as the time necessary to reach breakpoint.

4.7.1 The impact of flow rate on MBD biosorption

The flow rate has an effect on the biosorbent performance and efficiency in a continuous column biosorption operation. The influence of MBD flow rate on the breakthrough curves and biosorption capacity was investigated by varying the MBD flow rate while keeping other process parameters such as bed height and initial MBD concentration constant. The breakthrough curves of the plot of (C/C_o) against t (min) for various flow rates are shown in Figure (4.18). Table (4.9) Shows the detailed results different experiments. The breakthrough and saturation periods were lowered when the MBD flow rate was increased from 10 ml/min to 20 ml/min, as shown in Figure (4.18). The breakthrough time was lowered from 480 to 165 minutes as the MBD flow rate was raised, as shown in Table (4.9). The volume of MBD solution entering the column rises as more adsorbate molecules come into contact with the fixed bed biosorbent at

greater flow rates, resulting in a quicker breakthrough time. Furthermore, when the flow rate rises, the flow becomes more turbulent, decreasing the outer bulk phase mass transfer resistance to the solid biosorbent's surface, resulting in a rapid migration of bulk phase MBD molecules into the biosorbent surface. The breakthrough curve got steeper with increased flow rate, as shown in Figure (4.18), due to shorter contact time of MBD molecules with the mixed-biosorbent bed, which resulted in decreased biosorption capacity. This explains that a lower flow rate leads to a higher dye removal percentage. As a consequence, the lower flow rate values were picked as the most suitable for current experiments. Similar tendencies were seen in the removal of dyes by fixed bed columns (Cruz-Olivares et al., 2013; Mangaleshwaran et al., 2015; Shak et al., 2017).

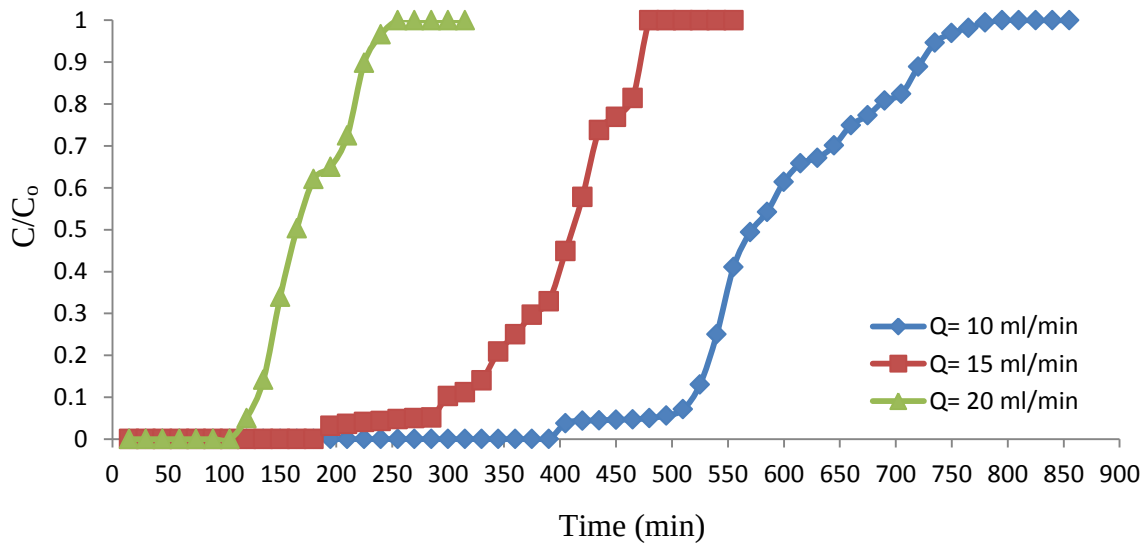

Fig. (4.18): Breakthrough curves for MBD biosorption at different flow rates.

Table (4.9): Experimental data analysis for biosorption of MBD onto SAC in a fixed-bed column mode at different operating conditions and breakthrough point of C/C_o was 0.05.

Biosorbent	Initial MBD concentration C_o (mg/l)	Flow rate Q_v (ml/min)	Bed depth H (cm)	t_b (min)	t_e (min)	m_{total} (mg)	q_{exp} (mg/g)	q_{total} (mg)	V_b (ml)	V_{eff} (ml)	Total remoal (R%)
SAC	25	10	15	480	795	198.75	19	160	4800	7950	80
	25	15	15	270	480	180	15.31	128.61	4050	7200	71.45
	25	20	15	120	255	127.5	10.16	85.34	2400	5100	67
	25	10	20	570	960	240	20.13	206.13	5700	9600	85.90
	25	10	30	720	1440	360	25	362.5	7200	14400	100
	50	10	15	240	570	285	26.5	222.6	2400	5700	78.11
	75	10	15	165	450	337.5	30.08	252.7	1650	4500	74.90

4.7.2 Impact of bed height of biosorbent on breakthrough curves

Adsorbate aggregation, all breakthrough curves steepness, and column adsorption efficiency are affected by the quantity of fixed bed biosorbent materials present in a fixed bed column. Figure (4.19) shows the breakthrough curves attained from MBD biosorption on the SAC for different bed heights with a constant flow rate and initial MBD concentration. The breakthrough curves parameters utilized in the MBD column analysis are listed in Table (4.9). The data revealed that when the height of the bed was raised, the time it took for the breakthrough to occur increased as well. By raising the bed height from 15 cm to 30 cm, the percentage dye removal rose from 80.5 to 100% Table (4.9). With a rise in bed height, the detected breakthrough period (t_b) is predicted to increase. The biosorbent SAC grew as the bed height increased, and the overall biosorption capability of the bed increased as well. As the biosorbent loading increased, the contact duration improved, resulting in greater removal efficiency. Furthermore, a long breakthrough time promotes intra-particle diffusion and increases column biosorption capacity (Vilvanathan and Shanthakumar, 2017). So, it was revealed that the volume of wastewater

treated increased when the bed depth was increased. This is due to an increase in surface area and the number of binding sites accessible for biosorption. Similar observations have been observed by a number of researchers (Sadaf and Bhatti, 2013 ; Rouf and Nagapadma, 2015; Alardhi et al., 2020).

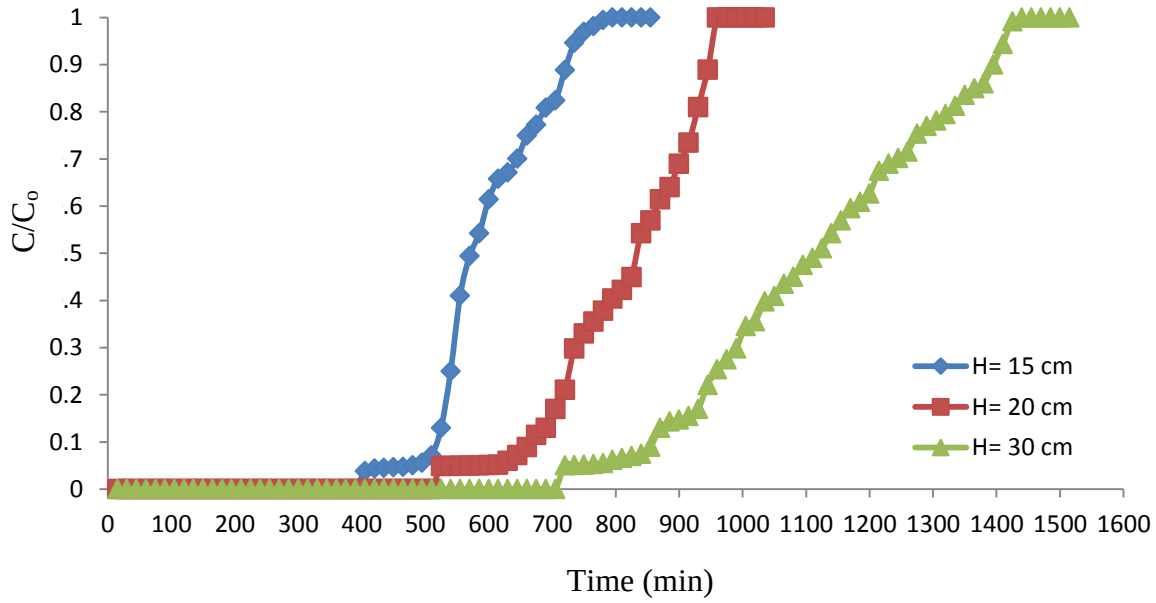

Fig. (4.19): Breakthrough curves for MBD biosorption at different column bed height.

4.7.3 Impact of initial MBD concentration on breakthrough curves

As shown in Figure (4.20), the effect of initial MBD concentration on the breakthrough curves and biosorption capacity was investigated by altering the initial MBD concentrations while keeping the other process parameters constant. The breakthrough curves of the plot of (C/C_o) versus t (min) for different initial MBD concentration were gotten from the test information as appeared in Figure (4.20) and the breakthrough curve parameters were calculated and displayed in Table (4.9). Figure (4.20) shows that increasing the primary dye concentration from 25 to 75 mg/l reduced the breakthrough time and saturation time because the fixed bed adsorbent became saturated quickly. As demonstrated in Table (4.9), the breakthrough

time dropped from 480 to 165 min as the MBD concentration increased. Figure (4.20) illustrates that the breakthrough time was flatter at lower MBD concentrations, indicating a broader MTZ and film control procedure. The breakthrough curve was sharper at increasing dye concentrations, indicating a smaller MTZ and an intraparticle diffusion controlled process (Afroze et al., 2015). The fixed bed biosorbent becomes saturated more slowly at lower MBD concentrations, increasing the breakthrough time. With increases in primary dye concentration, the total quantity of MBD adsorbed, q_{total} was raised from 160 to 252.7 mg, but the percentage dye removal was lowered from 80.50 percent to 74.9 %, as shown in Table (4.9). This is because the active binding sites of fixed bed biosorbent were quickly filled and saturated, resulting in a shorter breakthrough time. Additionally, a higher initial adsorbate concentration offers more pushing power for the transfer process to overcome mass transfer resistance. In addition, as indicated in Table (4.9), the total volume of MBD effluents was reduced from 7950 to 4500 ml when the initial dye concentration was increased. Other studies have made similar observations in the removal of other dyes including as (Ahmad and Hameed, 2009 ; Vilvanathan and Shanthakumar, 2017).

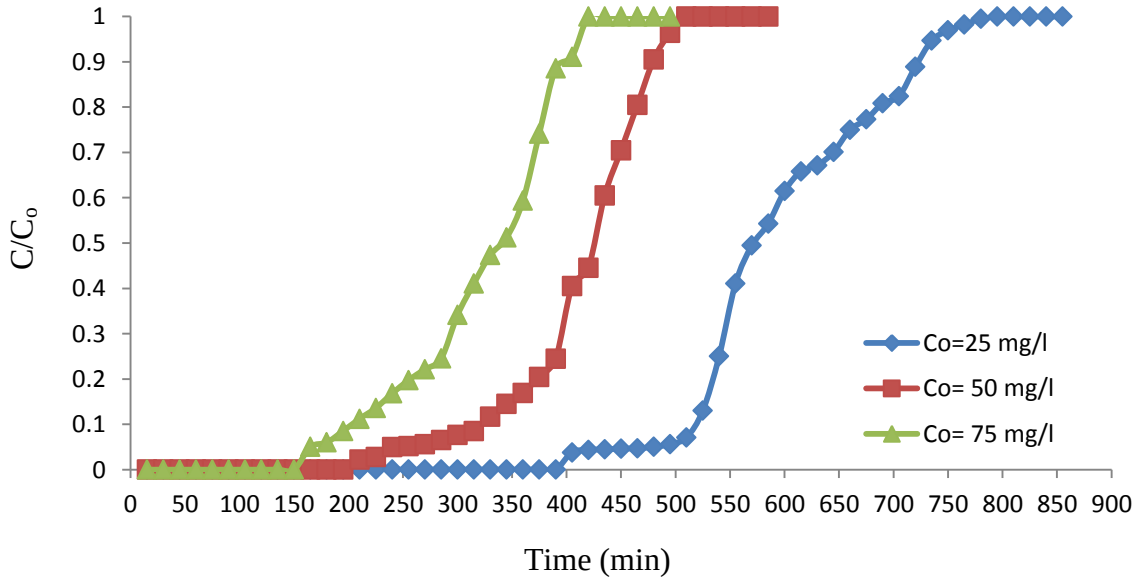

Fig. (4.20): Breakthrough curves for MBD biosorption at different initial MBD concentrations.

4.8 Dynamic modeling of a SAC fixed-bed biosorption column

The breakthrough curve is used to explain the performance and successful design of a fixed-bed column. Breakthrough time and the form of the breakthrough curve are two critical features that determine the operation and dynamic responsiveness of a fixed-bed biosorption column. Three models are including Bed Depth Service Time (BDST), Thomas models, and Yoon–Nelson models suggested in this study to anticipate the breakthrough curves observed at various experimental conditions (Jerold et al., 2016; Rangabhashiyam and Selvaraju, 2015).

4.8.1 The BDST (Bed Depth Service Time) model application.

To determine the influence of bed depth on the mode of the breakthrough curves, the experimental data obtained in the removal of MBD by SAC in a fixed bed column were fitted into the BDST model. The graph was drawn between service time and bed depth in the bed depth service time model for 0.05, 0.1, 0.2, 0.4, 0.6, and 0.8 values of C/C_o ratio at constant flow rate of 10 ml/min and initial concentration of MBD of 25 mg/l Figure (4.21). Table (4.10) shows the values of q_B, K_B, Z_c, and R^2. The slope and intercept values were used to estimate the value of biosorption capacity q_B (mg/g) and rate constant K_B for the corresponding C/C_o. The rate constant K_B indicates the rate at which MBD is transferred from its solution to the surface of the SAC (Noreen et al., 2013). By increasing the C/C_o ratio value from 0.05 to 0.8 at a constant flow rate of 10 ml/min and 25 mg/l initial concentration of MBD, the results showed an increase in q_B value from 3.55 to 9.56 (mg/g) and a reduction in K_B value from $47 * 10^{-5}$ to $12 * 10^{-5}$ l/mg.min (Balci et al., 2011). As a result of MBD continuing biosorption onto the biosorption surface (Kumar and Chakraborty, 2009). As a result, the dynamic biosorption capacity at such low breakthrough conditions was

certain to be lower than the biosorbent full bed capacity. However, the BDST theory of Bohart and Adams implies a rectangular isotherm with constant dynamic adsorption capacity (Kumar and Bandyopadhyay, 2006). Higher R^2 results ($R^2 > 0.98$) show that the BDST model for MBD biosorption on the biosorbent is valid (Table 4.10). The time it takes for all of an biosorbent active binding sites to become fully filled by adsorbate molecules until regeneration is required is known as column service time. Shows the low deviation between the experimental and calculated time using this model Table (4.11). Table (4.10) shows the critical bed depth values for MBD biosorption by SAC at various C/C_o ratios. As the C/C_o rose, the value of critical bed depth decreased from 12.37 to 10.57 cm for SAC (Dissanayake et al., 2016; Shak et al., 2017).

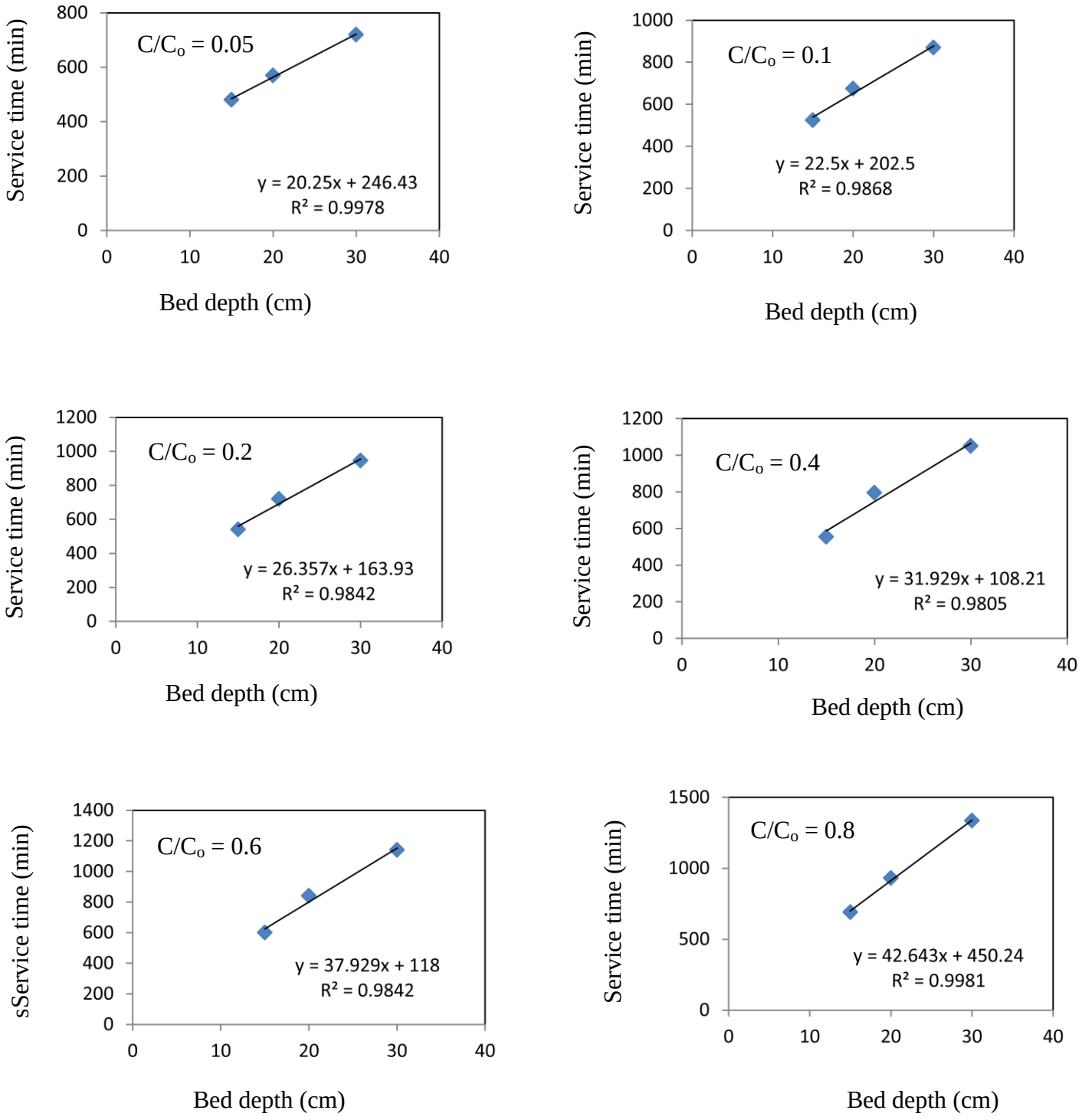

Fig. (4.21): BDST model plot at different values of C/C_o in fixed-bed column for MBD biosorption onto SAC (C_o =25 mg/l, flow rate=10 ml/min).

Table (4.10): Estimated BDST model parameters at different bed depth height with Q =10 ml/min and C_o =25 mg/l for MBD biosorption onto SAC column.

BDST model parameters for MBD biosorption onto SAC						
Parameters	q_B (mg/l)	q_B (mg/g)	K_B(l/mg.min)	U_f(cm/min)	Z_c (cm)	R^2
C/C_o =0.05	810	3.55	-0.00047	3.18	12.37	0.9978
C/C_o = 0.1	900	5.046	-0.00043	3.18	1.53	0.9868
C/C_o=0.2	1054.28	5.91	-0.00033	3.18	6.22	0.9842
C/C_o=0.4	1277.16	7.16	-0.00014	3.18	3.62	0.9805
C/C_o=0.6	1517.16	8.51	0.00013	3.18	3.12	0.9842
C/C_o=0.8	1705.72	9.56	0.00012	3.18	10.57	0.9981

Table (4.11): Comparison between $t_{cal.}$ & $t_{exp.}$ for MBD biosorption onto SAC at different breakthrough point (C/C_o) using estimated BDST model parameters at different bed depth height with Q =10 ml/min and C_o= 25 mg/l for column.

Parameters	**Bed depth, H (cm)**	**Flow rate, Q_v (ml/min**	**Initial MBD concentration, C_o (mg/l)**	**$t_{cal.}$**	**t_{exp}**
C/C_o=0.05	15	10	25	554.34	480
	20	10	25	655.595	570
	30	10	25	858.1	720
C/C_o=0.1	15	10	25	541	525
	20	10	25	654.4	675
	30	10	25	879.4	870
C/C_o=0.2	15	10	25	563.3	540
	20	10	25	695.2	720
	30	10	25	958.74	945
C/C_o=0.4	15	10	25	594.78	555
	20	10	25	754.43	795
	30	10	25	1073.72	1050
C/C_o=0.6	15	10	25	693.68	600
	20	10	25	883.33	840
	30	10	25	1262.62	1140
C/C_o=0.8	15	10	25	685.85	690
	20	10	25	899.1	930
	30	10	25	1325.49	1335

4.8.2 Thomas dynamic model of application

One of the most extensively used approaches for describing column biosorption data is Thomas model. Thomas model is obtained with the sorption that the rate driving force obeys second-order reversible reaction kinetics, which assumes Langmuir kinetics of sorption and no axial dispersion (Vijayaraghavan and Prabu, 2006). Thomas model is a simplistic model based on the mass conservation equation in a flow system. Thomas model was used to compute the maximum solid-phase concentration of MBD, q_{TH} (mg/g), and the Thomas kinetic rate constant, K_{Th} (l/mg.min), using the column experimental data from the breakthrough curve. The slope and intercept of the linear equation were used to get the values of k_{TH}, q_{TH}, and R^2, which were then summarized in Table (4.12). Figures (4.22 a-c) and (4.23 a-c) show the fitted linear plot of ln $[(C_o/C - 1)]$ versus time (t) for various bed heights and MBD flow rates (4.23 a-c). The K_{TH} values fell as the biosorbent bed height increased, as shown in Table (4.12). K_{TH} levels, for example, were reduced from $48 * 10^{-5}$ to $31* 10^{-5}$ l/min.mg. Slower mass transfer is the cause of the decline in K_{TH} values. However, when the flow rate rose, the K_{TH} value nearly doubled. The increased K_{TH} in the Thomas model can be attributed to quicker mass transfer at higher flow rates. It should be emphasized that this rapid mass transfer might be attributable to the biosorbent macropores (Bhaumik et al., 2013; Ataei-Germi and Nematollahzadeh, 2016). Furthermore, the q_{TH} values increased from 17.65 to 24.88 mg/g as the fixed bed biosorbent bed height raised, however the value of q_{TH} reduced as the flow rate rose. A large driving force is produced by the concentration difference between the dye in the solution and the dye on the biosorbent surface, resulting in higher column adsorption performance. Although the model showed high R^2 values the calculated q_{TH} value always exceeded the experimental values (Table 4.12). When the internal and exterior diffusions are not the limiting step, Thomas model fits

well with the experimental data. Thomas constant for other systems have been observed in a similar way by others (Bhaumik et al., 2013; Afroze et al., 2015; Amiri et al., 2019). The experimental findings fit Thomas model well, demonstrating that exterior and internal diffusion are not the limiting steps and that there is no axial dispersion.

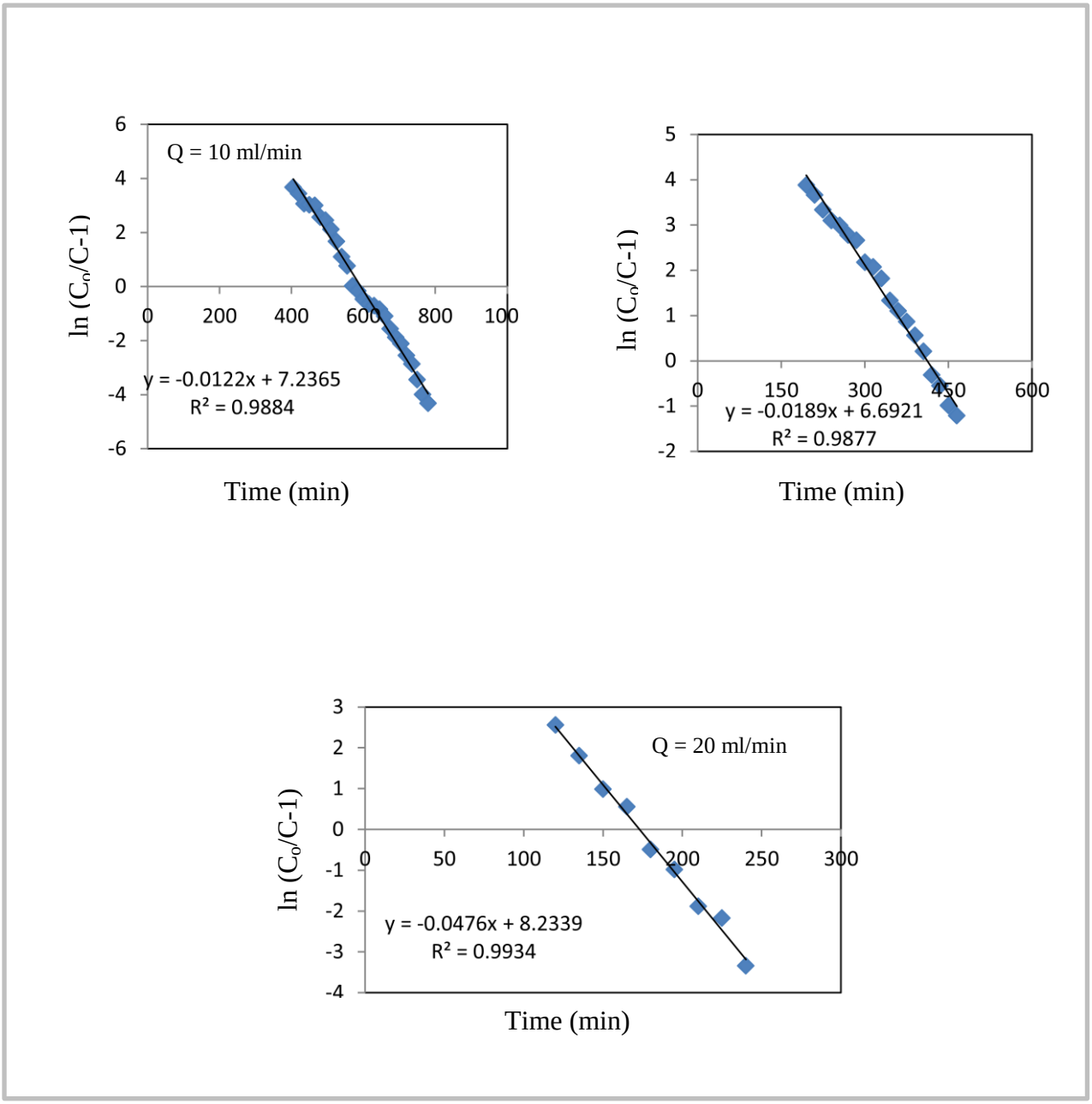

Fig. (4.22): Thomas kinetic plots for biosorption of MBD under various effect flow rate (C_o= 25 mg/l, H = 15).

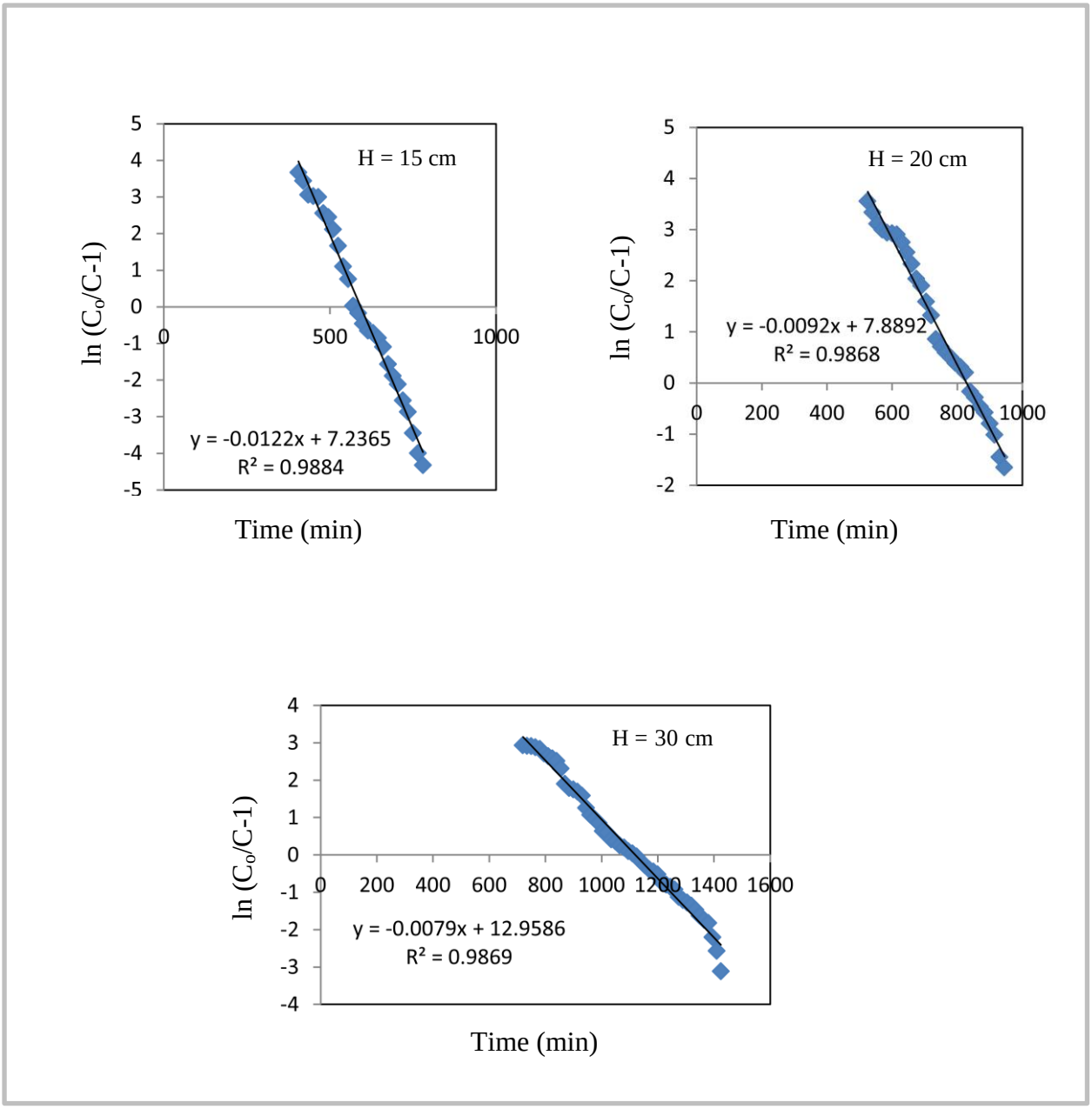

Fig. (4.23): Thomas kinetic plots for biosorption of MBD under various effect bed depth (Q =10 ml/min, C_o= 25 mg/l).

Table (4.12): Kinetic models parameters for biosorption of MBD onto SAC fixed bed column at different feed flow rate and bed height.

Experimental conditions							
Flow rate, Q_v(ml/min)		10	15	20	10	10	10
Bed depth (cm)		15	15	15	15	20	30
Initial concentration (mg/l)		25	25	25	25	25	25
qe, exp (mg/g)		17.50	15.31	10.16	17.50	20.13	25
Thomas Model Parameters	K_{TH} (l/mg.min)	0.00048	0.00075	0.0019	0.00048	0.00036	0.00031
	q_{TH}(mg/g)	17.65	15.81	10.29	17.65	20.93	24.88
	R^2	0.9884	0.9877	0.9934	0.9884	0.9868	0.9869
Yoon-Nelson Model Parameters	$K_{YN}(min^{-1})$	0.0195	0.0214	0.044	0.0195	0.0124	0.0079
	τ_{exp}(min)	585	420	165	585	840	1125
	τ_{Cal}(min)	601.53	399.81	173.64	601.53	826.93	1171.67
	q_{YN}(mg/g)	17.90	17.84	10.33	17.90	20.18	24.25
	R^2	0.9833	0.9837	0.9901	0.98330	0.9826	0.9847

4.8.3 Application of Yoon-Nelson dynamic model

The breakthrough behavior of MBD biosorption onto SAC was investigated using a simple theoretical model established by Yoon–Nelson. As a result, the values of K_{YN} (a rate constant) and τ (the time necessary for a 50% MBD breakthrough) could be calculated. For SAC, the values of K_{YN} and τ are provided in Table (4.12). Figure (4.24a-c) and Figuer (4.25a-c) show graphs of ln (C/C_o -C) against time for various bed heights and inlet flow rates derived from equation (2.22). The values of K_{YN} and are determined from the linear plot slop and intercept, and the findings are provided in Table (4.12) together with other determined values. The Yoon-Nelson constant K_{YN} was found to rise as the inflow flow rate increased and decrease as the bed height increased. The increased driving force of mass transfer in the liquid film was responsible for the rise in K_{YN} value which explains why breakthrough and saturation occurred faster at higher flow rates and initial concentrations. These results match those reported by previous researchers in fixed-bed adsorption investigations (Tsai et al. 2016; Liu et al., 2017). As the flow rate increased, the q_{YN} and τ for dye dropped. With increasing column bed height, the q_{YN} and τ time required for 50

percent sorbate breakthrough (min) were also shown to rise. The value of τ exhibited a distinct pattern, as greater adsorption reaction constants resulted in fast adsorption saturation, resulting in a shorter breakthrough time. A higher bed height means more time for the solution to come into touch with the fixed bed. Furthermore, a lower rate constant indicates that the MBD has had enough time to migrate from bulk solution to the SAC surface, and the value of correlation coefficients (R^2) listed in Table (4.12) demonstrated the model applicability ($R^2 > 0.9833$) to the experimental data under various conditions. A similar trend was also reported for the adsorption of MBD by Djelloul and Hamdaoui, 2014; Banerjee et al., 2017).

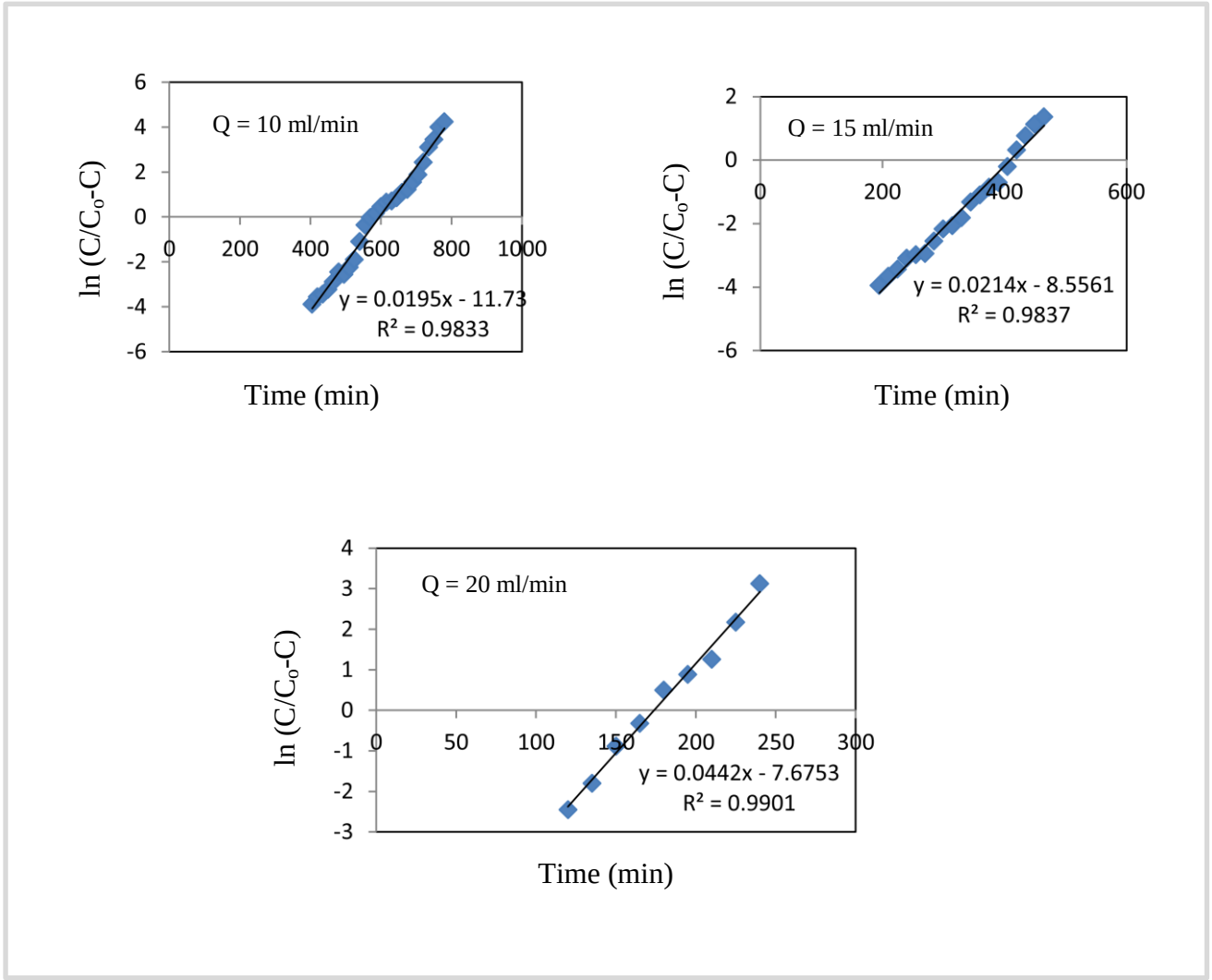

Fig. (4.24): Yoon-Nelson kinetics plots for the biosorption of MBD on SAC under different flow rate effect (C_o = 25 mg/l, H =15 cm).

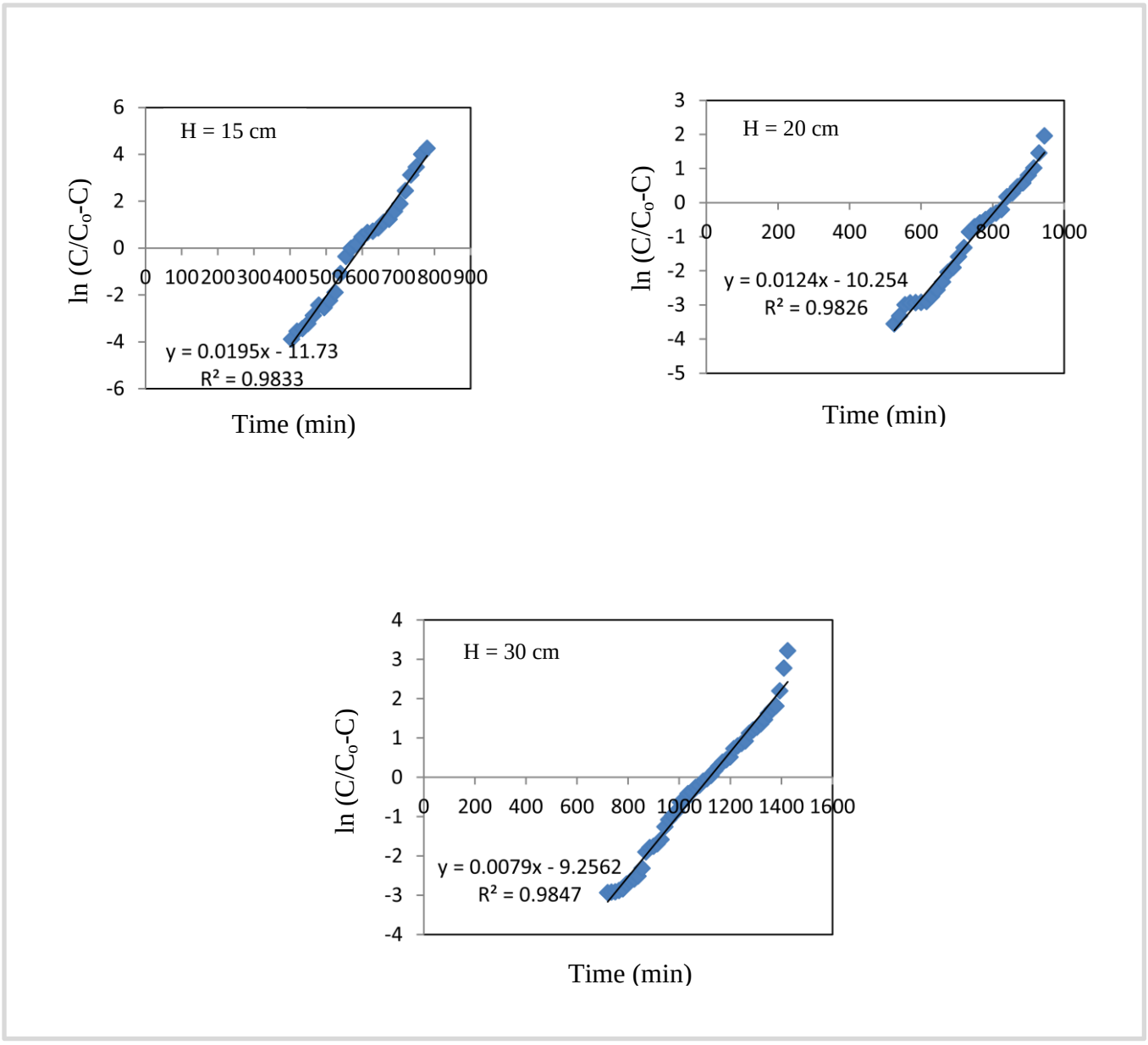

Fig. (4.25): Yoon-Nelson kinetics plots for the biosorption of MBD on SAC under different effect of bed depth (C_o = 25 mg/l, Q = 5 ml/min).

Chapter Five

Conclusions and Recommendations

Chapter Five

Conclusions and Recommendations

5.1 Conclusions

The following conclusions are reached from the present investigation based on the data stated.

5.1.1 Batch experiments mode

1. Naturally occurring plant based activated carbon (SAC) seems to be an effective and an alternative biosorbent for the removal of MBD from aqueous solutions.
2. Various operational factors were studied and the percentage dye removal increased as the pH of the solution and biosorbent dosage increased and the optimal value was reported at pH 9 and 0.8 g/100ml of dye solution respectively biosorbent dosage increased, but it decreased as the initial dye concentration increased
3. The biosorption of MBD was reached to equilibrium time at 75 min.
4. The Langmuir isotherm model was well-fitted to the SAC equilibrium biosorption of MBD, resulting in a homogeneous monolayer coverage of MBD on the SAC surface. The maximum biosorption potential was stated to be 33.34 mg/g. Also, the dimensionless separation factor (R_L) indicates the favourable biosorption process.
5. The MBD biosorption mechanism followed a pseudo-second-order model as shown by virtually identical experimental and measured q_e values and a high degree of determination R^2 0.9997 indicating the occurring of chemisorption of MBD using SAC.

6. The multi-linearity of the intraparticle diffusion kinetic model revealed that two or more steps, including intraparticle diffusion, control MBD biosorption.

5.1.2 Continuous flow mode

1. The synthesized SAC was found to be feasible media for using as a bed column for removal of MBD from colored water.
2. The breakthrough and exhaustion times decreased as the initial MBD concentration and flow rate increased, but they increased as the biosorbent bed depth increased. The biosorption capacity and the MBD removal efficiency were increased with increased of biosorbent mass leading to increase the exhaustion time of the column, but they lowered as flow rate was speed up. The biosorption capacity increased with increased the initial dye concentration, but the removal efficiency was dropped.
3. The mode of fixed bed column was based to study the dynamic biosorption of MBD and it was depended on feed flow rate, primary dye concentration and bed height of biosorbent.
4. The parameters of column kinetic were found through the kinetic study and the breakthrough curves were predicted under various conditions using the kinetic model of BDST, Thomas and Yoon-Nelson. Obtaind results showed that the three models can describe a whole breakthrough curve with high R^2 . Referred to the findings, it was reported that SAC can be effectively used as an biosorbent in mode of fixed bed column to continuously remove MBD from aqueous solutions.
5. The BDST model was effectively used to evaluate the model parameter and examine the column performance.

6. The value of q_e raised as the bed depth increased and reduced the flow rate decreased, according to the Thomas model and experimental MBD adsorption data. K_{Th} increased in value as the flow rate rose, but declined as the bed depth grew.
7. The rate constant K_{YN} for the Yoon-Nelson model rose with increasing flow rate and decreased with increasing bed depths for SAC. The 50 percent breakthrough time τ for SAC, on the other hand, reduced with increasing flow rate and improved with increasing bed depths.

5.1.3 Recommendations for future researchs

Future studies should consider the following recommendations:

1. Under similar operating conditions, a similar research could be carried out on the development of biomass-based activated carbon utilizing other locally available biomass solid wastes such as pine cone leaves, pine cone bark, eucalyptus leaves, wheat straw, and so on. This work can be extended to study the competitive biosorption with the presence of other dye or heavy metal ion, in batch and continuous flow mode.

2. Since real industrial effluents produce a wide variety of organic contaminants at the same time, real wastewater samples can be used as biosorbates to assess the effectiveness of biomass-based activated carbon biosorbents.
3. This work can be extended to study the competitive biosorption with the presence of other dye or heavy metal ion, in batch and continuous flow mode.

References

- Abbas, A.H, Ahmed, M.A.M., Ali, W.H., 2018, "biosorption of methyelen blue from aqueous solution using wastes micelium of fungl biomass type withe rot fungl", Journal of Engineering and Sustainable Development, 22.4.
- Abdelhafez, A.A., Li, J.H., 2016, "Removal of Pb(II) from aqueous solution by using biochars derived from sugar cane bagasse and orange peel", J. Taiwan Inst. Chem.Eng. 61, 367–375.
- Abdelkarim, S., Mohammed, H., Nouredine, B., 2017, "Sorption of Methylene Blue Dye from Aqueous Solution Using an Agricultural Waste", Trends in Green Chemistry, 03(01).
- Abdolali, A., Guo, W. S., Ngo, H. H., Chen, S. S., Nguyen, N. C., Tung, K. L., 2014, "Typical lignocellulosic wastes and by-products for biosorption process in water and wastewater treatment: A critical review", Bioresource Technology, 160, 57–66.
- Abdolali, A., Ngo, H.H., Guo, W., Zhou, J.L., Zhang, J., Liang, S., Chang, S.W., Nguyen, D.D., Liu, Y., 2017, "Application of a breakthrough biosorbent for removing heavy metals from synthetic and real wastewaters in a lab-scale continuous fixed bed column", Biores Technol 229:78–87.
- Acemiolu, B., Kertmen, M., Digrak, M. Alma, M.H, 2010, "Use of Aspergillus wentii for biosorption of methylene blue from aqueous solution", frican Journal of Biotechnology Vol. 9(6), pp. 874-881.
- Adebayo, M.A., Prola, L.D.T., Lima, E.C., Puchana-Rosero, M.J., Cataluña, R., Saucier, C., Ruggiero, R., 2014, "Adsorption of procion blue MX-R dye from aqueous solutions by lignin chemically modified with aluminium and manganese", Journal of Hazardous Materials, 268, 43–50.

- Adegoke, K. A., Bello, O. S., 2015, " Dye sequestration using agricultural wastes as adsorbents", Water Resources and Industry, 12, 8–24.
- Afroze, S., Sen, T. K., Ang, H.M., 2015, "Adsorption performance of continuous fixed bed column for the removal of methylene blue (MB) dye using Eucalyptus sheathiana bark biomass", Research on Chemical Intermediates, 42(3), 2343–2364.
- Ahmad, A.A., Hameed, B.H., 2009, "Fixed-bed adsorption of reactive azo dye onto granular activated carbon prepared from waste", Journal of Hazardous Materials, 175(1-3), 298–303.
- Ahmed, M.J., 2016, "Application of agricultural based activated carbons by microwave and conventional activations for basic dye adsorption: Review", Journal of Environmental Chemical Engineering, 4(1), 89–99.
- Ait, A.H., Zbair, M., Anfar, Z., Naciri, Y., El Haouti, R., El Alem, N., Ezahri, M., 2018, "Cationic dyes adsorption onto high surface area almond shell activated carbon: kinetics, equilibrium isotherms and surface statistical modelling", Mater Today Chem. 8, 121–132.
- Akkaya, G., Güzel, F., 2013, "Application of some domestic wastes as new low cost biosorbents for removal of methylene blue:Kinentic and equilibrium studies. Chemical Engineering Communications, 201(4), 557–578.
- Alardhi, S.M., Albayati, T.M., Alrubaye, J.M., 2020 "Adsorption of the methyl green dye pollutant from aqueous solution using mesoporous materials MCM-41 in a fixed-bed column", Heliyon, 6(1),03,253.
- Al-Ghouti, M.A, Al-Absi, R.S., 2020, "Mechanistic understanding of the adsorption and thermodynamic aspects of cationic methylene

blue dye onto cellulosic olive stones biomass from wastewater", Scientific Reports., 10:15928.

- Al-Husseiny, H.A., 2014, "Adsorption of methylene blue dye using low cost adsorbent of sawdust: batch and continues studies," Journal of Babylon University/Engineering Sciences., 2,22.
- Ali, I., 2014, "Water treatment by adsorption columns: evaluation at ground level", Sep Purif Rev43:175–205.
- Almeida, E.J.R., Corso, C.R., 2014, "Comparative study of toxicity of azo dye Procion Red MX-5B following biosorption and biodegradation treatments with the fungi Aspergillus niger and Aspergillus terreus", Chemosphere, 112, 317–322.
- Amin, M.T., Alazba, A.A, Shafiq, M., 2017, "Effective adsorption of methylene blue dye using activated carbon developed from the rosemary plant: isotherms and kinetic studies", Desalination and Water Treatment, 1-10.
- Amiri, M. J., Khozaei, M., Gil, A., 2019, "Modification of the Thomas model for predicting unsymmetrical breakthrough curves using an adaptive neural-based fuzzy inference system", Journal of Water and Health, 17(1), 25–36.
- Anastopoulos, I., Bhatnagar, A., Hameed, B.H., Ok, Y. S., Omirou, M., 2017, "A review on waste-derived adsorbents from sugar industry for pollutant removal in water and wastewater", Journal of Molecular Liquids, 240, 179–188.
- Ani, J.U., Akpomie, U.C., Okoro, L.E., Aneke, O.D., Onukwuli, Ujam, O.T., 2020, "Potentials of activated carbon produced from biomass materials for sequestration of dyes, heavy metals, and crude oil components from aqueous environment", Applied Water Science.

- Ansari, S. A., Khan, F., Ahmad, A., 2016., Cauliflower leave, an agricultural waste biomass adsorbent, and its application for the removal of MB dye from aqueous solution: equilibrium, kinetics, and thermodynamic studies", International Journal of Analytical Chemistry, 2016, 1–10.
- Asghar, A., Abdul Raman, A.A., Wan Daud, W.M.A., 2015, "Advanced oxidation processes for in-situ production of hydrogen peroxide/hydroxyl radical for textile wastewater treatment: a review", Journal of Cleaner Production, 87, 826–838.
- Ataei-Germi, T., Nematollahzadeh, A., 2016, "Bimodal porous silica microspheres decorated with polydopamine nano-particles for the adsorption of methylene blue in fixed-bed columns. Journal of Colloid and Interface Science, 470.
- Auta, M., Hameed, B.H., 2013, "Acid modified local clay beads as effective low-cost adsor-bent for dynamic adsorption of methylene blue", J. Ind. Eng. Chem. 19, 1153–1161
- Auta, M., Hameed, B.H., 2014, "Chitosan–clay composite as highly effective and low-cost adsorbent for batch and fixed-bed adsorption of methylene blue", Chemical Engineering Journal, 237, 352–361.
- Aydın, H., Baysal, G., 2005, "Adsorption of acid dyes in aqueous solutions by shells of bittim (Pistacia khinjuk Stocks)", Desalination, 196(1-3), 248–259.
- Azha, S. F., Ahmad, A. L., & Ismail, S., 2016, "Coating paint for dyes removal: Performance and characteristic", Journal of Water Process Engineering, 15, 18–25.
- Azzaz, A.A., Jellali, S., Akrout, H., Assadi, A.A. Bousselmi, L., 2017, "Optimization of a cationic dye removal by a chemically modified agriculture by-product using response surface

methodology: biomasses characterization and adsorption properties", Environmental Science and Pollution Research 24(11), 9831-9846.

- Badran, I., Qut, O., Abdallah D. Manasrah, A.D., Abualhasan, M., 2020, "Continuous adsorptive removal of glimepiride using multi-walled carbon nanotubes in fixed-bed column", Environmental Science and Pollution Research.
- Balci, B., Keskinkan, O., Avci, M., 2011, "Use of BDST and an ANN model for prediction of dye adsorption efficiency of Eucalyptus camaldulensis barks in fixed-bed system", Expert Syst. Appl. 38, 949–956.
- Banerjee, M., Bar, N., Basu, R.K., Das, S.K., 2017, "Comparative study of adsorptive removal of Cr(VI) ion from aqueous solution in fixed bed column by peanut shell and almond shell using empirical models and ANN", Environmental Science and Pollution Research, 24(11), 10604–10620.
- Banerjee, S., Sharma, G.C., Gautam, R.K., Chattopadhyaya, M.C., Upadhyay, S.N., Sharma, Y.C., 2016, "Removal of malachite green, a hazardous dye from aqueous solutions using avena sativa (oat) hull as a potential adsorbent", Journal of Molecular Liquids, 213, 162–172.
- Banerjee, S., Sharma,Y.C., 2013, "Equilibrium and kinetic studies for removal of malachite green from aqueous solution by a low cost activated carbon", J. Ind. Eng. Chem. 19, 1099-1105.
- Bansal, R.C., Goyal, M., 2005, "Activated carbon adsorption", Florida, United States: CRC Press.
- Baruah, S., Devi, A., Bhattacharyya, K. G., Sarma, A., 2016, "Developing a biosorbent from aegle marmelos leaves for removal

of methylene blue from water", International Journal of Environmental Science and Technology, 14(2), 341–352.

- Bayomie, O.S., Kandeel, H., Shoeib, T., Yang, H., Youssef, N., El-Sayed, M.M.H., 2020, "Novel approach for effective removal of methylene blue dye from water using fava bean peel waste", Scientific Reports, 10(1).
- Belhouchat, N., Zaghouane-Boudiaf, H.,Viseras, C., 2017, "Removal of anionic and cationic dyes from aqueous solution with activated organo-bentonite/sodium alginate encapsulated beads", Applied Clay Science, 135, 9–15.
- Bello, O. S., Ahmad, M.A., Ahmad, N., 2012, "Adsorptive features of banana (Musa paradisiaca) stalk-based activated carbon for malachite green dye removal. Chemistry and Ecology, 28(2), 153–167.
- Benkaddour, S., Slimani, R., Hiyane, H., El Ouahabi, I., Hachoumi, I., El Antri, S., Lazar, S., 2018, "Removal of reactive yellow 145 by adsorption onto treated watermelon seeds: Kinetic and isotherm studies. Sustainable Chemistry and Pharmacy, 10, 16–21.
- Bhatnagar, A., Jain, A.K., 2005, "A comparative adsorption study with different industrial wastes as adsorbents for the removal of cationic dyes from water", Journal of Colloid and Interface Science, 281(1), 49–55.
- Bhaumik, M., Setshedi, K., Maity, A., Onyango, M.S., 2013" Chromium(VI) removal from water using fixed bed column of polypyrrole/Fe3O4 nanocomposite", Separation and Purification Technology, 110, 11–19.
- Bohart, G. S., Adams, E.Q., 1920, "Adsorption in columns", J. Chem. Soc. 42.

- Boudechiche, N., Mokaddem, H., Sadaoui, Z., Trari, M., 2016, "Biosorption of cationic dye from aqueous solutions onto lignocellulosic biomass (Luffa cylindrica): characterization, equilibrium, kinetic and thermodynamic studies", International Journal of Industrial Chemistry, 7(2), 167–180.
- Boulaiche W, Hamdi B, Trari M, 2019, "Removal of heavy metals by chitin: equilibrium, kinetic and thermodynamic studies", Appl
- Bulut, Y, Aydın, H., 2006, "A kinetics and thermodynamics study of methylene blue adsorption on wheat shells", Desalination, 194(1):259–67.
- Cai, Y., Liu, L., Tian, H., Yang, Z., Luo, X., 2019, "Adsorption and desorption performance and mechanism of tetracycline hydrochloride by activated carbon-based adsorbents derived from sugar cane bagasse activated with ZnCl2", Molecules, 24(24), 4534.
- Calvete, T., Lima, E.C., Cardoso, N.F., Vaghetti, J.C.P., Dias, S.L.P., Pavan, F.A., 2010, "Application of carbon adsorbents prepared from Brazilian-pine fruit shell for the removal of reactive orange 16 from aqueous solution: Kinetic, equilibrium, and thermodynamic studies", Journal of Environmental Management, 91(8), 1695–1706.
- Cencen, F., Aktas, O., 2011, "Activated carbon for water and wastewater treatment: Integration of adsorption and biological treatment", Hoboken, New Jersey, United States: John Wiley and Sons.
- Chen, H., Wang, X., Li, J., Wang, X., 2015, "Cotton derived carbonaceous aerogels for the efficient removal of organic pollutants and heavy metal ions", J Mater Chem A, 3:6073–6081.

- Chen, J., Wang,Y., Liu,Y., Tang, M., Wang, R., Tian, Y., Jia, C., 2019, "Bacterial community shift and antibiotics resistant genes analysis in response to biodegradation of oxytetracycline in dual graphene modified bioelectrode microbial fuel cell", Bioresour. Technol. 276, 236–243.
- Chen, J., Yang, Y., Liu, Y., Tang, M., Wang, R., Zhang, C., Jiang, J., Jia, C., 2019 a, "Bacterial community shift in response to a deep municipal tail wastewater treatment system", Bioresour. Technol. 281, 195–201.
- Chen, Y., Zhai, S.-R., Liu, N., Song, Y., An, Q.-D., Song, X.-W., 2013, "Dye removal of activated carbons prepared from NaOH-pretreated rice husks by low-temperature solution-processed carbonization and H_3PO4 activation", Bioresource Technology, 144, 401–409.
- Cheng, P.J., Wang, X., 2000, "Aspect of kaolinite characterization and retention of Pb and Cd, App. Clay Sci., 22, 39-45.
- Cherifi, H., Fatiha, B., Salah, H., 2013, "Kinetic studies on the adsorption of methylene blue onto vegetal fiber activated carbons", Applied Surface Science, 282, 52–59.
- Cheriti, A., Fouzi, M., Belboukhari, N., Taleb, S., 2011, "Copper Ions biosorption properties of biomass derived from algerian sahara plants", Expanding Issues in Desalination.
- Chinoune, K., Bentaleb, K., Bouberka, Z., Nadim, A., Maschke, U., 2016, "Adsorption of reactive dyes from aqueous solution by dirty bentonite", Applied Clay Science, 123, 64–75.
- Choo, K.H., Chang, D.I., Park, K.W., Kim, M.H., 2008, "Use of an integrated photocatalysis/hollow fiber microfiltration system for the removal of trichloroethylene in water", J. Hazard. Mater. 152, 183–190.

- Chowdhury, Z.Z., Hamid, S.B.A., Zain, S.M., 2015, "Evaluating design parameters for breakthrough curve analysis and kinetics of fixed bed columns for Cu(II) cations using lignoccellulosic wastes", BioResources, 10(1), 732-749.
- Crawford, C. B., Quinn, B., 2017, "The interactions of microplastics and chemical pollutants", Microplastic Pollutants, 131–157.
- Crini, G., 2003, "Studies on adsorption of dyes on beta-cyclodextrin polymer", Bioresour Technol90:193–198.
- Crini, G., Lichtfouse, E., Wilson, L.D., Morin-Crini, N., 2018, "Adsorption-oriented processes using conventional and non-conventional adsorbents for wastewater treatment", Green Adsorbents for Pollutant Removal, 23–71.
- Cruz-Olivares, J., Pérez-Alonso, C., Barrera-Díaz, C., Ureña-Nuñez, F., Chaparro-Mercado, M.C. and Bilyeu, B. (2013) "Modeling of lead (II) biosorption by residue of allspice in a fixedbed column". Chemical Engineering Journal 228(Supplement C), 21-27
- Dahiru, D., Zango, Z.U., Haruna, M.A., 2018, "Cationic dyes removal using low-cost banana peel biosorbent", American Journal of Materials Science, 8,2. 32-38.
- Dai, Y., Sun, Q., Wang, W., Lu, L., Liu, M., Li, J., Zheng, W., 2018, "Utilisations of agricultural waste as adsorbent for the removal of contaminants", A review.Chemosphere 211, 235–253.
- Danwittayakul, S., Jaisai, M., Dutta, J., 2015, "Efficient solar photocatalytic degradation of textile wastewater using ZnO/ZTO composites", Applied Catalysis B: Environmental, 163, 1–8.

- Das, N., Das, D., 2013, "Recovery of rare earth metals through biosorption: An overview", Journal of Rare Earths, 31(10), 933–943.
- Das, R., Mukherjee, A., Sinha, I., Roy, K., Dutta, B.K., 2020, "Synthesis of potential bio‑adsorbent from indian neem leaves (Azadirachta indica) and its optimization for malachite green dye removal from industrial wastes using response surface methodology: kinetics, isotherms and thermodynamic studies", Applied Water Science, 10:117.
- Dawood, S., Sen, T.K., 2012, "Removal of anionic dye congo red from aqueous solution by raw pine and acid-treated pine cone powder as adsorbent: Equilibrium, thermodynamic, kinetics, mechanism and process design", Water Research, 46(6), 1933–1946.
- De Gisi, S., Lofrano, G., Grassi, M., Notarnicola, M., 2016, "Characteristics and adsorption capacities of low-cost sorbents for wastewater treatment", A review. Chem. Eng.Trans. 9, 10–40.
- Dileepa Chathuranga, P.K, Priyantha, N., Iqbal, S., Mohomed Iqbal, M.C., 2013, "Biosorption of Cr (III) and Cr(VI) species from aqueous solution by Cabomba caroliniana: kinetic and equilibrium study", Environ Earth Sci 70:661–671.
- Dissanayake, D.M.R.E.A., Chathuranga, P.K.D., Perera, P.I., Vithanage, M., Iqbal, M.C.M. 2016, "Modeling of Pb(II) adsorption by a fixed-bed column", Bioremediation Journal, 20(3), 194–208.
- Djelloul, C., Hamdaoui, O., 2014, "Dynamic adsorption of methylene blue by melon peel in fixed-bed columns", Desalination and Water Treatment, 1–10.

- Dod, R., Banerjee, G., Saini, S., 2012, "Adsorption of methylene blue using green pea peels (Pisum sativum): A cost-effective option for dye-based wastewater treatment", Biotechnology and Bioprocess Engineering, 17(4), 862–874.
- El maguana, Y., Elhadiri, N., Benchanaa, M., Chikri, R., 2020, "Activated carbon for dyes removal: Modeling and understanding the adsorption process", Journal of Chemistry, 2020, 1–9.
- El Messaoudi, N., El Khomri, M., Dbik, A., Bentahar, S., Lacherai, A., Bakiz, B., 2016, "Biosorption of Congo red in a fixed-bed column from aqueous solution using jujube shell: Experimental and mathematical modeling", Journal of Environmental Chemical Engineering, 4(4), 3848–3855.
- El-Haddad, M., Regti, A., Slimani, R., Lazar, S., 2014, "Assessment of the biosorption kinetic and thermodynamic for the removal of safranin dye from aqueous solutions using calcined mussel shells", J Ind Eng Chem 20:717–724.
- El-Maghraby, A., El Deeb., H.A., 2011, "Removal of a basic dye from aqueous solution by adsorption using rice hulls", Journal Glob. NEST ,13: 90–98.
- El-Maghraby, A., Nahla, A., Taha, N.A., 2014, "Equilibrium and kinetic studies for the removal of cationic dye using banana pith" Advances in Environmental Research, 3. 3,217-230.
- ElSayed, E.E., 2018, "Natural diatomite as an effective adsorbent for heavy metals in water and wastewater treatment (a batch study)", journal Water Science, 32, 1, 32-43.
- Enenebeaku, C.K., Okorocha, N.J., Enenebeaku, U.E., Onyeachu, B.I., 2017, "Adsorption of methylene blue dye onto bush cane bark powder", International Letters of Chemistry, Physics and Astronomy Submitted, 76, 12-26.

- Enniya, I., Rghioui, L., Jourani, A., 2018, "Adsorption of hexavalent chromium in aqueous solution on activated carbon prepared from apple peels", Sustainable Chemistry and Pharmacy. 7, 9–16.
- Etim, U.J., Umoren, S.A., Eduok, U.M. 2016, "Coconut coir dust as a low cost adsorbent for the removal of cationic dye from aqueous solution", Journal of Saudi Chemical Society, 20, S67–S76.
- Ezechi, E.H., Kutty, S.R.b.M., Malakahmad, A., Isa, M.H., 2015, "Characterization and optimization of effluent dye removal using a new low cost adsorbent: Equilibrium, kinetics and thermodynamic study", Process Safety and Environmental Protection 98, 16-32.
- Fahad, B.M., Ali, N.S., Hameed, T.T., 2018, "Using paper waste as adsorbent for methyl violet dye removal from waste water", Journal of Engineering and Sustainable Development Vol. 22, No. 01.
- Farooq, U., Kozinski, J.A., Khan, M.A., Athar, M., 2010, "Biosorption of heavy metal ions wheat based biosorbent – A review of the recent literature", Biores. Technol. 101, 5043–5053.
- Fathi, M.R., Asfaram, A., Hadipour, A., Roosta, M., 2014, "Kinetics and thermodynamic studies for removal of acid blue 129 from aqueous solution by almond shell", J Environ Health Sci Eng 12(1):62.
- Fathy, N.A, Ahmed, S.A.S., El-enin, R.M.M.A., 2012, "Effect of activation temperature on textural and adsorptive properties for activated carbon derived from local reed biomass: Removal of p Nitrophenol" Environmental Reseach,Engineering and Management 59.

- Fauzi, N.A.B.M., 2015, " Biomass for green removal of dyes", A project dissertation submitted to the Chemical Engineering Programme Universiti Teknologi PETRONAS.
- Felista, M.M., Wanyonyi, W.C., Gilbert, O., 2020, "Utilization of Macadamia seed husks as alow-cost sorbent for removing cationic dye (basic blue 3 dye) from aqueous solution", Journal Pre-proof, S2590-1826(20)30024-2.
- Fernandez, M.E., Nunell, G.V., Bonelli, P.R., Cukierman, A.L., 2014, "Activated carbon developed from orange peels: Batch and dynamic competitive adsorption of basic dyes", Industrial Crops and Products, 62, 437–445.
- Fideles, R.A., Ferreira, G.M.D., Teodoro, F.S., Adarme, O.F.H., da Silva, L.H.M., Gil, L.F., Gurgel, L.V.A., 2018, "Trimellitated sugarcane bagasse: A versatile adsorbent for removal of cationic dyes from aqueous solution. Part I: Batch adsorption in a mono component system", Journal of Colloid and Interface Science, 515, 172–188.
- Foo, K.Y., Lee, L.K., Hameed, B.H., 2013, "Preparation of tamarind fruit seed activated carbon by microwave heating for the adsorptive treatment of landfill leachate: A laboratory column evaluation", Bioresource Technology, 133, 599–605.
- Francisco, S., Lorena, N., Matheus, B., Kleber, d.S., Waldomiro, P.J., Roberto, F., 2019, "Biosorption of methylene blue dye using natural biosorbents made from weeds", Journal of Materials, 12, 2486.
- Freundlich, H.M.F., 1906, "Over the adsorption in solution", J Phys. Chem 57:385–470.
- Fu, J., Chen, Z., Wang, M., Liu, S., Zhang, J., Zhang, J., Xu, Q., 2015, "Adsorption of methylene blue by a high-efficiency

adsorbent (polydopamine microspheres): Kinetics, isotherm, thermodynamics and mechanism analysis", Chemical Engineering Journal, 259, 53–61.

- Fuat, G., 2015, "Conversion of grape industrial processing waste to activated carbon sorbent and its performance in cationic and anionic dyes adsorption", J. Clean. Prod. 93, 84–93.
- Gao, W., Zhao, S., Wu, H., Deligeer, W., Asuha, S., 2016, "Direct acid activation of kaolinite and its effects on the adsorption of methylene blue", Applied Clay Science, 126, 98–106.
- Gebrezgiher, M., Kiflie, Z., 2020, "Utilization of cactus peel as biosorbent for the removal of reactive dyes from textile dye effluents", Journal of Environmental and Public Health, 1–10.
- Geetha, P., Latha, M.S., Koshy, M., 2015, "Biosorption of malachite green dye from aqueous solution by calcium alginate nanoparticles: equilibrium study", Journal of Molecular Liquids, 212.723–730.
- Georgin, J., Dottob, G.L., Mazuttib, M.A., Foletto, E.L., 2016, J. Environ. Chem. Eng, 4, 266–275 .
- Giannakoudakis, D.A., Hosseini-Bandegharaei, A., Tsafrakidou, P., Triantafyllidis, K.S., Kornaros, M., Anastopoulos, I., 2018, "Aloe vera waste biomass-based adsorbents for the removal of aquatic pollutants: a review", J. Environ. Manag. 227: 354–364.
- Guarín, J. R., Moreno-Pirajan, J. C., Giraldo, L., 2018, "Kinetic Study of the bioadsorption of methylene blue on the surface of the biomass obtained from the algae D. antarctica", Journal of Chemistry, 2018, 1–12.
- Gulipalli,C.S.,Kailas L,B.P., Wasewar, 2011, "Batch Study,equilibrium and kinetics of adsorption of selenium using rice

husk ash(RHA)", Journal of engineering science and technology, 6 ,5.586-605.

- Gunturu, B., Palukuri, N. R., Sahadevan, R., 2018, "Decolorisation of basic textile dye from aqueous solutions using a biosorbent derived from the spesia populnea used biomass", IOP conference series: Materials science and engineering, 330, 012036.
- Gupta, V. K., Ali, I., 2012, "Environmental Water: Advances in Advances in Treatment", Remediation and Recycling Book.
- Hameed, B., Daud, F., 2008, "Adsorption studies of basic dye on activated carbon derived from agricultural waste: Hevea brasiliensis seed coat", Chemical Engineering Journal, 139(1), 48–55.
- Hameed, B.H., 2009, "Removal of cationic dye from aqueous solution using jackfruit peel as non-conventional low-cost adsorbent", Journal of Hazardous Materials, 162(1), 344–350.
- Hameed, B.H., El-Khaiary, M.I., 2008, "Batch removal of malachite green from aqueoussolutions by adsorption on oil palm trunk fibre: Equilibrium isotherms and kinetic studies", J. Hazard. Mater. 154 (2008) 237-244.
- Han, X., Wang, W., Ma, X., 2011, "Adsorption characteristics of methylene blue onto low cost biomass material lotus leaf", Chemical Engineering Journal, 171(1), 1–8.
- Hassan, A.F., Abdel-Mohsen, A.M., Fouda, M.M.G., 2014, "Comparative study of calcium al-ginate, activated carbon and their composite beads on methylene blue adsorption.Carbohydr",Polym. 102, 192–198.
- Hassan, W., Farooq, U., Ahmad, M., Athar M., Khan, M.A., 2017, "Potential biosorbent, haloxylon recurvum plant stems, for the

removal of methylene blue dye", Arabian Journal of Chemistry, 10: S1512–S1522.

- Hassan, W., Farooq, U., Ahmad, M., Athar, M., Khan, M.A., 2013, "Potential biosorbent, Haloxylon recurvum plant stems, for the removal of methylene blue dye", Arabian Journal of Chemistry, 10, S1512–S1522.
- Heidarinejad, Z., Rahmanian, O., Fazlzadeh, M., Heidari, M., 2018, "Enhancement of methylene blue adsorption onto activated carbon prepared from Date Press Cake by low frequency ultrasound", J. Mol. Liq. 264, 591–599.
- Hesas, R.H., Arami-Niya, A., A.N., Daud, W.M.A.W., Sahu, J.N., 2013, "Preparation and characterization of activated carbon from apple waste by microwave-assisted phosphoric acid activation: Application in methylene blue", BioResources, 8, 2: 2950-2966.
- Ho, Y.S., Mckay, G., 1999, "Pseudo-second order model for sorption processes", Process Biochem., 34,451.
- Hong, G.-B., Wang, Y.-K., 2017, "Synthesis of low-cost adsorbent from rice bran for the removal of reactive dye based on the response surface methodology", Applied Surface Science, 423, 800–809.
- Hu, H., Xu, K., 2020, "Physicochemical technologies for HRPs and risk control", High-Risk Pollutants in Wastewater, 169–207.
- Hussin, Z.M., Talib, N., Hussin, N.M., Hanafiah, M.A.K.M., Hanafiah, M.A.K.M., Khalir, W.K.A.W., 2015, "Methylene Blue Adsorption onto NaOH Modified Durian Leaf Powder: Isotherm and Kinetic Studies", American Journal of Environmental Engineering , 5(3A): 38-43.
- Hutchins, R.A., 1973, "New method simplifies design of activated carbon systems", Chem. Eng. 80 (19), 133-138.

- Hynes, N.R.J., Kumar, J.S., Kamyab, H., Sujana, J.A. J., Al-Khashman, O.A., Kuslu, Y., Suresh, B., 2020, "Modern Enabling Techniques and Adsorbents based Dye Removal with Sustainability Concerns in Textile Industrial Sector -A comprehensive review", Journal of Cleaner Production.
- Iftekhar, S., Ramasamy, D.L., Srivastava, V., Asif, M.B., Sillanpää, M., 2018, "Understanding the factors affecting the adsorption of Lanthanum using different adsorbents: A critical review", Chemosphere, 204, 413–430.
- Inam, E., Etim, U.J., Akpabio, E.G., Umoren, S.A., 2016, "Process optimization for the application of carbon from plantain peels in dye abstraction", Journal of Taibah University for Science, 11(1), 173–185.
- Inamuddin, 2018, "Xanthan gum/titanium dioxide nanocomposite for photocatalytic degradation of methyl orange dye", International Journal of Biological Macromolecules.
- Jabar, J.M., Odusote, Y.A., Alabi, K.A., Ahmed, I.B., 2020, "Kinetics and mechanisms of congo‑red dye removal from aqueous solution using activated Moringa oleifera seed coat as adsorbent", Applied Water Science, 10:136.
- Jamiu, M.J., Yisau, A.O. Kazeem, A.A., Ibrahim, B.A., 2020, "Kinetics and mechanisms of congo‑red dye removal from aqueous solution using activated Moringa oleifera seed coat as adsorbent", Journal of Applied Water Science, 10:136.
- Jawad, A.H., Ismail, K., Ishak, M.A.M., Wilson,L.D., 2019, "Conversion of malaysian low-rank coal to mesoporous activated carbon: structure characterization and adsorption properties", Chinese. J Chem Eng., Vol. 27, no. 7, pp. 1716–1727.

- Jawad, A.H., Ngoh, Y.S., Radzun, K.A., 2018, "Utilization of water- melon (Citrullus lanatus) rinds as a natural low-cost biosorbent for adsorption of methylene blue: kinetic, equilibrium and thermodynamic studies", J Taibah Univ Sci ,12(4):371–381.
- Jawad, A.H.,Waheeb, A.S., Rashid, R.A., Nawawi, W.I., Yousif, E., 2018 a, "Equilibrium isotherms, kinetics, and thermodynamics studies of methylene blue adsorption on pomegranate (Punica granatum) peels as a natural low-cost biosorbent", DWT. 105:322–331.
- Jerold, M., Joseph, D., Patra, N., Sivasubramanian, V., 2016, "Fixed-bed column studies for the removal of hazardous malachite green dye from aqueous solution using novel nano zerovalent iron algal biocomposite", Nanotechnology for Environmental Engineering, 1(1).
- Kalhori, E.M., AL-Musawi, T.J., Ghahramani, E., Kazemian, H., Zarrabi, M., 2017, "Enhancement of the adsorption capacity of the light-weight expanded clay aggregate surface for the metronidazole antibiotic by coating with MgO nanoparticles: Studies on the kinentic, isotherm, and effects of environmental parameters", Journal of Chemosphere, 175:8-20.
- Kannan, N., and Sundaram, M.M., 2001, "Kinetics and mechanism of removal of methylene blue by adsorption on various carbons- A comparative study", Dyes and Pigments, 51(1). 25-40.
- Kanthasamy, S., Hadibarata, T., Hidayat, T., Alamri, S.A., Al-Ghamdi, A.A., 2020, "Adsorption of azo and anthraquinonec dye by using watermelon peel powder and corn peel powder: equilibrium and kinetic studies", Journal of Biointerface Research in Applied Chemistry, 10, 1: 4706-4713.

- Kapur, M., Mondal, M.K., 2015, "Design and model parameters estimation for fixed-bed column adsorption of Cu(II) and Ni(II) ions using magnetized saw dust", Desalination and Water Treatment, 1-12.
- Karthikeyan, S., Gupta, V.K., Boopathy, R., Titus, A., Sekaran, G., 2012, "A new approach for the degradation of high concentration of aromatic amine by heterocatalytic fenton oxidation: kinetic and spectroscopic studies", J. Mol. Liq. 173, 153–163.
- Kaveeshwar, A.R., Kumar, P.S., Revellame, E.D., Gang, D.D., Zappi, M.E., Subramaniam, R., 2018, "Adsorption properties and mechanism of barium (II) and strontium (II) removal from fracking wastewater using pecan shell based activated carbon", Journal of Cleaner Production, 193, 1–13.
- Koçer, O., Acemioğlu, B., 2016, "Adsorption of basic green 4 from aqueous solution by olive pomace and commercial activated carbon: process design, isotherm, kinetic and thermodynamic studies", Desalination and Water Treatment 57(35), 16653-16669.
- Kodal, S.P., Aksu, Z., 2017, "Cationic surfactant-modified biosorption of anionic dyes by dried Rhizopus arrhizus", Environmental technology, Taylor & Francis, 38, 2551–2561.
- Kooh, M.R.R., Dahri, M.K, Lim, L.B., 2016, "Jack fruit seed asa sustainable adsorbent for the removal of rhodamine B dye", Journal of Environment & Biotechnology Research,4.7–16.
- Kratochvil, D., Volesky,B., 2000, "Multicomponent biosorption in fixed beds", Water Res., 34: 3186-3196.
- Krishna, L.S., Yuzir, A., Yuvaraja, G., Ashokkumar, V., 2017 "Removal of acid blue25 from aqueous solutions using bengal gram fruit shell (BGFS) biomass", International Journal of Phytoremediation 19(5), 431-438.

- Kuang, Y., Zhang, X., Zhou, S., 2020, "Adsorption of methylene blue in water onto activated carbon by surfactant modification. water", 12(2), 587.
- Kulkarni, M. R., Revanth, T., Acharya, A., Bhat, P., 2017, "Removal of Crystal Violet dye from aqueous solution using water hyacinth: Equilibrium, kinetics and thermodynamics study", Resource-Efficient Technologies, 3(1), 71–77.
- Kumar, A., Jena, H.M., 2016, "Removal of methylene blue and phenol onto prepared activated carbon from Fox nutshell by chemical activation in batch and fixed-bed column", J. Clean. Prod. 137, 1246–1259.
- Kumar, P. A., Chakraborty, S., 2009, "Fixed-bed column study for hexavalent chromium removal and recovery by short-chain polyaniline synthesized on jute fiber", Journal of Hazardous Materials, 162(2-3), 1086–1098.
- Kumar, S., Gunasekar, V., Ponnusami, V., 2012, "Removal of methylene blue from aqueous effluent using fixed bed of groundnut shell powder", Journal of Chemistry, 2013, 1–5.
- Kumar, U., Bandyopadhyay, M., 2006, "Fixed bed column study for Cd(II) removal fromwastewater using treated rice husk", J. Hazard. Mater. 129 (1–3) 253–259.
- Kushwaha, A.K., Gupta, N., Chattopadhyaya, M.C., 2014, "Removal of cationic methylene blue and malachite green dyes from aqueous solution by waste materials of Daucus carota", Journal of Saudi Chemical Society, 18(3), 200–207.
- Labied, R., Benturki, O., Eddine, A. Y.E., Donnot, A., 2018, "Adsorption of hexavalent chromium by activated carbon obtained from a waste lignocellulosic material (Ziziphus jujuba cores):

Kinetic, equilibrium, and thermodynamic study", Adsorption Science & Technology, 36(3-4), 1066–1099.

- Lakshmipathy, R., 2015 a, "A fixed bed column study for the removal of Pb2+ ions by Watermelon rind", Environ. Sci. Water Res. Technol., 1, 244-250.
- Lakshmipathy, R., Sarada, N.C., 2015, "Methylene blue adsorption onto native watermelon rind: Batch and fixed bed column studies", Desalalin. Water Treat. 1–14.
- Langmuir, I., 1916, "The adsorption of gases on plane surface of glass, mica and platinum", J Am Chem Soc 40:1361–1403.
- Latif, S., Rehman, R., Imran, M., Iqbal, S., Kanwal, A., Mitu, L., 2019, "Removal of acidic dyes from aqueous media using citrullus lanatus peels: An agrowaste-based adsorbent for environmental safety", Journal of Chemistry.
- Lee, H.M., An, K.H., Kim, B.J., 2014, "Effects of carbonisation temperature on poredevelopment in polyacrylonitrile-based activated carbon nanofibers", Carbon Lett.15 (2), 146–150.
- Li, G., Zhang, D., Li, Q., Chen, G., 2014, "Effects of pH on isotherm modeling and cation competition for Cd(II) and Cu(II) biosorption on myriophyllum spicatum from aqueous solutions", Environ Earth Sci 72:4237–4247.
- Liu, J., Xia, S., Lü, X., Shen, H., 2017, "Adsorption of tricresyl phosphate onto grapheme nanomaterials from aqueous solution", Water Sci. Technol, 76, 1565–1573.
- Liu, Q.-X., Zhou, Y.-R., Wang, M., Zhang, Q., Ji, T., Chen, T.-Y., Yu, D.-C., 2019, "Adsorption of methylene blue from aqueous solution onto viscose-based activated carbon fiber felts: Kinetics and equilibrium studies", Adsorption Science & Technology, 026361741982743.

- Luo, L., Wu, X., Li, Z., Zhou, Y., Chen, T., Fan, M., & Zhao, W. (2019). Synthesis of activated carbon from biowaste of fir bark for methylene blue removal. Royal Society Open Science, 6(9), 190523.
- Lopez-Cervantes, J., Sanchez-Machado, D.I., Sanchez-Duarte, R.G., Correa-Murrieta, M.A., 2017, "Study of a fxed-bed column in the adsorption of an azo dye from an aqueous medium using a chitosan–glutaraldehyde biosorbent", Adsorpt Sci Technol 36:215–232.
- Mafra, M.R., Igarashi-Mafra, L., Zuim, D.R., Vasques, É.C., Ferreira, M.A., 2013, "Adsorption of remazol brilliant blue on an orange peel adsorbent", Brazilian Journal of Chemical Engineering, 30(3), 657–665.
- Mahamadi, C., Mawere, E., 2019, "Continuous flow biosorptive removal of methylene blue and crystal violet dyes using alginate-water hyacinth beads. Cogent Environmental Science, 0(0).
- Mahmoud, M.A., 2015, "Kinetics and thermodynamics of aluminum oxide nanopowder as adsorbent for Fe (III) from aqueous solution", Beni−Suef University Journal of Basic and Applied Sciences. 4: 142−149.
- Malik, P.K., 2004, "Dye removal from wastewater using activated carbon developed from sawdust: adsorption equilibrium and kinetics", Journal of Hazardous Materials,113. 81-88.
- Mall, M.I, Srivastava,V.C., Agarwal, N.K., 2005, "Adsorptive removal of malachite green dye from aqueous solution by bagasse fly ash and activated carbon-kinetic study and equilibrium isotherm analyses", Colloids Surf A Physicochem Eng Asp., vol. 264, pp. 17–28.

- Mane, V.S., Deo Mall, I., Chandra Srivastava, V., 2007, "Kinetic and equilibrium isotherm studies for the adsorptive removal of Brilliant Green dye from aqueous solution by rice husk ash", Journal of Environmental Management, 84(4), 390–400.
- Mangaleshwaran, L., Thirulogachandar, A., Rajasekar, V., Muthukumaran, C., Rasappan, K., 2015 "Batch and fixed bed column studies on nickel (II) adsorption from aqueous solution by treated polyurethane foam". Journal of the Taiwan Institute of Chemical Engineers 55, 112- 118.
- Marrakchi, F., Ahmed, M.J., Khanday, W.A., Asif, M., Hameed, B.H., 2017, "Mesoporous-activated carbon prepared from chitosan flakes via single-step sodium hydroxide activation for the adsorption of methylene blue", International Journal of Biological Macromolecules, 98, 233–239.
- Mashkoor, F., Nasar, A., 2020, "Magnetized tectona grandis sawdust as a novel adsorbent: preparation, characterization, and utilization for the removal of methylene blue from aqueous solution", Cellulose, 27,2613- 2635.
- Mashkoor, F., Nasar, A., 2019, "Preparation ,characterization and adsorption studies of the chemically modified luffa aegyptica peel as a potential adsorbent for the removal of malachite green from aqueous solution", J. Mol. Liq. 274, 315 327.
- Mhemeed, A.H., 2018, " A general overview on the adsorption" , Indian Journal of Natural Sciences Vol.9 /Issue 51 / December / 2018.
- Michalak, I., Chojnacka, K., Witek-Krowiak, A., 2013, "State of the art for the biosorption process—A review", Applied Biochemistry and Biotechnology, 170(6), 1389–1416.

- Mittal, A., Thakur, V., Mittal, J., Vardhan, H., 2014, "Process development for the removal of hazardous anionic azo dye Congo red from wastewater by using hen feather as potential adsorbent, "Desalination and Water Treatment, Taylor & Francis, 52, 227–237.
- Miyah, Y., Lahrichi, A., Idrissi, M., Boujraf, S., Taouda, H., Zerrouq, F., 2016, "Assessment of adsorption kinetics for removal potential of crystal violet dye from aqueous solutions using moroccan pyrophyllite", Journal of the Association of Arab Universities for Basic and Applied Sciences, 23(1), 20–28.
- Mo, J., Yang, Q., Zhang, N., Zhang, W., Zheng, Y., Zhang, Z., 2018, "A review on agro-industrial waste (AIW) derived adsorbents for water and wastewater treatment", Journal of Environmental Management, 227, 395–405.
- Mohebali, S., Bastani., D., Shayesteh, H., 2019, "Equilibrium, kinetic and thermodynamic studies of a low-cost biosorbent for the removal of Congo red dye: acid and CTAB-acid modified celery (Apium graveolens)", J Mol Struct. 1176:181–193.
- Mohseni-Bandpi, A., Al-Musawi, T. J., Ghahramani, E., Zarrabi, M., Mohebi, S., & Vahed, S. A. (2016). Improvement of zeolite adsorption capacity for cephalexin by coating with magnetic Fe3O4 nanoparticles. Journal of Molecular Liquids, 218, 615–624.
- Mopoung, S., Moonsri, P., Palas, W., Khumpai, S., 2015, "Characterization and properties of activated carbon prepared from tamarind seeds by KOH activation for Fe(III) adsorption from aqueous solution", The Scientific World Journal, 2015, 1–9.
- Mosbah, M.B., Mechi, L., Khiari, R., Moussaoui, Y., 2020, "Current state of porous carbon for wastewater treatment", Jouranl of processes, 2020,8, 1651.

- Moyo, M., Pakade, V.E., Modise, S.J., 2017, "Biosorption of lead(II) by chemically modifed Mangifera indica seed shells: adsorbent preparation, characterization and performance assessment", Process Saf Environ Prot 111:40–51.
- Muralik,K., Uma, R.N., 2016, "Emoval of basic dye (methylene blue) using low cost biosorbent: Water hyacinth", International Journal of Advanced Engineering Technology.
- Muthuraman, G., 2011, "Extractive removal of astacryl blue BG and astacryl golden yellow dyes from aqueous solutions by liquid–liquid extraction", Desalination, 277(1-3), 308–312.
- Najim, A. A., 2018, "Biosorption of Nickel Ions and Methylene Blue Dye from Simulated Wastewater by Three Phase Circulated Fluidized Bed Using Mixed Algae", Iraqi Journal of Chemical and Petroleum Engineering, 19(4), 1-11.
- Nanganoa, L.T., Ketcha, J.M., Ndi, J.N., 2014, "Kinetic and equilibrium modeling of the adsorption of amaranth from aqueous solution onto smectite clay", Research Journal of Chemical Scienc, vol. 4(2), 7-14.
- Naskar, A., Majumder, R., 2017, "Understanding the adsorption behaviour of acid yellow 99 on aspergillus niger biomass", Journal of Molecular Liquids 242 (1), 892–899.
- Nasuha, N., Hameed, B.H., 2011, "Adsorption of methylene blue from aqueous solution onto NaOH-modified rejected tea", Chem. Eng. J. 166, 783–786.
- Naushad, M., Alothman, ZA., Inamuddin Javadian, H., 2015, "Removal of Pb(II) from aqueous solution using ethylene diamine tetra acetic acid-Zr(IV) iodate composite cation exchanger: kinetics, isotherms and thermodynamic studies", J Ind Eng Chem ;25:35–41.

- Nazarzadeh Zare, E., Mansour Lakouraj, M., Ramezani, A., 2016, "Efficient sorption of Pb(ii) from an aqueous solution using a poly(aniline-co-3-aminobenzoic acid)-based magnetic core–shell nanocomposite", New Journal of Chemistry, 40(3), 2521–2529.
- Nemeş, L., Bulgariu, L., 2016, "Optimization of process parameters for heavy metals biosorption onto mustard waste biomass", Open Chemistry, 14(1).
- Nethaji, S., Sivasamy, A., Mandal, A.B., 2012, "Adsorption isotherms, kinetics and mechanism for the adsorption of cationic and anionic dyes onto carbonaceous particles prepared from Juglans regia shell biomass", International Journal of Environmental Science and Technology, 10(2), 231–242.
- Nibret, G., Ahmad, S., Rao, D.G., Ahmad, I., Shaikh, M.A.M.U., Rehman, Z.U., 2019, "Removal of methylene blue dye from textile wastewater using water hyacinth activated carbon as adsorbent: Synthesis, characterization and kinetic studies", SSRN Electronic Journal.
- Nirmal, A., Swamy, A., Sakpal, Q., Shingare, S.P., 2019, " Removal of methylene blue from aqueous solution using agricultural wastes as adsorbent" , International Journal of Innovative Research in Science, Engineering and Technology, Vol. 8, Issue 5.
- Noreen, S., Bhatti, H.N., Nausheen, S., Sadaf, S., Ashfaq, M., 2013, "Batch and fixed bed adsorption study for the removal of Drimarine Black CL-B dye from aqueous solution using a lignocellulosic waste: A cost affective adsorbent", Industrial Crops and Products, 50, 568–579.
- Obayomia, K.S., Autab, M., Kovo, A.S., 2019, "Isotherm, kinetic and thermodynamic studies for adsorption of lead(II) onto

modified Aloji clay", Desalination and Water Treatment, 181.376–384.

- Oguntimein, G.B., 2015, "Biosorption of dye from textile wastewater effluent onto alkali treated dried sunflower seed hull and design of a batch adsorber", Journal of Environmental Chemical Engineering, 3(4), 2647–2661.
- Orzechowska-Zięba, A., Jodłowski, G., Wójcik, M, 2019, "Biosorbents for waste water cleaning from coloring agents", IOP Conference Series: Earth and Environmental Science, 214, 012031.
- Ozdemir, I., Sahin, M., Orhan, R., Erdem, M., 2014, "Fuel process" Technol, 25, 200–206 .
- Pang, J., Fu, F., Ding, Z., Lu, J., Li, N., Tang, B., 2017, "Adsorption behaviors of methylene blue from aqueous solution on mesoporous birnessite", J. Taiwan Inst. Chem. E 77, 168–176.
- Patel, H., 2019, "Fixed-bed column adsorption study: a comprehensive review", Applied Water Science, 9(3).
- Patel, H., Vashi, R.T., 2012, "Fixed bed column adsorption of acid yellow 17 dye onto tamarind seed powed", Can. J.Chem.Eng., 90:180-185.
- Pathania, D., Sharma, S., Singh, P., 2017, "Removal of methylene blue by adsorption onto activated carbon developed from ficus carica bast", Arabian Journal of Chemistry, 10, S1445–S1451.
- Pavan, F.A., Camacho, E.S., Lima, E.C., Dotto, G.L., Branco, V.T.A., Dias, S.L.P. 2014, "Formosa papaya seed powder (FPSP): Preparation, characterization and application as an alternative adsorbent for the removal of crystal violet from aqueous phase", Journal of Environmental Chemical Engineering, 2(1), 230–238.
- Pezoti, O., Cazetta, A.L., Souza, I.P.A.F., Bedin, K.C., Martins, A.C., Silva, T.L., Almeida, V.C., 2014, "Adsorption studies of

methylene blue onto ZnCl2-activated carbon produced from buriti shells (Mauritia flexuosa L.)", Journal of Industrial and Engineering Chemistry, 20(6), 4401–4407.

- Pholosi, A., Naidoo, E.B., Ofomaja, A.E., 2020, "Intraparticle Diffusion Of Cr(Vi) Through Biomass And Magnetite Coated Biomass: A Comparative Kinetic And Diffusion Study", South African Journal of Chemical Engineering.
- Ponnusami, V., Gunasekar, V., Srivastava, S. N., 2009, "Kinetics of methylene blue removal from aqueous solution using gulmohar (Delonix regia) plant leaf powder: Multivariate regression analysis", Journal of Hazardous Materials, 169(1-3), 119–127.
- Prola, L.D.T., Acayanka, E., Lima, E.C., Umpierres, C.S., Vaghetti, J.C.P., Santos, W.O., Djifon, P.T., 2013, "Comparison of Jatropha curcas shells in natural form and treated by non-thermal plasma as biosorbents for removal of Reactive Red 120 textile dye from aqueous solution", Industrial Crops and Products, 46, 328–340.
- Quansah, J.O., Hlaing, T., Lyonga, F.N., Kyi, P.P., Hong, S.H., Lee, C.G., Park, S.J., 2020, "Nascent rice husk as an adsorbent for removing cationic dyes from textile wastewater", applied sciences,10, 3437.
- Rafatullah, M., Sulaiman, O., Hashim, R., Ahmad, A., 2010, "Adsorption of methylene blue on low-cost adsorbents: a review", Journal of Hazardous Materials, 177(1-3), 70-80.
- Rahman, S.A.M., Amin, M.A., Alam, A.R.R., 2012, "Removal of methylene blue from wastewater using activated carbon prepared from rice husk", Dhaka Univ. J. Sc., 60. 185–189.
- Ramrakhiani, L., Halder, A., Majumder, A., Mandal, A. K., Majumdar, S., Ghosh, S., 2017, "Industrial waste derived

biosorbent for toxic metal remediation: mechanism studies and spent biosorbent management", Chemical Engineering Journal, Elsevier, 308, 1048–1064.

- Rangabhashiyam, S., Selvaraju, N., 2015, "Adsorptive remediation of hexavalent chromium from synthetic wastewater by a natural and ZnCl2 activated Sterculia guttata shell", Journal of Molecular Liquids, 207, 39–49.
- Rangabhashiyam, S., Anu. N., Selvaraju, N., 2013, "Sequestration of dye from textile industry wastewater using agricultural waste products as adsorbents", Journal of Environmental Chemical Engineering, 1, 629-641.
- Razi, M.A.M, Hishammudin, M.N.A.M., Hamdan, R.H., 2017, "Factor affecting textile dye removal using adsorbent from activated carbon: A review ", 710 30 MATEC Web of Conferences matecconf.
- Reddy, D.H.K., Lee, S.M., Seshaiah, K., 2012, "Removal of Cd(II) from aqueous solution by agro biomass: equilibrium, kinetic and thermodynamic studies", J. Environ. Eng.Res., 17, 3: 125-132.
- Reddy, N.A., Lakshmipathy, R., Sarada, N.C., 2014, "Application of citrullus lanatus rind as biosorbent for removal of trivalent chromium from aqueous solution", Journal of Alexandria Engineering, 53, 969-975.
- Rizzi, V., D'Agostino, F., Fini, P., Semeraro, P., Cosma, P., 2017, "An interesting environmental friendly cleanup: The excellent potential of olive pomace for disperse blue adsorption/desorption from wastewater", Dyes and Pigments, 140, 480–490.
- Robinson, T., McMullan, G., Marchant, R., & Nigam, P. (2001). Remediation of dyes in textile effluent: a critical review on current

treatment technologies with a proposed alternative. Bioresource Technology, 77(3), 247–255.

- Rouf ,S., Nagapadma , M., 2015, " Modeling of Fixed Bed column studies for adsorption of azo dye on chitosan Impregnated with a Cationic Surfactant" , International Journal of Scientific & Engineering Research, 6, 2.
- Rubio, J., Souza, M., Smith, R., 2002, "Overview of flotation as a wastewater treatment technique", Minerals Engineering, 15(3), 139–155.
- Sadaf, S., Bhatti, H.N., 2013, "Evaluation of peanut husk as a novel, low cost biosorbent for the removal of indosol orange RSN dye from aqueous solutions: batch and fixed bed studies", Clean Technologies and Environmental Policy, 16(3), 527–544.
- Sajab, M.S., Chia, C.H., Zakaria, S., Sillanpää, M., 2014, "Fixed-bed column studies for the removal of cationic and anionic dyes by chemically modified oil palm empty fruit bunch fibers: single- and multi-solute systems", Desalination and Water Treatment, 1–8.
- Salam, M.A., 2013, "Removal of heavy metal ions from aqueous solutions with multi-walled carbon nanotubes: kinetic and thermodynamic studies", Int J Environ Sci Technol 10(4):677–688.
- Saleem, M., Wongsrisujarit, N., Boonyarattanakalin, S., 2016, "Removal of nickel (II) ion by adsorption on coconut copra meal biosorbent", Desalination and Water Treatment, 57, 12,5623–5635.
- Salisua, A., Sanagi, M.M., Naim, A.A., Karim, K.J., 2015, "Removal of methylene blue dye from aqueous solution using alginate grafted polyacrylonitrile beads", Pharma Chem. 7, 237–242.

- Salleh, M.A.M., 2011, "Cationic and anionic dye adsorption by agricultural solid wastes: A comprehensive review", Desalination, . 280(1): p. 1-13.
- Samiey, B., Ashoori, F., 2012, "Adsorption removal of methylene blue by agar: Effects of NaCl and ethanol", Chemistry Central Journal 6(14), 1-13.
- Santhi, T., Manonmani, S., Vasantha, V.S., Chang, Y.T. 2011, "A new alternative adsorbent for the removal of cationic dyes from aqueous solution", Arabian Journal of Chemistry, 9, S466–S474.
- Saravanan, A., Senthil Kumar, P., Yaswanthraj, M., 2018, "Modeling and analysis of a packed-bed column for the effective removal of zinc from aqueous solution using dual surface modifed biomass", Part Sci Technol Int J 36(8):934–944.
- Saroyan, H.S., Giannakoudakis, D.A., Sarafidis, C.S., Lazaridis, N.K., Deliyanni, E.A., 2017, "Effective impregnation for the preparation of magnetic mesoporous carbon: application to dye adsorption", J. Chem. Technol. Biotechnol. 92: 1899–1911.
- Saxena, Bhardwaj, M., Allen, T., Kumar, S., Sahney, R., 2019, "Adsorption of heavy metals from wastewater using agricultural-industrial wastes as biosorbents", WaterSci. 31, 189–197.
- Schiewer, S. and Patil, S.B., 2008, "Pectin-rich fruit wastes as bio-sorbents for heavy metal removal: equilibrium and kinetics", Bioresource Technology, 99, 6: 1896-1903.
- Sen, S.K., Raut, S., Bandyopadhyay, P., Raut, S., 2016, "Fungal decolouration and degradation of azo dyes: a review", Fungal Biology Reviews 30 (3), 112–133.
- Senthil Kumar, P., Ramalingam, S., Senthamarai, C., Niranjanaa, M., Vijayalakshmi, P., Sivanesan, S., 2010, "Adsorption of dye from aqueous solution by cashew nut shell: Studies on equilibrium

isotherm, kinetics and thermodynamics of interactions", Desalination, 261(1-2), 52–60.

- Senthil, k.P., Palaniyappan, M., Priyadharshini, M., Vignesh, A.M., Thanjiappan, A., Sebastina, A.F.P., Tanvir, A.R., Srinath, R., 2014, "Adsorption of basic dye onto raw and surface-modified agricultural waste", Environmental Progress & Sustainable Energy 33(1), 87-98.
- Sentruk, H.B., Ozdes, D., Duran, C., 2010, "Biosorption of rhodamine 6G from aqueous solutions onto almond shell (Prunus dulcis) as a low cost biosorbent", Desalination, 252, 81-87.
- Seow, T.W, Lim, C.K, 2016, "Removal of dye by adsorption: A review", Int. J. Appl. Eng. Res. 11, 2675–2679.
- Seshadri, S., Bishop, P.L., Agha, A.M., 1994, "Anaerobic/aerobic treatment of selected azo dyes in wastewater", Waste Management, 14(2), 127–137.
- Shayesteh, H., Rahbar-Kelishami., A., Norouzbeigi., R., 2016, "Adsorption of malachite green and crystal violet cationic dyes from aqueous solution using pumice stone as a low-cost adsorbent: kinetic, equilibrium, and thermodynamic studies", Desalin Water Treat. 57(27): 12822–12831.
- Sheng, L., Zhang, Y., Tang, F., Liu, S., 2018, "Mesoporous/microporous silica materials: preparation from natural sands and highly efficient fxed-bed adsorption of methylene blue in wastewater", Microporous Mesoporous Mater 257:9–18.
- Singh, H., Chauhan, G., Jain, A. K., Sharma, S.K., 2017, "Adsorptive potential of agricultural wastes for removal of dyes from aqueous solutions", Journal of Environmental Chemical Engineering, 5(1), 122–135.

- Sivarajasekar, N., Baskar, R., 2015, " Agriculture waste biomass valorisation for cationic dyes sequestration: A concise review", Journal of Chemical and Pharmaceutical Research, 2015, 7(9):737-748.
- Somaia, G.M., Sahar, M.A., 2017, "Preparation of environmentally friendly activated carbon for removal of pesticide from aqueous media", Int J Ind Chem, 8:121–132.
- Shak, A., Dawood, S., Sen, T.K., 2017, "Performance and dynamic modelling of mixed biomass-kaolin packed bed adsorption column for the removal of aqueous phase methylene blue (MB) dye". Desalination and Water Treatment 82, 67-80.
- Srivastava, V., Sillanpää, M., 2017, "Synthesis of malachite@clay nanocomposite for rapid scavenging of cationic and anionic dyes from synthetic wastewater", Journal of Environmental Sciences, 51, 97–110.
- Sulyman, M., Namiesnik, J., Gierak, A., 2016, "Low-cost adsorbents derived from agricultural by-products/wastes for enhancing contaminant uptakes from wastewater: A review", Pol. J. Environ. Stud, 26, No. 2, 479-510.
- Sun, S., Zhang, T., 2020, " Review of classical reservoir simulation", Reservoir Simulations, 23–86.
- Swamy, M.M. , Nagabhushana, B.M., Krishna, R.H., Kottam, N., Raveendra, R.S., Prashanth, P.A., 2017, "Fast adsorptive removal of methylene blue dye from aqueous solution onto a wild carrot flower activated carbon: isotherms and kinetics studies", Desalin Water Treat,71.399–405.
- Tabrez, A. K., Ved, V., 2010, "Removal of cadmium (II), lead (II), and chromium (VI) ions from aqueous solution using clay",

Toxicological And Environmental Chemistry, Vol.92, No.8, PP. 1435–1446.

- Tan, I. A. W., Ahmad, A. L., Hameed, B. H., 2008, " Adsorption of basic dye on high-surface-area activated carbon prepared from coconut husk: Equilibrium, kinetic and thermodynamic studies", Journal of Hazardous Materials, 154(1-3), 337–346.
- Teutscherova, N., Houska, J., Navas, M., Masaguer, A., Benito, M., Vazquez, E., 2018, "Leaching of ammonium and nitrate from Acrisol and Calcisol amended with holm oak biochar: a column study", Geoderma 323:136–145.
- Thomas, H.C., 1944, "Heterogeneous ion exchange in a flowing system" J. Am. Chem.Soc. 66 1466–1664.
- Thommes, M., 2010, "Physical adsorption characterization of nanoporous materials", Chemie Ingenieur Technik, 82(7), 1059–1073.
- Thuong, N.T., Nhi, N.T.T., Nhung, V.T.C., Bich, H.N, Quynh, B.T.P., Bach, L.G., Nguyen, T.D.N., 2018, "A Fixed-bed column study for removal of organic dyes from aqueous solution by pre-treated durian peel waste", Indones. J. Chem., 2019, 19 (2), 486 – 494.
- Tsai, W.C., Luna, M.D.G., Arriesgado, H.L., Futalan, C.M., Colades, J. I., Wan, M.W., 2016, "Competitive fixed-bed adsorption of Pb(II), Cu(II), and Ni(II) from aqueous solution using chitosan-coated bentonite", Int. J. Polym. Sci. (2016), 1–11.
- Uddin, M. T., Rahman, M. A., Rukanuzzaman, M., Islam, M.A., 2017, "A potential low cost adsorbent for the removal of cationic dyes from aqueous solutions", Applied Water Science, 7(6), 2831–2842.

- Ukanwa, Patchigolla, Sakrabani, Anthony, Mandavgane., 2019, "A Review of Chemicals to Produce Activated Carbon from Agricultural Waste Biomass", Sustainability, 11(22), 6204.
- Üner, O., GeÇgel, Ü., Bayrak, Y., 2015, "Preparation and characterization of mesoporous activated carbon from waste watermelon rind by using the chemical activation method with zinc chloride", Arabian Journal of Chemistry, 12, 8: 3621-3627.
- Unuabonah, E.I., OIu-Owolabi, B.I., Fasuyi, E.I., Adebowale, K.O., 2015, "Modeling of fixed bed column studies for the adsorption of cadmium onto novel polymer-clay composite adsorbent", J.Hazard.Mater., 179:415-423.
- Vardhan, K.H., Kumar, P.S., Panda, R.C., 2019, "A review on heavy metal pollution, toxicity and remedial measures: Current trends and future perspectives", Journal of Molecular Liquids, 290, 111197.
- Vijayaraghavan, K., Prabu, D., 2006, "Potential of Sargassum wightii biomass for copper(II) removal from aqueous solutions: Application of different mathematical models to batch and continuous biosorption data", Journal of Hazardous Materials, 137(1), 558–564.
- Vilvanathan, S., Shanthakumar, S., 2017, "Column adsorption studies on nickel and cobalt removal from aqueous solution using native and biochar form of Tectona grandis". Environmental Progress & Sustainable Energy
- Volesky, B., 2001, "Detoxification of metal-bearing effluents: biosorption for the next century", Hydrometallurgy 59:203–216.
- Vučurović, V.M., Razmovski, R.N., DMiljić, U., 2014, "Removal of cationic and anionic azo dyes from aqueous solutions by

adsorption on maize stem tissue", J.Taiwan Inst. Chem. Eng., 45, 1700–1708.

- Vučurović, V.M., Razmovski, R.N., Tekić, M.N., 2012, "Methylene blue (cationic dye) adsorption onto sugar beet pulp: Equilibrium isotherm and kinetic studies", Journal of the Taiwan Institute of Chemical Engineers, 43(1), 108–111.
- Wang, L., Shi, C., Pan, L., Zhang, X., Zou, J., 2020, "Rational design, synthesis, adsorption principles and applications of metal oxide adsorbents: A review", : Nanoscale Accepted Manuscript.
- Wang, X., Jiang, C., Hou, B., Wang, Y., Hao, C., Wu, J., 2018, "Carbon composite lignin-based adsorbents for the adsorption of dyes", Chemosphere 206, 587–596.
- Weber, J., Morriss, J.C., 1963, "Kinentics of adsorption on carbon from solution", J. Sanitary Eng. Div Am. Soc. Civ. Eng., 89,1-60.
- Weng, C.H., Pan, Y.F., 2007, " Adsorption of a cationic dye (methylene blue) onto spent activated clay", Journal of Hazardous Materials, 144(1-2), 355–362.
- Wong, K.T., Eu, N. C., Ibrahim, S., Kim, H., Yoon, Y., Jang, M., 2016, "Recyclable magnetite-loaded palm shell-waste based activated carbon for the effective removal of methylene blue from aqueous solution", Journal of Cleaner Production, 115, 337–342.
- Worch, E., 2012, "Adsorption technology in water treatment: Fundamentals, processes and modeling", Berlin, Germany: Walter de Gruyter.
- Wu, J.S., Liu, C.H., Chu, K.H., Suen, S.Y., 2008, "Removal of cationic dye methyl violet 2B from water by cation exchange membranes", J. Membr. Sci. 309, 239–245.

- Xu, Z., Cai, J., Pan, B., 2013, "Mathematically modeling fixed-bed adsorption in aqueous systems", Journal of Zhejiang University SCIENCE A, 14(3), 155–176.
- Yagub, M.T., Sen, T.K., Afroze, S., Ang, H.M., 2014, "Fixed-bed dynamic column adsorption study of methylene blue (MB) onto pine cone", Desalination and Water Treatment, 55(4), 1026–1039.
- Yahya, M.A., Al-Qodah, Z., Ngah, C.W.Z., 2015, "Agricultural bio-waste materials as potential sustainable precursors used for activated carbon production: A review", Renewable and Sustainable Energy Reviews, 46, 218–235.
- Yoon, Y.H., Nelson, J.H., 1984, "Application of gas adsorption kinetics. Part 1. A theoreti-cal model for respirator cartridge service time", Am Ind. Hyg, Assoc. J. 45 .509–516.
- Yu, J., Zhu, J., Feng, L., Cai, X., Zhang, Y., Chi, R., 2015, "Removal of cationic dyes by modified waste biosorbent under continuous model: Competitive adsorption and kinetics", Arabian Journal of Chemistry.
- Yuan, N., Cai, H., Liu, T., Huang, Q., & Zhang, X., 2019, Adsorptive removal of methylene blue from aqueous solution using coal fly ash-derived mesoporous silica material. Adsorption Science & Technology, 026361741982743
- Zarrabi, M., 2016, "Improvement of zeolite adsorption capacity for cephalexin by coating with magnetic Fe_3O_4 nanoparticles", Journal of Molecular Liquids , 218, 615-624.
- Zazouli, M. A., Azari, A., Dehghan, S., Salmani Malekkolae, R., 2016, "Adsorption of methylene blue from aqueous solution onto activated carbons developed from eucalyptus bark and Crataegus oxyacantha core", Water Science and Technology, 74(9), 2021–2035.

- Zhang, J., Landry, M.P., Barone, P.W., 2013, "Molecular recognition using corona phase complexes made of synthetic polymer adsorbed on carbon nanotubes", Nature Nano-Technology, 8, 12: 959-968.
- Zhang, X., Hao, Y., Wang, X., Chen, Z., 2017, "Rapid removal of zinc(II) from aqueous solutions using a mesoporous activated carbon prepared from agricultural waste", Journal of Materials, 10: 1002–1019.
- Zhou,Y., Zhang, L., Cheng, Z., 2015, "Removal of organic pollutants from aqueous solution using agricultural wastes: a review", J Mol Liq. 212: 739–762.
- Zou, W., Bai, H., Gao, S., Li, K., 2013, "Characterization of modified sawdust, kinetic and equilibrium study about methylene blue adsorption in batch mode", Korean Journal of Chemical Engineering, . 30(1): p. 111-122.

الخلاصـــــــــة

تتحرى هذه الدراسة عن قدرة الكربون المنشط المشتق من نبات طبيعي (SAC) كمادة حيوية منخفضة الكلفة (نبات شانجينيا (Schanginia / sp)، كمادة مازة لإزالة صبغة الميثيلين الزرقاء (MBD) من مياه الفضلات. أجريت سلسلة من التجارب المختبرية بنوعيها نظام الدفعة ونظام الامتزاز بالجريان المستمر لتقييم معالجة المحاليل المائية الصناعية باستخدام SAC. تم استخدام تقنيات متنوعة لإجراء تحاليل التمييز قبل وبعد إزالة MBD وتشمل ايجاد المساحة السطحية (S_{BET}) و FTIR و SEM و SPM.

تمت دراسة العوامل المختلفة التي تؤثر على عملية امتزاز الصبغة في درجة حرارة الغرفة بنظام الدفعة مثل الدالة الحامضية لمحلول الصبغة، وقت التلامس ، جرعة المادة المازة، وتركيز الصبغة الأولي . تم التوصل الى ان درجة الحموضة 9 وجرعة 0.8 غم/ 100 مل من محلول الصبغة ، و 75 دقيقة من وقت التلامس لتركيز الصبغة البالغ 50 ملغم / لتر وسرعة الرج البالغة 250 rpm ، هي الظروف المثلى لإزالة الصبغة باستخدام SAC.

تم تحليل البيانات التجريبية عند الاتزان باستخدام موديلي لانكمير وفراندلش ، ووجد ان البيانات توافق موديل لانكمير ليكون افضل موديل لمحاكاة امتزاز الصبغة على سطوح SAC. تم ايجاد قيمة الامتزاز القصوى (q_{max}) والبالغة 33.34 ملغم / غم ومعامل تحديد (R^2) يبلغ 0.9954.

تم تحليل البيانات الخاصة بدراسة ديناميكية الامتزاز وفق عدة موديلات رياضية لتحديد نوع ومعدل وميكانيكية الامتزاز وتبين ان الامتزاز كيمياوي ويتخلله الانتشار داخل الجسيمات.

تم استخدام طبقة ثابتة من الامتصاص المستمر من مادة الامتصاص الحيوي SAC لإزالة MBDمن المحاليل المائية عند درجة حرارة الغرفة (٢٥ ± ٥ درجة مئوية) لدراسة تأثيرات معدل التدفق ، وارتفاع الحشوة ، وتركيزات الصبغة عند كفاءة الإزالة .لوحظ أن نسبة الإزالة تزداد مع زيادة إرتفاع الحشوة وتنقص كلما زاد معدل التدفق وزيادة تركيز MBD تزداد قدرة الامتصاص مع زيادة ارتفاع الحشوة وتركيزه وتقل مع زيادة معدل التدفق.

تم تحليل بيانات العمود التي تم الحصول عليها وأظهرت أن منحنيات الاختراق (breakthrough curves) تأثرت بقوة بهذه العوامل. تم استخدام موديلات رياضية لوصف تصرف المفاعل مع امكانية التنبؤ بالاعتماد على مجموعة البيانات التجريبية وشملت هذه الموديلات Bed Depth Surface Time (BDST) و Thomas و Yoon-Nelson .

وجد ان الموديلات المعتمدة لوصف امتزاز الصبغة تغطي التصرف الكامل لمنحني الاختراق مع تثبيت افضل بالاعتماد على قيمة R^2 العالية والانحراف القليل جدا بين القيم التجريبية والمخمنة .تشير النتائج إلى أن SAC يمكن استخدامه بكفاءة لإزالة صبغة الميثيلين الزرقاء من المحاليل المائية.

جمهورية العراق
وزارة التعليم العالي والبحث العلمي
جامعة بابل
كلية الهندسة
قسم الهندسة البيئية

ازالة الصبغة المثيلين الزرقاء من مياه الصرف الملونه باستخدام ماده مازه طبيعيه

رسالة مقدمه الى
قسم الهندسة البيئية كلية الهندسة
في جامعة بابل كجزء من متطلبات نيل
درجة الماجستير في الهندسة / الهندسة البيئية

من قبل
معالي الامجاد حسن حسين جواد الحميري

بكالوريوس هندسة بيئية،(٢٠١٧)

اشراف

أ.م.د. اسراء سعدي عبد الامير سماكه

1443 هـ 2021 م